Health and Environmental Risks of Synthetic Nanoparticles Assessed by Human Cell Lines

Abdulmajeed Almutary (MSc Medical Biotechnology)

Department of Medical Biotechnology, College of Medicine and Public Health, Flinders University of South Australia

A thesis submitted in fulfilment of the requirement for the degree of Doctor of Philosophy

February 2018

Thesis Summary

Toxicity of synthetic nanoparticles (NPs) to human keratinocyte cell line (HaCaT) and human colon carcinoma cell line (Caco-2) were determined by 3-(4,5-Dimethylthiazol-2-yl)-2,5-diphenyltetrazolium bromide (MTT) , lactate dehydrogenase (LDH) and crystal violet assays. Eight nanoparticles were spiked in MTT and crystal violet assays and tested with HaCaT human skin cells to determine any possible interference. The MTT assay standard curve optical density (OD) measurements were shifted by the presence of trisilanol phenyl and trisilanol isooctyl polyhedral oligomeric silsesquioxane particles. The crystal violet standard curve OD measurements were significantly altered by AuNPs, but they did not affect the MTT assay. Carbon black decreased ODs in the MTT and crystal violet assays and was localised in the cell cytoplasm. The toxicity of 12-nm amorphous silica (SiO_2) NPs following 4, 24 and 48h exposure was investigated using HaCaT cell line with MTT and crystal violet assays. Eleven concentrations of 12-nm SiO_2 (ranging between 0.05-10 mg/mL) were tested. At 4, 24 and 48h exposure, a dose dependent increase in cell death with increasing concentration were observed when screened with the MTT assay. At 24h for concentrations $\geq$ 2 mg/mL, relative survival decreased when assayed by the MTT assay and relative cell number decreased when assayed with the crystal violet assay. After 48h treatment, cytotoxicity was observed at every treatment concentration assessed with the MTT and crystal violet assays. SiO_2 nanoparticles are toxic to cultured human skin cells at a concentration as low as 0.05 mg/mL for 48h treatment when screen by the crystal violet assay. The toxicity of SiO_2 NPs synthesised by the Stöber method and NDMA as a potent known carcinogen during chlorination on HaCaT and Caco-2 cell lines for 4, 24 and 48h detected by MTT and LDH assays. The morphology and size of SiO_2 NPs was determined by SEM (200 nm in diameter). After exposure to SiO_2 (concentrations 0.05–2mg/mL), the concentration 2 mg/mL inactivated LDH in both cell lines; however, it did not reduce their metabolic activity when MTT assay used. NDMA (concentrations 0.1–1000 µg/mL) inactivated LDH leakage in HaCaT and Caco-2 and reduced the metabolic activity of HaCaT cells at 48-h exposure. This suggests that a concentration of SiO_2 <2 mg/mL used in water treatment can reduce the risk of nanomaterial toxicity to humans and possibly the ecosystems.

Thiolated silica (SiO_2) NPs were synthesised using the Stöber method and then coated with low-fouling zwitterionic SBMA using thiol-ene addition. SEM revealed monodispersed spherical particles with DLS showing a small increase in nanoparticle average diameter after modification with SBMA. Toxicity of the SiO_2-SBMA NPs (concentrations of 0.05–2.00mg/mL) was investigated using the MTT, LDH and crystal violet assays on the Caco-2 and HaCaT cell lines for 4, 24 and 48 h. The SiO_2-SBMA NPs increased LDH leakage and decreased relative cell number at 2.00 mg/mL, as clearly observed after the particles were exposed to UV light. These results indicate that concentrations ≤1.50 mg/mL of SiO_2-SBMA is of low toxicity are biocompatible and show potential as a chemotherapy drug conjugate.

Table of Contents

List of Tables

List of Figures

List of Abbreviations

AB	Alamar Blue
AgNP	Silver nanoparticle
ANOVA	Analysis of variance
ATCC	American Type Culture Collection
AuNP	Gold nanoparticle
CdM2	Dimethyl cadmium
CdS	Cadmium sulphide
CdSe	Cadmium–selenide
CdTe	Cadmium–tellurium
COPD	Chronic obstructive pulmonary disease
CWP	Coal workers pneumoconiosis
DLS	Dynamic light scattering
DMEM	Dulbecco's Modified Eagle Medium
DMSO	Dimethyl sulfoxide
ED	Electrodialysis
ENM	Engineered nanomaterial
EPR	Enhanced permeability and retention
FBS	Foetal bovine serum
FCS	Foetal calf serum
FP	Formation potential
IARC	International Agency for Research on Cancer
INT	Iodonitrotetrazolium chloride
LDH	Lactate dehydrogenase
MDR	Multidrug resistance
MED	Multiple effect distillation

MPTMS	3-Mercaptopropyl)trimethoxysilane
MQ	Milli-Q
MTS	3-(4,5-dimethylthiazol-2-yl)-5-(3-carboxymethoxyphenyl)-2-(4- sulfophenyl)-2Htetrazolium
MTT	3-(4,5-Dimethylthiazol-2-yl)-2,5-diphenyltetrazolium bromide
MWCNT	Multi-walled carbon nanotube
NAD	β-Nicotinamide adenine dinucleotide
NADH	β-Nicotinamide adenine dinucleotide hydrate
NDBA	*N*-nitrosodi-n-butylamine
NDEA	*N*-nitrosodiethylamine
NDMA	*N*-nitrosodimethylamine
NDPhA	*N*-nitrosodiphenylamine
NIOSH	National Institute of Occupational Safety and Health
NM	Nanomaterial
NMEA	*N*-nitrosomethylethylamine
NMor	*N*-nitrosomorpholine
NP	Nanoparticle
NR	Neutral Red
nZVI	Zerovalent iron
OD	Optical density
PBS	Phosphate buffered saline
PEG	Polyethylene glycol
PES	polyether sulfone
PLA	polylactic acid
PMS	Phenazine methosulfate
POSS	Polyhedral oligomeric silsesquioxane
PS	Polysulfone

QD	Quantum dot
RES	Reticuloendothelial system
RO	Reverse osmosis
ROS	Reactive oxygen species
RPM	Revolutions per minute
RPMI	Roswell Park Memorial Institute
SA	Surface area
SBMA	Sulfobetaine methacrylate
SD	Standard deviation
SDS	Sodium dodecyl sulphate
SE	Standard error
SEM	Scanning electron microscopy
SPB	Sodium phosphate buffer
SWCNT	Single-walled carbon nanotubes
TEM	Transmission electron microscopy
TEOS	Tetraethyl orthosilicate
TOP	Trioctyl phosphine
TOPO	Trioctyl phosphine oxide
UF	Ultrafiltration
UV	Ultraviolet
WST-1	2-(4-iodophenyl)-3-(4-nitrophenyl)-5-(2,4-disulfophenyl)-2H-tetrazolium
ZnO	Zinc oxide
ZnS	Zinc sulphide

Declaration

I certify that this thesis does not incorporate without acknowledgment any material previously submitted for a degree or diploma in any university; and that to the best of my knowledge and belief it does not contain any material previously published or written by another person except where due reference is made in the text

Abdulmajeed Almutary

19/07/2017

Acknowledgments

I would like to thank my amazing parents for their support, love, care and concern while I pursued my dreams in science. My deep gratitude goes to my brothers and sisters for their help and for supporting me.

I would like thank my PhD supervisor Associated Prof Barbara Sanderson for guiding me and teaching me so much, and for always explaining things to me with such kindness and good cheer. It was an honour to know her and be under her supervision for many years. Also I would like to thank my co-supervisor Prof Amanda Ellis in the School of Chemistry, Physics & Earth and Sciences, Flinders University, for providing the nanoparticles studied in this project and for all her helpful information.

My deepest gratitude goes to all the staff in the department of Medical Biotechnology, Flinders University, Prof Christopher Franco for his great leadership and Barbara Kupke and Hanna Krysinska for taking care of us in the lab and keeping the lab functioning perfectly and with no shortages in resources.

Publications and Conferences

1. **ALMUTARY, A**. & SANDERSON, B. 2016. The MTT and Crystal Violet Assays Potential Confounders in Nanoparticle Toxicity Testing. *International Journal of Toxicology*, DOI: 10.1177/1091581816648906

2. **ALMUTARY, A**. & SANDERSON, B. 2017. Toxicity of four novel polyhedral oligomeric silsesquioxane (POSS) particles used in anti-cancer drug delivery. *Journal of Applied Pharmaceutical Science Vol,* 7, 101-105. DOI: 10.7324/JAPS.2017.70212

3. **ALMUTARY, A**. Ellis, A. SANDERSON, B 2016. Amorphous silica nanoparticles show concentration and time-dependent toxicity on Huma HaCaT Cells. *International Journal of Sciences and Applied Research*.

4. **ALMUTARY, A**. Ellis, A. SANDERSON, B 2017. Toxicity of N-Nitrosodimethylamine and SiO2 nanoparticles to HaCaT and caco-2 cell lines found in wastewater treatment. *Journal of Toxicology and Health. DOI:10.7243/2056-3779-4-4*

5. **ALMUTARY, A**. Ellis, A. SANDERSON, B 2017. Toxicity of thiolated silica nanoparticles modified with sulfobetaine methacrylate for potential use in chemotherapy drug conjugation. *Journal of Applied Pharmaceutical science.*

6. **ALMUTARY, A**, SANDERSON, B 2017. Up to date in vitro artefacts in the detection of nanoparticle toxicity: Short review. *Journal of Ecology and Toxicology.*

Conferences

1. Sanderson BJS, Young F, Shapter J, Cooksley C, Munir S, **Almutary A**, Wubuli A (2012) Cytotoxicity of synthetic nanoparticles towards human cells in culture. AMSR Conference, Adelaide, S.A.

2. **Almutary, A**, Sanderson, BJS, Ellis A (2014) in Vitro Cytotoxicity of Silica Nanoparticles on Human Skin Cells, AMSR Conference, Adelaide S.A

Chapter 1: Introduction

1.1 Nanotechnology

Nanotechnology is the science of production of new materials at the atomic levels (Wilson et al., 2002). It involves the synthesis of particles smaller than 100 nm using manipulative techniques (Agnihotri et al., 2014). The importance of this field stems from its potential to revolutionise fields such as medicine and engineering. In the past two decades, the number of commercial nanoparticle (NP)-based therapeutic products has increased (Anselmo and Mitragotri, 2016). Globally, twenty-four NP-based therapeutic products have been approved for clinical use (Kateb and Heiss, 2013). Among these products, two dominant classes are the liposomal drugs and polymer–drug conjugates. Liposomal drugs were the first closed bilayer phospholipid systems to be described (in 1965) and to then become drug delivery systems (Allen and Cullis, 2013). The cooperation of many liposome researchers led to the development of critical technical advances such as extrusion for homogenous size, drug loading and long-circulating (PEGylated; i.e. coated with polyethylene glycol) liposomes. These technical developments have led to many clinical trials of a variety of anti-fungal, anti-cancer, antibiotic and anti-inflammatory drugs (Lee et al., 2006, Panáček et al., 2009). Lipidic NPs became the first nanomedicine delivery system to be used in clinical application, and they are a new technology platform with considerable clinical application.

1.1.1 Nanotechnology in Australia

In Australia, a strategic plan in the field of nanotechnology was unveiled in the year 2002 (Braach-Maksvytis, 2002). The strategic plan brought together isolated activities into a multidisciplinary infrastructure (Braach-Maksvytis, 2002). Recent activities aimed to bring together a wide range of groups to create a network that links different approaches in nanotechnology (Braach-Maksvytis, 2002). This was an important step in fostering nanotechnology in Australia. As part of this plan, national science bodies such as the Commonwealth and Industrial Research Organisation, the Australian Research Council and the Australian Academy of Science have described nanotechnology as a crucial science investment field (Braach-Maksvytis, 2002). Many Australian universities offer, or are willing to offer in the near future, nanotechnology

undergraduate studies (Braach-Maksvytis, 2002). Flinders University of South Australia is one of the few universities offering undergraduate nanotechnology studies. In 2002, the Department of Nanotechnology at the university entered its third year. The Flinders Centre for NanoScale Science and Technology has been created and the Molecular Technologies Research Cluster will be an important area for nanotechnology research investment.

Nanotechnology in Australia is well supported and approved by governments. According to *Nanotechnology in Australia—Towards a National Initiative (2002)*, the federal government in August 2001 granted financial support for nanotechnology headquartered at the University of Sydney (Braach-Maksvytis, 2002). The Queensland Government and the University of Queensland announced an AU$60 million initiative in the field of biotechnology and nanotechnology (Braach-Maksvytis, 2002).

NanoMac, based at the University of Queensland, is the first nanomaterials research centre in Australia. NanoMac is headed by Prof GQ Max Lu, chair of chemical engineering in the field of nanotechnology (Braach-Maksvytis, 2002). NanoMac aims to promote research and development in the field of nanomaterials in Australia and globally. According to a survey conducted by the Australian Academy of Science (2009) examining collaboration and research trends, nanotechnology is stronger than many fields, but is at an earlier stage of development (Simmons and Barlow, 2009). Collaborations are perhaps equal between Australia and international partners; also collaboration can involve sharing ideas and data, and joint publication.

1.1.2 Nanotechnology Applications

Nanotechnology applications cover communications, electronics, cosmeceuticals, food, energy and agricultural industries, among others (Lee et al., 2008; Simmons and Barlow, 2009) . Currently, nanomaterials are used in environmental remediation, medical devices and pharmaceutical areas, giving scientists a chance to modify matter in various aspects of work and life (Martin, 1994). The production of nanoscale applications on a commercial level has already begun. For example, in 2002, 140 organisations globally were producing nanoscale particles. The first generation application was functioning scientific tools, for example, atomic force microscopes and the development of simple nanoscale compounds and particles for use in cosmetics,

sunscreen, paint and coatings; other uses include stain-resistant clothing and dirt-resistant bathtubs (Colvin, 2003). The second generation is expected to be developed within 5–15 years. The future of second generation applications might be the midpoint between scientific function and scientific fiction. The British Royal Academy of Engineering and the Royal Society suggested that the changes would vary from fundamental nanoscale components and composites to more complex nano-structures (Rogers-Hayden and Pidgeon, 2007). These complex structures are produced using a bottom-up pattern of manufacturing and self-assembly in which molecular synthesis occurs in a manner resulting in molecules and atoms attaching together in distinct models to create complex structures (Rogers-Hayden and Pidgeon, 2007). If the second generation of nanotechnology applications becomes real, mid-term applications would cross over into different sectors (Rogers-Hayden and Pidgeon, 2007).

1.1.3 Nanotechnology Risk Assessment

Nanotechnology application is an important part of enhancing quality of life through the production of light materials, cleaner energy, less expensive clean water and the development of new drugs (Savolainen et al., 2010). The unique properties of engineered nanomaterials (ENMs) and their wide application show great promise for industries using materials at the nanoscale. The uses of ENMs have been the cornerstone of many industrial sectors, such as paper, textiles, energy and cosmetics (Chaudhry et al., 2008). In 2015, products containing ENMs turned over US$1.1–2.5 trillion (Holman et al., 2006). These days, ENMs occur in more than 800 consumer products, including cigarette filters, fabrics, sprays, sunscreen and cleaning products (Savolainen et al., 2010). Although these ENMs might be beneficial for technological applications, they can have genotoxic effects and can lead to inflammation or cancer due to some of their features (Borm et al., 2006; Chaudhry et al., 2008; Donaldson et al., 2005; Schiavo et al., 2016). ENM features such as large surface area (SA), mass ratio size and dose play an important role in their toxicity to some nanoparticles and is a question waiting resolved (Savolainen et al., 2010, Schiavo et al., 2016). ENM dose is connected to the amount of materials engaged in the exposure, which is linked to total mass concentration (Savolainen et al., 2010). However, aerosol exposure to NPs is connected to particle number and SA; this has been the concern in establishing the correct metric for particle toxicity (Hoet et al., 2004; Yang et al., 2009). Several

researchers have concluded that ENM SA is the correct metric for dose definition (Savolainen et al., 2010), which has led to a vast amount of research on ENMs and the correlation between their features and toxic effects, to ensure safe use of NPs (Fubini et al., 2010). The nanotechnology–biology interface has received increased attention to provide a better understanding. Therefore, many organisations and countries have emphasised the safety of nanotechnologies (Kuzma, 2006).

1.1.3.1 Issues related to Engineered Nanomaterial Risk Assessment

The steps used in risk assessments for other types of chemicals are similarly used in the evaluation of ENM risk. The first step is to identify the ENM properties that may have health effects (Jia et al., 2005; Nel et al., 2009). Second, ENM hazard characterisation is defined by the dose responses for targeted organs and cells and the mechanism of toxicity (Chou et al., 2008). In addition, assessment of ENM includes their reactions with constituents at the point of human body entry and their capacity to cross internal barriers such as the blood–placenta, blood–testicular and blood–brain barrier (Cedervall et al., 2007). The third step in the risk assessment of ENM is to estimate the exposure (Savolainen et al., 2010). ENM can be produced from substances in many forms, sizes and surface coatings; hence, these features require validation of analytical methods for their characterisation in bulk samples and measurements in the air in workplaces. ENM concentrations will be higher in occupational environments; therefore, occupational settings hold the most potential for human exposure (Peters et al., 2008). Risk assessments also need to account for the transport process between the source of action and human receptors. The fourth step in risk assessment/hazard identification is hazard characterisation, exposure assessment and risk characterisation, which make up the risk assessment process (Savolainen et al., 2010). Risk assessment combines these four steps to help understand the possibility of a hazard substance posing a health issue in a certain exposure situation.

1.1.4 Silica Nanoparticles

Silica is the common name of silicon dioxide (SiO_2), which can have a crystalline or non-crystalline (amorphous) structure (Street, 2005). In crystalline silica, the silicon and oxygen atoms are bound in a stable geometric pattern, whereas in amorphous silica, the atoms are in an uncoordinated pattern (see Figure 1.1) (Street, 2005). Amorphous silica

occurs naturally or can be obtained under uncontrolled conditions or as manufactured synthetic silica (Street, 2005). Naturally occurring amorphous silica is diatomaceous earth, in which particles are the fossils of marine plants known as diatoms (Merget et al., 2002). Dust from non-calcined diatomaceous earth was found to contain 0.1–4% crystalline silica, while processing leads to contamination with crystalline silica of up to 60% (Street, 2005). Exposure to other naturally occurring biogenic amorphous silica was reported for farmers during agricultural settings (Lawson et al., 1995). The handling of these silica particles could lead to exposure to the crystalline type of silica. Amorphous silica produced under controlled conditions can be classified into three groups (Merget et al., 2002): wet process silica such as precipitated silica and silica gels; pyrogenic silica; and post-treatment silica, for example, chemically or physically treated silica. Fused silica is a phase of heated silica, when it becomes liquid and cools down without becoming crystallised.

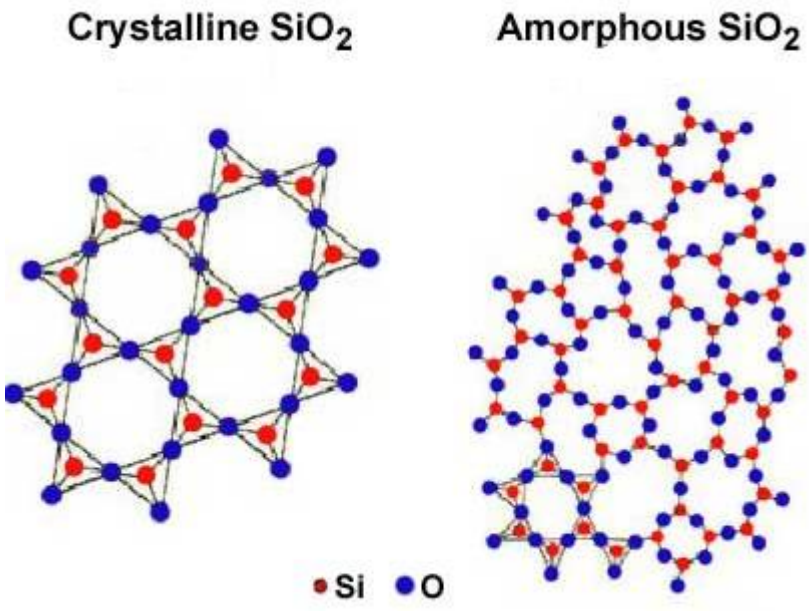

Figure 1.1: Schematic representation of crystalline and non-crystalline silica (Balaguru and Jeyaprakash, 2012).

1.1.4.1 Crystalline and Non-crystalline Silica Particles

Crystalline types of silica are found in nature and can be synthesised in forms that clearly have no natural counterpart (Grose and Flanigen, 1977). The most common type of crystalline silica is quartz; two less common forms are cristobalite and tridymite, each of which has polymorphic forms that are stable at different temperatures (Marinelli

et al., 2001; Shinohara and Kohyama, 2004). At normal temperatures, the stable form is alpha-quartz, which is reversed at 573°C to beta-quartz. Beta-quartz is stable up to 867°C (Flanigen and Patton, 1978). Tridymite can be stable from this temperature up to 1470°C. Beyond this temperature, cristobalite is stable and stays that way to around 1713°C (Flanigen and Patton, 1978). Quartz is a solid component of most natural mineral dust (Flanigen and Patton, 1978). Human exposure to quartz occurs most often during occupational activities that demand movement of earth or handling of silica-containing products, or during manufacturing of silica-containing products (Flanigen and Patton, 1978). Environmental exposure to surroundings with quartz dust can occur during industrial and agriculture activities (Howard, 1991). Respirable quartz dust particles deposit in the lungs if inhaled and little is known of their clearance kinetics in humans (Borm et al., 2004, Morrow et al., 1967). There are a shortage of data on quartz dust load in human lungs (Crosera et al., 2009). In addition, it has been noticed that deposition and clearance of quartz in animals is dependent on species (Dagle et al., 1986). Exposure to quartz particles in rats has been shown to lead to the formation of discrete silicotic nodules (Corrin and King, 1969). Moreover, inhalation of aerosolised quartz particles reduced alveolar macrophage clearance function and caused progressive lesions and oxidative stress in rats after intratracheal instillation or inhalation of quartz (Warheit et al., 2007).

1.1.4.2 Toxicity of Non-crystalline Amorphous Silica

Amorphous silica NPs are currently used in industrial and biomedical applications such as cosmetics, food additives and drug delivery systems (Merget et al., 2002). However, there is no conclusive information about their cytotoxicity, genotoxicity or carcinogenicity potential (Uboldi et al., 2012). Occupational exposure to crystalline silica dust is connected with an increase in pulmonary diseases including silicosis, chronic bronchitis, tuberculosis and chronic obstructive pulmonary disease (COPD). Not many studies have estimated the effect of synthetic amorphous silica in relation to airway or lung diseases (Merget et al., 2002). Workplace concentrations have been assessed in some studies. The European Chemical Industrial Council reported that the average total dust concentration in a workplace ranged from <1 to ~10 mg/m^3 (Kauppinen et al., 2000). The known health effects of amorphous silica on humans are discussed in the following section.

1.1.4.3 Health Hazards of Amorphous Silica

1.1.4.3.1 Pneumoconiosis

Silicosis and coal workers pneumoconiosis (CWP) are serious cases of occupational lung disease (Castranova and Vallyathan, 2000). CWP and silicosis continue to occur frequently despite strong precautions to control environmental dust. Even though the mechanisms of silicosis and CWP initiation and progression are understood, this has not prevented these occupational diseases. The knowledge obtained from research has been highly valuable in determining the cause and progression, which had led to the recommendation and implementation of exposure limits (Castranova and Vallyathan, 2000). Many studies have reported a large number of cases of pneumoconiosis in workers in the diatomite industry. However, some studies did not clearly state if the cause was from crystalline or amorphous silica (Pandurangi et al., 1990). Other studies have suggested that contamination of crystalline silica is causative of pneumoconiosis in diatomite workers after finding that exposure to natural diatomite was connected with simple fibrosis; while exposure to calcined diatomite was associated with progressive pulmonary fibrosis (Føreland et al., 2008; Smart and Anderson, 1952). In epidemiological studies, no silicosis was observed in workers exposed to long-term manufactured silica; however, in another study, silicosis was found in 4–28 cases caused by amorphous silica not contaminated with quartz (Merget et al., 2002).

1.1.4.3.2 Bronchiolitis Obliterans

In one case study, a non-smoking animal feed worker was found to suffer from irreversible airflow obstruction after two years of occupational exposure to proteolytic enzymes, microorganisms and both amorphous and synthetic silicates (Spain et al., 1995). Despite being removed from the work place and undergoing treatment, the worker's pulmonary dysfunction did not improve. A lung biopsy showed peribronchial inflammation and neolumen formation consistent with bronchiolitis obliterans (Spain et al., 1995). Energy dispersive analysis of biopsy specimens and bronchoalveolar lavage fluid uncovered the presence of silica particles. The finding may link potential silica exposure with the pathological discovery. This case study suggests bronchiolitis obliterans can occur as a result of occupational exposure in the animal industry.

Therefore, this case should be considered in the evaluation of symptomatic patients with possible exposure to amorphous silica (Spain et al., 1995).

1.1.4.3.3 Carcinoma

Confirming a clear relationship between exposure to silica in the workplace and cancer is often difficult (Parent et al., 2000). Cancer's slow development can make it complicated to identify a particular cause–effect relationship (Brown, 2009). Moreover, variable job histories, exposure to other carcinogenic compounds and other factors such as genetic sensitivity and poor nutrition influence detection of silica carcinogenicity in the workplace (Colditz et al., 2006). Detailed records on workers is crucial for finding and preventing exposure to carcinogens (Brown, 2009). Thus, the only precaution that can be taken is limiting or removing exposure to probable and known carcinogens. Two studies of cohort mortality caused by the diatomaceous earth industry and a refractory brick factory revealed an increased risk of bronchial carcinoma among workers (Merget et al., 2002). Neither study examined the cause of mortality; that is, whether it was amorphous or crystalline silica. However, an independent effect of amorphous silica cannot be concluded. Further research is necessary to understand the complex pattern of influence leading to lung cancer among silica-exposed workers and to know whether and how to limit exposure to other workplace lung carcinogens. The overall respirable dust, surface size and age of silica particles affects the carcinogenic potential of silica (Brown, 2009). In addition, the apparent paradox of a lower lung cancer risk in some workplaces that have high-level silica exposure needs further investigation (Brown, 2009).

1.1.5 Polyhedral Oligomeric Silsesquioxane (POSS)

Molecular nanocomposites are attracting strong interest in the materials community (Waddon and Coughlin, 2003). Molecular nanocomposites hold the potential to improve the engineering properties of conventional materials and create new properties. Many types of systems and approaches to fabrication have been implemented (Waddon and Coughlin, 2003). One of the most exciting class of nanocomposites is the polyhedral oligomeric silsesquioxanes (POSS) (Schwab and Lichtenhan, 1998), first discovered in 1946 by Scott (as cited in Li et al., 2001) figures 1.2 &1.3. Studies on POSS molecules focussing on synthesis, structure and properties were noted from the 1940s (Phillips et

al., 2004). Two landmark 1946 publications were those by Scott on condensed POSS cages and by Scott, Brown and Vogt on uncondensed POSS 'triol' characterisation (as cited in Phillips et al., 2004). After 1990, the field developed rapidly in the hands of two research groups: the Feher group at the University of California and the Lichtenhan group at the Airforce Research Laboratory, in the United States. The Feher group advanced the methods for synthesising and modifying a structurally well-defined Si/O framework while the Lichtenhan group led the use of discrete POSS in polymer-related applications (Mark, 2007). A recent composite review categorised POSS structure as having sphere-like or dimensionality structure (Phillips et al., 2004). This is a useful initial assignment of the possibility to create higher-dimensionality structures by crystallisation or aggregation of POSS macromers into the polymer matrix, and led to the building of the 1–3-dimensional stage (Phillips et al., 2004).

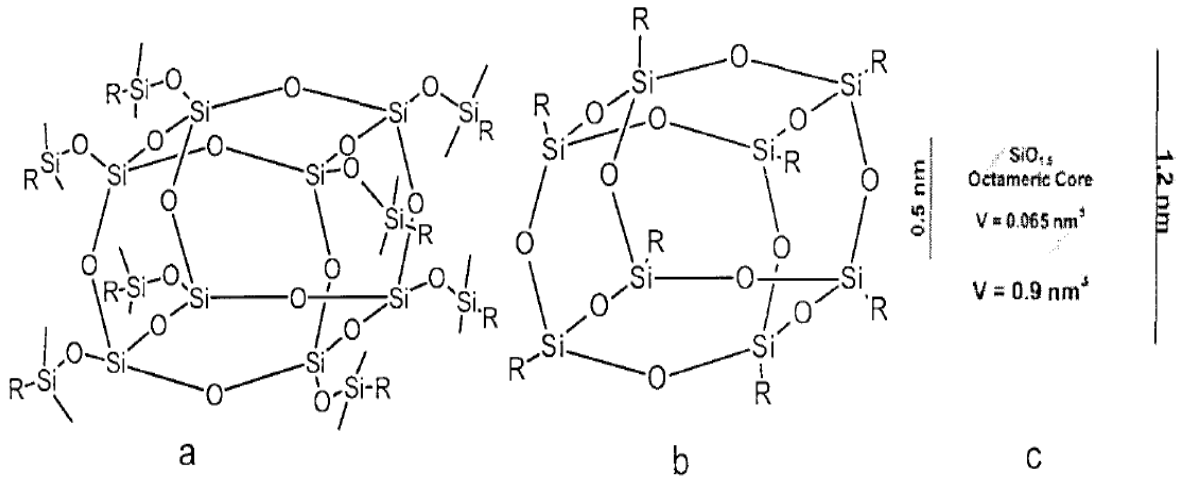

Figure 1.2: Silsesquioxanes: (a) Q8 (Q = SiO2/2) and R can be H, epoxy, vinyl or methacrylate; (b) R8T8—T8 is T = R-SiO3/2 and R is alkene, alkyl oracetylene; (c) typical sizes/volumes (Wallace et al., 1999).

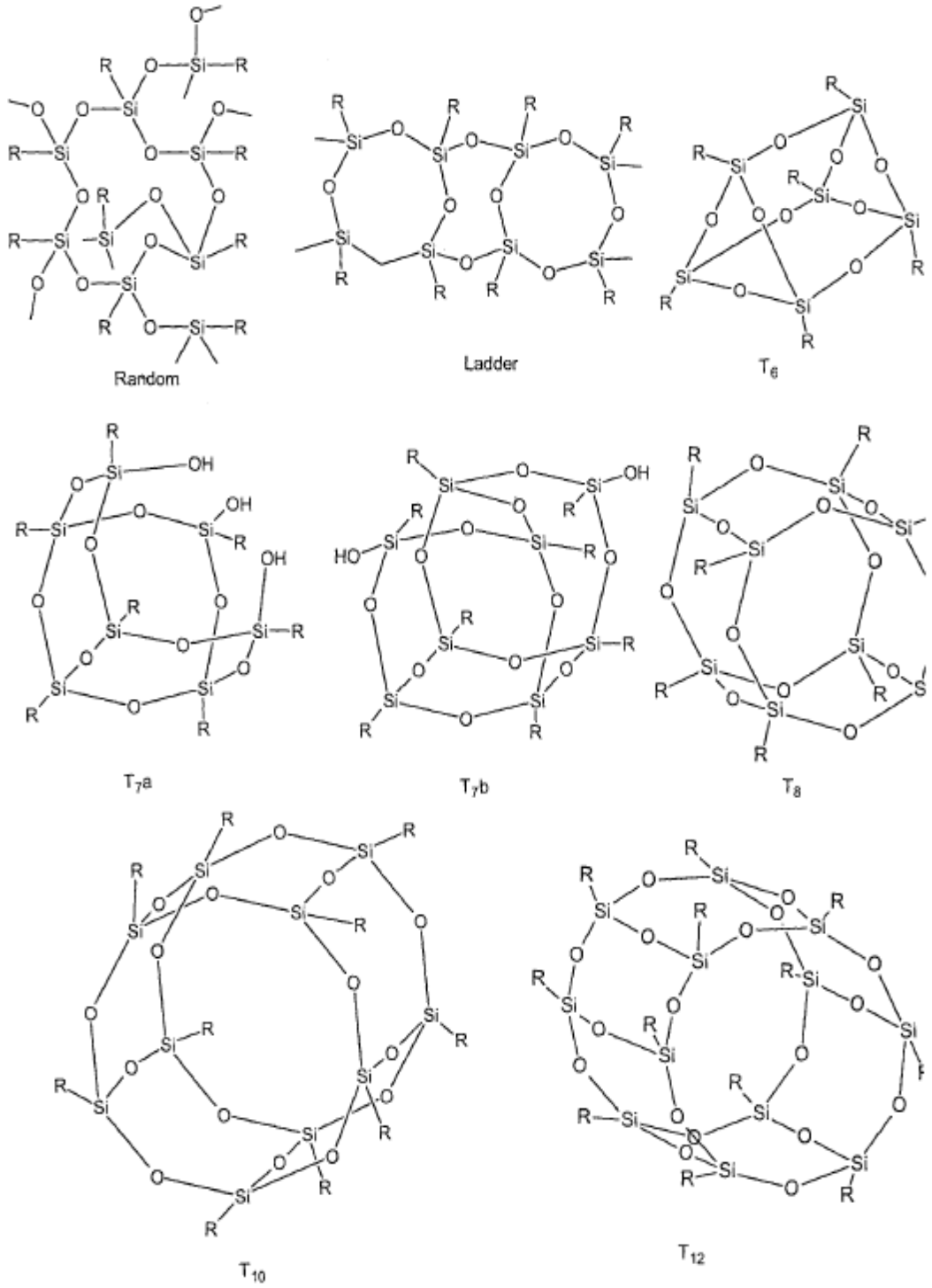

Figure 1.3: Chemical structures of various types of silsesquioxanes (Gnanasekaran et al., 2009).

1.1.5.1 Basic Structure of POSS

POSS molecules have a cage-like structure measuring 1–3 nm with a hybrid chemical composition ($RSiO_{1.5}$) (H_2O) (Zhao and Schiraldi, 2005). This chemical composition

lies between silicones (R2SiO) and silica (SiO_2), and is well defined spatially where R is an organic group such as ethyl, phenyl, cyclopentyl, cyclohexyl, isooctyl or a hydrogen atom; and *a* and *b* are integers, with $a + b = 2n$ where *n* is an integer and $b = a + 2$ (see Figure 1.2). The structure of silsesquioxanes could be cage, random or ladder. The cage structure could contain eight atoms positioned at cube vertices. Cubic structure compounds are mostly shown as T6, T7, T8 and T12. This depends on how many silicon atoms are in the cubic structure (Figure 1.3) (Wallace et al., 1999). This well-defined structure has a stable inorganic Si-O core covered by substituents that provide a wide range of polarities and reactivate if the structure modified (Zhao and Schiraldi, 2005). POSS molecules can be combined into a polymer system by grafting, blending or copolymerisation (Zhao and Schiraldi, 2005).

1.1.5.2 Synthesis of POSS

The framework for synthesising a fully condensed POSS starts with the hydrolysis and condition of a trifunctional organosilicon monomer such as organotrichlorosilane as represented in Figures 1.4 and 1.5 (Feher et al., 1999). Isolated POSS precursors from the hydrolysis mixture can be used in polymerisation reactions directly; however, extra functionalisation is often needed. Limiting the number of functional groups to one or two is necessary to incorporate POSS reagents into a linear polymer system, which helps avoid cross-link networks (Schwab and Lichtenhan, 1998). In Figures 1.4 and 1.5, functionalisation of the POSS framework can be easily achieved by corner capping the POSS-trisilanols with silane coupling agents suitable for polymerisation or grafting reactions. There are a few reactions that could lead to the formation of POSS and its derivatives (Li et al., 2001). These can be classified into two major stages depending on the nature of the beginning materials employed. The first stage is reactions that gave rise to new Si-O-Si bonds with consecutive formation of a polyhedral cage framework. These reactions are complex and there are multistep processes leading to oligomers and polymers that include oligosilsesquioxanes and their derivatives (Li et al., 2001). The second stage involves shuffling the substituents at the silicon atom without changing the silicon oxygen skeleton of the molecules (Li et al., 2001).

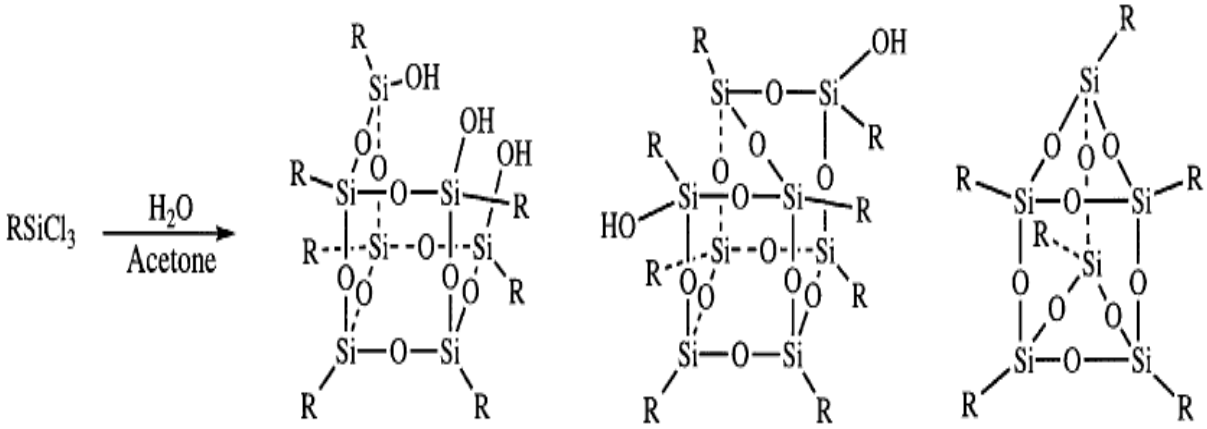

Figure 1.4: The POSS product obtained from the hydrolysis of cyclohexyltrichlorosilane (R = c-C6H11) (Feher et al., 1999).

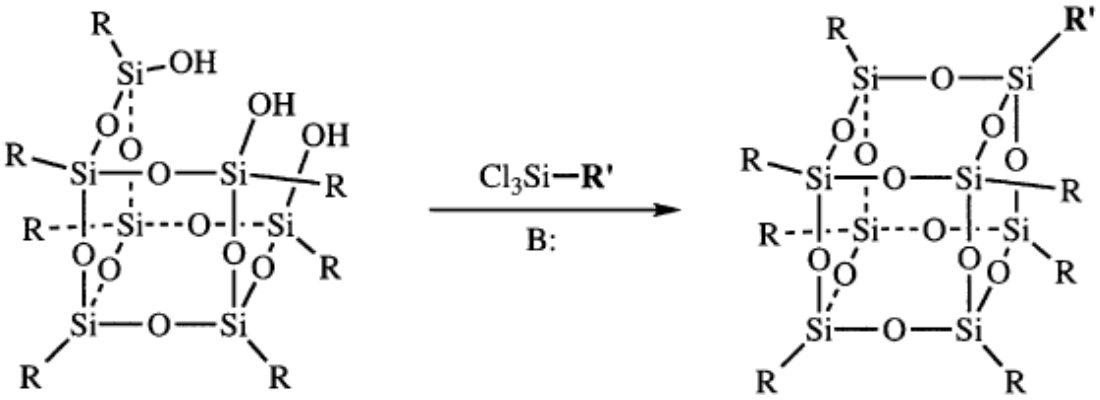

Figure 1.5: Synthesis of polymerisable POSS reagents. R is for non-reactive functionality; R' for polymerisable or grafting functionality (Schwab and Lichtenhan, 1998).

1.1.5.3 Properties of POSS

A recent study has shown that the thermal stability and mechanical properties of polymer materials such as polycarbonate, polymethyl methacrylate, phenolic resin and cyanate ester have been improved by the incorporation of POSS (Du et al., 2010). Benzoxazine and incomplete trisilanol POSS were prepared and, after curing, the corresponding composites were gained. Dynamic mechanical analysis , differential scanning calorimetry and x-ray diffraction were used to characterise curing behaviour, structures and thermal properties. It was found that chemical bonds were created

between trisilanol phenyl POSS and polybenzoxazines , and that trisilanol phenyl POSS had a better affinity with the matrix than did trisilanol isobutyl POSS. The composite's thermal stability and dynamic viscoelasticity have been perfected by the incorporation of trisilanol phenyl POSS (Du et al., 2010). It is becoming clear that incorporation of POSS into linear polymers or network resins could provide nanocomposites with good thermal and mechanical properties (Li et al., 2001). Many nanocomposites have been developed following increases in the synthesis of a variety of POSS-containing monomers with functionalised substituents (Li et al., 2001). In this way, this technique can be used to change the matrix of composites such as carbon filters (Li et al., 2001).

1.1.5.4 Application of POSS

POSS nanostructures have potential value in many biomedical applications such as dental composites, drug delivery, biomedical devices, biosensors and tissue engineering (Ghanbari et al., 2011). Cyto-compatibility and nontoxicity are features that make POSS suitable for biomedical applications (Crowley et al., 2016). One of the most valuable applications of POSS was in the development of cardiovascular implants where incorporation of POSS with biocompatible polymers led to the development of nanocomposite materials that enhanced anti-thrombogenicity and haemocompatibility, and reduced inflammatory response and calcification resistance (Ghanbari et al., 2011). Currently, POSS-containing polymers are under intensive investigation to develop a new generation of cardiovascular implants such as bypass grafts, heart valve prostheses and coronary stents (Ghanbari et al., 2011; Naghavi et al., 2013).

1.1.5.5 Classification of POSS

Due to their chemical structure, a variety of POSS-containing polymers and copolymers can be synthesised. Several groups known as 'R' can bind to the corner Si atoms. Those used in the current study on trisilanol POSS have an Si atom removed from the corner and an H atom bound to each surrounding-edge O atom. The R groups can be ethyl, phenyl, cyclopentyl, cyclohexyl or isooctyl groups. Figure 1.6 represents functionalities prepared from POSS-trisilanol precursors. The change in R groups would modify the composition, chain mobility and local structure (Marchesi et al., 2014; Mark, 2007).

These modifications would affect the dimensional, thermal and oxidative stability that leads to composites with improvements properties.

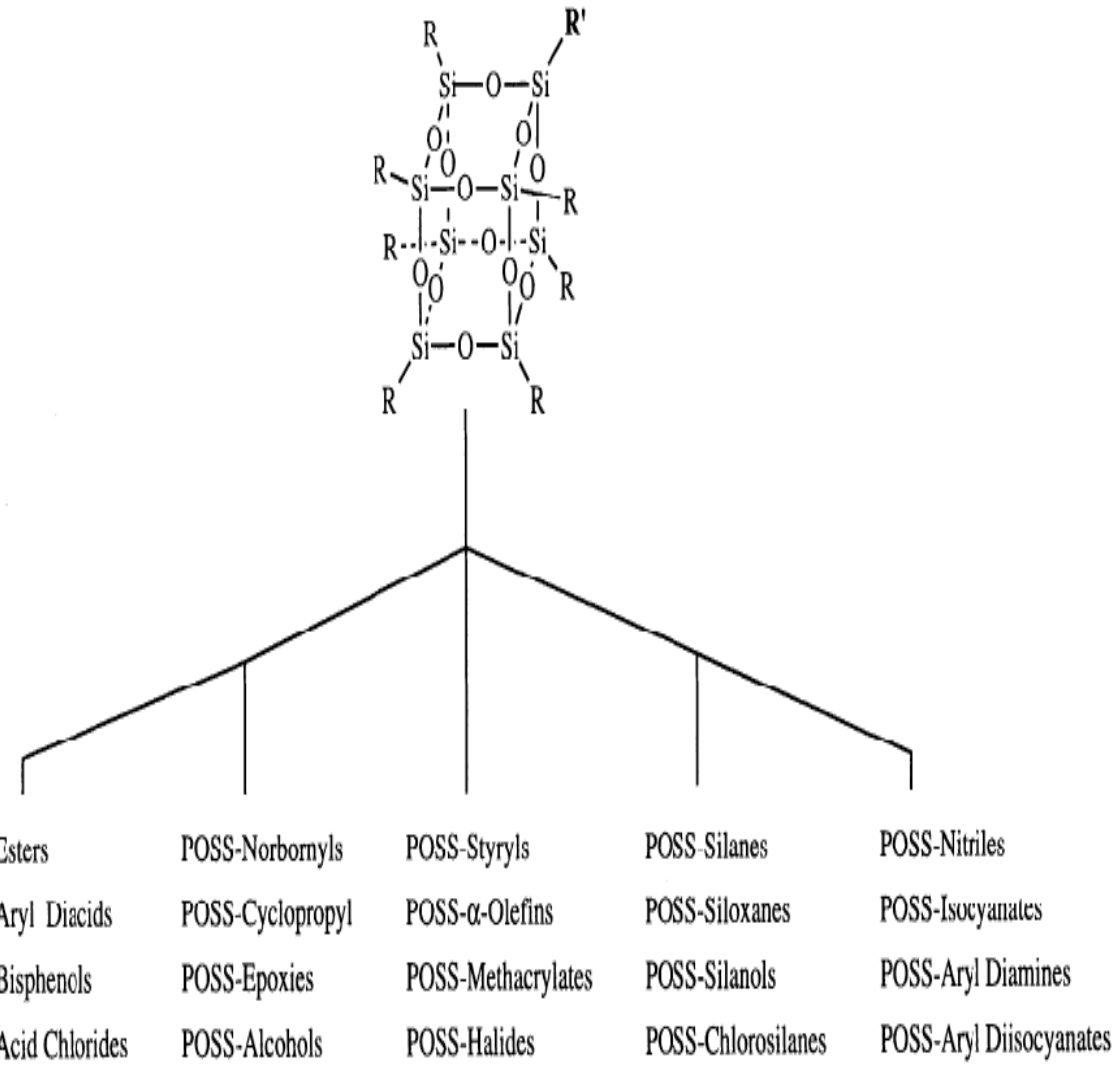

Figure 1.6: Functionalities resulting from POSS-trisilanol precursors (Marchesi et al., 2014).

1.1.5.6 Toxicity of POSS

In the literature, POSS nanocomposites have shown little or no toxicity to human cell lines. A recent review highlighted the physical properties of POSS polymer-based materials and their bio-stability and low toxicity. Bio-stability is one of the crucial considerations in the selection of polymer-based composites for medical applications (Wu and Mather, 2009). In a previous study related to the current research, the toxicity of five concentrations (0.001–100mg/mL) of POSS particles to the human keratinocyte

cell line (HaCaT) was investigated. Trisilanol isooctyl POSS particles significantly reduced the metabolic activity and relative cell number in HaCaT cell cultures after a 24-h exposure. Trisilanol phenyl, cyclopentyl and cyclohexal POSS particles did not show any sign of toxicity; therefore, toxicity may be attributed to the shape of the particle. Trisilanol phenyl, cyclopentyl and cyclohexal POSS particles show promising application in anti-cancer drug delivery (Almutary and Sanderson, 2016).

1.1.5.7 Guidelines for Using POSS Safely

Most studies are not concerned with investigating the cytotoxicity of POSS and their occupational safety, or even that of other NPs. A recent study described the effect of amine-functionalised POSS on COS-1 cells as being very low and amount of the particles founded in the cytoplasm (McCusker et al., 2005). Over the past 15 years, insufficient data were available on the health and environmental impacts of nanostructured materials, but this has been growing slowly (Maynard et al., 2006). ENMs depositing in the respiratory tract could lead to inflammation and transmission to other cells, and transport to sensitive target sites in the body (Michelson and Rejeski, 2006). Unfortunately, the rates of translocation of these nanomaterials are uncertain (Michelson and Rejeski, 2006; Mills et al., 2006).

1.1.6 Quantum Dots (QDs)

Cadmium is used in the construction of particles commonly called quantum dots (QDs) (Rzigalinski and Strobl, 2009). QDs are defined as semiconductor metalloid–crystal structures comprising 200–10,000 atoms and measuring 2–100 nm (Hardman, 2006; Juzenas et al., 2008; Rzigalinski and Strobl, 2009). QDs are characterised by bright and stable fluorescence caused by their unique opto-electronic properties arising out of their small size (Hardman, 2006; Juzenas et al., 2008; Rzigalinski and Strobl, 2009). Because of their petite size, QDs have a large SA, making it possible to functionalise them through targeting sites used in site-directed activity (Jaiswal et al., 2003). QDs have revolutionised biological imaging at the cellular level, targeted drug delivery and cancer detection. However, interest in expanding research on QDs in the field of medicine was not sustained because of the requirement for a substantial amount of cadmium in a highly reactive form, and associated health risks (Jaiswal et al., 2003).

Despite the uncertainty regarding risks of cadmium exposure, QDs were more useful than organic fluorophores for understanding biological interactions. QDs are inorganic fluorophores that could be used as an alternative to organic fluorophores (Jaiswal et al., 2003). Between ultraviolet (UV) and red light wavelengths, QDs can be excited because of their wide excitation spectra, unlike the restricted excitation of organic fluorophores (Jaiswal et al., 2003; Mazumder and Sun, 2009). Changes in the composition and size of QDs can widen excitation spectra and at the same time produce narrow emission spectra (Jaiswal et al., 2003). This feature allows the simultaneous detection of different-coloured QDs; thus facilitating the detection of several cells *in vivo* and multiple molecules at the same time *in vitro* (Coto-García et al., 2011; Jaiswal et al., 2003). More details are provided in Figure 1.7. Due to their properties, QDs are effective not only for imagining QD-tagged proteins over a longer period but also for imaging the growth and development of organisms for periods of weeks to months (Jaiswal et al., 2003).

1.1.6.1 Basic Structure of QDs

Structurally, QDs are composed of a metalloid crystalline core and a shell or a cap that protects the core and renders the QD bioavailable (see Figure 1.8) (Hardman, 2006). QD cores are made of a variety of metal complexes such as noble metals, semiconductors and magnetic transition metals (Dabbousi et al., 1995; Esparza et al., 2015; Smith et al., 2008). For example, semiconductor III–V series QDs consist of indium phosphate (InP), gallium arsenate (GaA), indium arsenate (InA), metalloid cores, and group II–IV series QDs are composed of zinc–selenium (ZnSe), zinc sulphide (ZnS), cadmium–tellurium (CdTe) and cadmium–selenium (CdSe) cores (Dabbousi et al., 1995).

Due to the large SA of CdTe and CdSe QDs, many atoms are shown at the surface (Rzigalinski and Strobl, 2009). These atoms have molecular orbitals with a full complement of electrons for stability. Therefore, another semiconductor with a broader bandgap, such as ZnS, is added over the CdSe core (Biju et al., 2008). Adding ZnS enhances fluorescence efficacy, and could reduce the toxicity resulting from the highly reactive core (Rzigalinski and Strobl, 2009). Growing a ZnS shell layer on the surface of the CdSe core is known to enhance photoluminescence efficiency (Smith et al., 2008). Hardman (2006) has shown that a QD core–shell could be added to a QD to obtain the desired bioactivity. A QD that is newly synthesised is inherently

hydrophobic; however, adding a hydrophobic cap to the metalloid core could render them biologically less active and improve their solubility.

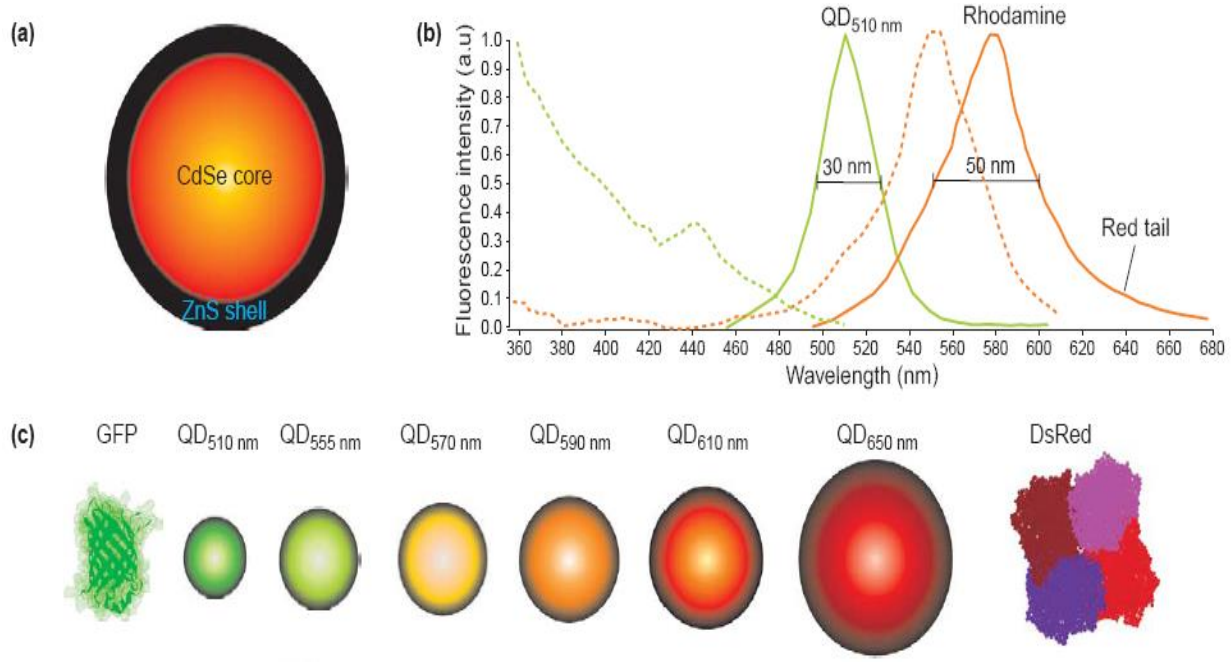

Figure 1.7: (a) A simple structure of quantum dots (QDs) comprising cadmium–selenide (CdSe) as the core and many layers of zinc sulphide (ZnS) as a thick shell to implement quantum yield and photostability; (b) Broken green lines indicate a broad QD excitation spectrum, whereas broken orange lines indicate a narrow organic dye excitation spectrum. The unbroken green line indicates a narrow QD emission spectrum, whereas the unbroken orange line indicates a broad QD emission spectrum for organic dye; (c) Red Fluorescent Protein DFP and (DsRed) are commonly used fluorescent proteins and the emission of QDs can be controlled by the size of the CdSe core and the ZnS shell (Jaiswal et al., 2003).

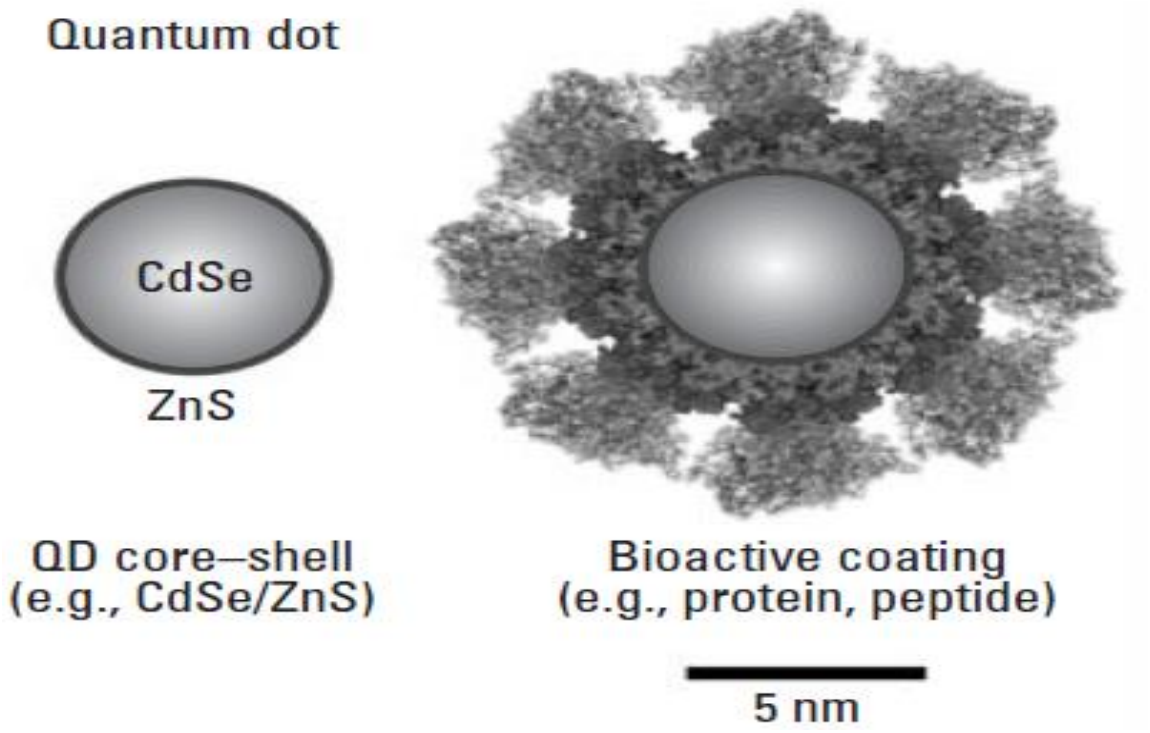

Figure 1.8: Quantum dots (QDs) composed of metalloid core and a shell or a cap such as cadmium–selenium (CdSe) or zinc sulphide (ZnS), which can render the QD bioavailable (Hardman, 2006).

1.1.6.2 Synthesis of QDs

In 1982, Efros and Ekimov described the synthesis of QDs (Efros et al., 2013). Top-down techniques such as lithography were widely used to prepare QDs. This technique made QDs that were unsuitable for advanced applications because of their poor optical properties, reduced productivity, crystal defects and size variations (Wang et al., 2014). A bottom-up technique was investigated for QD properties and applications by several researchers (Wang et al., 2014). CdSe QDs could be synthesised via pyrolysis of trioctyl phosphine/trioctyl phosphine oxide (TOP/TOPO) and a mixture of organometallic precursors such as dimethyl cadmium (CdM2) (Pradeep et al., 2017). This provided a hydrophobically capped CdSe, cadmium sulfide (CdS) and CdTe QDs. CdM2 was heated to 230–300°C with added TOP–selenide. TOPO was heated to 300°C for 20 min under vacuum followed by injection of the CdM2 mixture and selenide precursor (Biju et al., 2008). CdSe nanocrystal growth was carried out at 230–260°C (Coolen et al., 2009). The result was a sample of QDs with size distribution of 1.2–11.5 nm that could be separated using size-selective purification (Coolen et al., 2009). Due to CdM2's

toxicity, pyrophoric nature and volatility, researchers replaced CdM2 with a non-volatile cadmium precursor such as $CdCIO_4$, and used thioglycerol as a capping agent (Coolen et al., 2009).

A recent study has shown that most synthesised QDs are in a nonpolar organic solvent and solubilised in aqueous buffer as their hydrophobic surface had to be transformed to an amphiphilic one (Michalet et al., 2005). A variety of solubilisation methods has been discussed, including ligand exchange with simple thiol-containing molecules or much more accurate ones such as oligomeric phosphines and peptides. Another method was the encapsulation by a layer of triblock copolymers, or a philic diblock. In addition, a combination of different layers of molecules gave the required colloidal stability to QDs (Michalet et al., 2005). The purpose of functionalising QDs was to meet four key requirements (Mazumder and Sun, 2009): increasing stability in water; presence of functional groups for bioconjugation; lack of interference with the native properties of NPs; and non-immunogenicity and biocompatibility in living systems (Michalet et al., 2005).

1.1.6.3 Application of QDs

The use of QDs is increasing rapidly to include emerging technologies. The unique optical and electronic properties of QDs are a key feature to increase the use of QDs (Bruchez et al., 1998). Currently, QDs are applied in electronics and biomedical engineering; the most useful properties of QDs are their fluorescence spectrum, which make QDs the optimal fluorophores in the field of medical imaging (Li and Zhu, 2013; Michalet et al., 2005). For example, fluorescence QDs conjugated with antibodies could be targeted towards cellular structures or specific biological events (Chinen et al., 2015). Conjugated QDs could also be used in labelling of microorganisms, detection of biofilms, drug delivery, treatment of AIDS, labelling of breast cancer and tumour targeting and imaging (Sun et al., 2014).

1.1.6.4 Toxicity of QDs

The literature on the cytotoxic effect of QDs on cells *in vitro* and *in vivo* demonstrates mixed results. Michalet et al. (2005) reported that potential interference and cytotoxicity of QDs are related to the synthesis, solubilisation and functionalisation procedures. Rzigalinski and Strobl (2009) found that QD toxicity was related to multiple parameters

such as size, concentration, shape, activity surface coating, redox, charge and mechanical stability. Smith et al. (2008) mentioned that QDs were composed of toxic atoms (e.g. Cd, Hg, Pb) and the effects of these on the QDs were not clear. QDs were found to aggregate, bind nonspecifically to cellular membranes and induce the creation of reactive oxygen species (ROS) (Smith et al., 2008). However, other reports discussing cell viability function and morphology did not find adverse effects (Michalet et al., 2005). The following sections summarise the reports from *in vivo* and *in vitro* studies.

1.1.6.5 In Vitro Studies

Mazumder et al. (2009) found that CdSe QDs were strongly toxic to cultured cells in the presence of UV illumination for a prolonged period. A process called photolysis occurs when UV irradiation acts on chemical bonds leading to the dissolution of the particle. Thus, toxic cadmium could be released, causing immense harm to cells (Kirchner et al., 2005). Coating QDs with nontoxic organic compounds such as PEG or inorganic layers such as ZnS and silica could prevent toxicity. Nonetheless, QDs could access cells by endocytosis, and cell death is attributed to uptake quantity (Bernevig et al., 2006; Zhang et al., 2006). Another study of QD toxicity showed that CdSe-core QDs were acutely toxic under known conditions such as synthesis parameters, exposure to UV light and surface coating (Derfus et al., 2004). Jaiswal et al. (2003) reported that HeLa cells labelled with QDs for more than one week showed no observable effect on growth. A recent study observed no cytotoxicity or phototoxicity to prostate carcinoma Du145 cells exposed to CdSe/ZnS (0–100nM). However, cell growth decreased at the highest doses (200–400nM), which was attributed to the borate buffer used to suspend the QDs (Generalov et al., 2010).

1.1.6.6 In Vivo Studies

In experiments conducted on rats, 25% of the cadmium aggregated within the liver (Derfus et al., 2004). Even a low dose of cadmium ions *in vitro* (100–400µM) was shown to decrease the variability of hepatocytes. Metallothionein was a critical mitochondrial protein affected by the binding of cadmium to sulfhydryl groups, leading to mitochondrial stress and dysfunction (Derfus et al., 2004). The small amount of this protein was not sufficient when exposed to a high level of Cd^{2+}. Hepatocytes isolated

from rats grown *in vitro* showed typical metallothionein levels similar to those *in vivo*, suggesting that isolated cells were a representative model for *in vivo* hepatotoxicity (Liu et al., 1990). *Xenopus* embryos with 2×10^9 CdSe/ZnS QDs/cell and comparable control embryos showed similar growth patterns, suggesting there was no cytotoxic effect (Dubertret et al., 2002). However, at 5×10^9 QDs/cell, noticeable abnormalities were observed to influence the osmotic equilibrium of the cell (Dubertret et al., 2002).

The distribution of three different CdSe/ZnS QDs peptides (F3, GFE, LyP-1) coated on tissues of normal BalbC mice for 5–20 minutes showed accumulation of the three types in liver and spleen additional to the targeted tissue (lung) (Åkerman et al., 2002). The nonspecific aggregation decreased after adding PEG to the QD surface. Acute toxicity was not observed after 24 h of exposure. Another study reported that there were no adverse effects from injecting CdSe QDs into mice (Larson et al., 2003). However, Larson and his group did not give an exact time line; they only outlined the absence of toxicity when maintained for 'a long time'.

1.1.6.7 Guidelines for Using QDs Safely

In relation to investigation of the cytotoxic effect of QDs *in vitro* and *in vivo*, a shortage of work on Q safety and the potential hazards from inhaling or exposure was noted in the literature review. The cytotoxic effects of QDs and their long-term stability both *in vivo* and under environmental conditions remains unclear (Argyle and Robinson, 2006). The current study investigated the interference of cadmium sulphide (CdS) QDs using a protocol of two classical assays to identify any potential confounding effects.

1.1.7 Gold Nanoparticles

Gold NPs (AuNPs) have a long history in chemistry back to ancient Roman times when they were used to decorate glass (Kang et al., 2010). The new era of AuNP synthesis began nearly 150 years ago by Michael Faraday, who identified that colloidal gold has properties different from bulk gold (Faraday, 1857). Synthesis methods for spherical and non-spherical AuNPs have been developed over the last half-century (Kang et al., 2010). The AuNPs produced have unique properties such as their shape-dependent optical, size and electronic features. In addition, they have a high SA that can be readily modified with ligands having functional groups such as phosphines, thiols and amines, which display affinity for gold surfaces. When these functional groups are connected

with ligands such as proteins and antibodies, this increases functionality (Kang et al., 2010). The understanding of gold nanoconjugates has led to a wide range of investigations, including crystallisation of materials, programmed assembly, bioelectronics and detection methods. The literature on gold nanoconjugates in biodetection and biodiagnostics is vast. In recent years, the unique properties of gold and the use of conjugates have revealed exciting findings in medicine and biology. These findings have shown the potential for gold nanoconjugates enter living cells if functionalised with suitable surface moieties; thus, this could be a promising therapeutic agent in cellular biology (Kang et al., 2010).

1.1.7.1 Synthesis and Assembly

There are many traditional methods of synthesis of AuNPs by reduction of gold derivatives (Daniel and Astruc, 2004). The most popular one is using citrate reduction of $HAuCl_4$ in water (Ji et al., 2007). This conventional method was described by Turkevich in 1951 when he synthesised AuNPs at the size of 20 nm (Turkevich et al., 1951). In 1973, Frens reported AuNPs pre-chosen in size between 16 and 147 nm by varying the ratio between the reducing and stabilising agents' trisodium citrate to gold ratio (Frens, 1973). The method gained much attention and it is still used even now, especially when a loose shell of ligands is needed around the gold core. In recent research, sodium 3-mercaptopropionate was found to stabilise AuNPs by the simultaneous addition of citrate and an amphiphile surfactant (Yonezawa and Kunitake, 1999). By adopting this method, the size of AuNPs can be controlled by varying the stabiliser to gold ratio. In 1997, Mulvaney and colleagues stabilised AuNPs with alkanethiols (Mulvaney et al., 1997). This showed that thiols of different chain can be used in synthesis. In 1994, the establishment of the Brust–Schiffrin method for AuNP synthesis had an effect on the field of nanotechnology because it reduced dispersion and controlled the size of thermally stable and air-stable AuNPs (1.5–5.2 nm) (Brust et al., 1994; Liz-Marzán, 2013). These AuNPs can be frequently isolated and re-dissolved without aggregation and decomposition (Daniel and Astruc, 2004). Moreover, they can be handled and functionalised easily as molecular and stable organic compounds (Daniel and Astruc, 2004). Different sulphur-containing ligands such as di- and tri-thiols, xanthates and disulphides, and resorcinarene tetra-thiols can be used to stabilise AuNPs (Reznickova et al., 2015). Disulphide is not as efficient a stabilising agent as are

thiols but is useful for catalysis (Fernández-Rodríguez et al., 2006). Similarly, thioethers do not bind to AuNPs as strongly as do polythioether, as established by Rheinhout's group (Daniel and Astruc, 2004).

1.1.7.2 Gold Nanoparticles in Drug Delivery

It is well known that active targeting by modifying NPs with ligands has the ability to enhance the therapeutic activity and produce fewer side effects than conventional therapeutics (Cho et al., 2008). The ability to target specific cells rather than tissues means that ligand conjugate nanocarriers will outperform the first generation of non-targeted nanosystems (Das et al., 2009; Weissleder et al., 2005). Although targeting delivery systems relies on factors such as delivery vehicles, drugs and diseases, many important benefits have been reported (De Jong and Borm, 2008). In cancer therapy, targeting ligands demonstrated greatly enhanced retention and cellular uptake of NPs by receptor-mediated endocytosis (Chen et al., 2010; Qian et al., 2002). Identification of NP accumulation in tumours is dependent on their physiochemical properties, which can lead to a higher intracellular drug concentration that helps in increasing therapeutic activity (Petros and DeSimone, 2010). Targeting of endothelial tissue in cardiovascular disease by NP locating is achieved by ligand receptor interaction rather than enhanced permeability and retention (EPR) (Shi et al., 2007). In a similar way, ligand-mediated targeting is an important benefit of nano-drug transcytosis beyond epithelial and endothelial barriers (Georgieva et al., 2014). In such cases, targeted delivery is applied to combat multidrug resistance (MDR) or to longer circulate targeted NPs to locate and fight migrating cancer cells (Patil et al., 2009). Although three targeted NP systems are still in Phase I/II of clinical trials, the way of clinically translating these systems is not as smooth as predicted (Shi et al., 2010). One main obstacle is the complexity of manufacturing viable targeted NPs; also, production usually requires time-consuming steps such as biomaterial assembly, ligand infusion and purification, which demand quality assurance (Shi et al., 2010). The single-step synthesis of targeted NPs by pre-functionalised self-assembling provides an easy strategy for changing size and scale (Shi et al., 2010). Aside from NPs, targeting ligands is another important consideration in drug delivery, as are variables such as ligand biocompatibility, binding affinity, cell specify, mass production and purity (Shi et al., 2010). AuNPs employ their unique chemical and physical properties for transporting and unloading therapeutics (Hainfeld

et al., 2014). Gold core is essentially solid and nontoxic; also, synthesising monodispersing NPs is easy and they can be formed with core sizes of 1–150 nm. In addition, their photophysical properties could trigger release of the drug at a remote site (Skirtach et al., 2006). Several studies have highlighted the application of AuNPs for biosensing , drug delivery and diagnostics (Hainfeld et al., 2014).

1.2 Water Resources in Australia

Australia is known as the world's driest continent in terms of average precipitation per hectare (Quiggin, 2006). In some states rainfall occurs unevenly and only 12% runs off to collect in rivers. The rest of the rainfall evaporates, is used by plants or is held in wetlands, lakes or aquifers (Quiggin, 2006). Australia's water resources assessment in 2000 defined Australia's water resources as groundwater or surface water (Vertessy, 2010). Surface water is divided into 325 surface water management areas, 246 component river basins and 12 drainage divisions (Vertessy, 2010). Groundwater is divided into 538 groundwater management units and 69 groundwater provinces (Vertessy, 2010). The 2010 water resource assessment reported on the climatic conditions and rainfalls percentage in the Australian landscape from 2009–10 (Figure 1.9).

The central problem of water availability in Australia is water supply rather than low total volume of rainfall. The problem is that water may not be available where it is needed the most (Quiggin, 2006). Transporting water from one place to another is expected to create technological difficulties related to the requirements for dams and pipelines, and socio-political difficulties associated with conflicting claims to water (Shannon et al., 2008). Australian cities are facing severe or, in most cases, chronic shortages of water. Water restrictions have been necessary in most mainland capitals and are permanent or likely to become so in another places. At the same time, the agricultural sector consumes large quantities of water for irrigation (Quiggin, 2007). The problem with the water shortage is that it is diverse and complicated by the aggregate allocations of water in many catchments; in the Marry Darling Basin, water allocation is beyond the level that is environmentally sustainable in the long term. Moreover, climate change associated with global warming is a likely cause of the reduction of rainfall in much of south-eastern Australia, although this effect is not

constant (Quiggin, 2007). Below is a brief survey of water supply issues for major Australian cities.

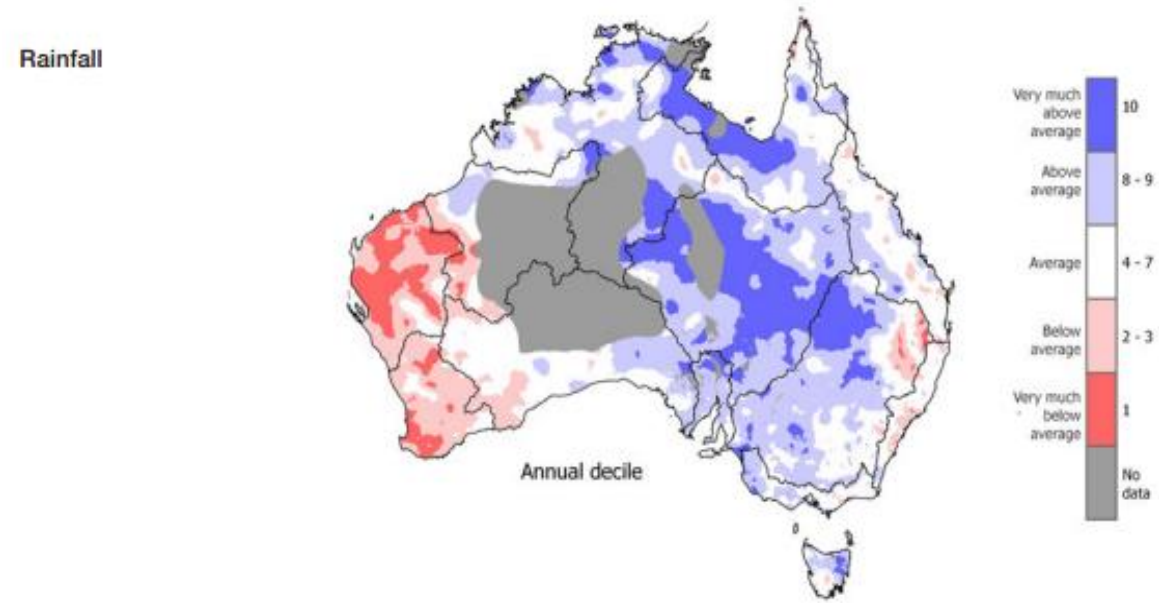

Figure 1.9: 2009-10 Assessment report of rainfalls percentage in Australian regions (Vertessy, 2010).

1.2.1 Adelaide

South Australia is considered the driest state in Australia (Warren, 1982). The Murray River and some water sources are the only water supplies and can barely cover the demands for water in Adelaide (Warren, 1982). The Murray River delivers up to 40% of the state's urban needs for water in an average year; however, this can reach as much as 90% in dry years (Mugavin, 2004). The Onkaparinga and Torrens Rivers are the main local sources in Adelaide (Australia, 1999). Water is held in a number of small reservoirs but Mount Bold is the largest reservoir in the state with a capacity of 46 GL (Australia, 1999). Per year total urban consumption is ~250 GL and ~150 GL of this is residential consumption, mostly in Adelaide (Australia, 1999). The urban water consumption is ~10% of the total water intake in South Australia (Australia, 1999). Adelaide is obliged to have permanent restrictions on water use, commonly prohibiting the use of sprinklers during the daylight. *Water Proofing Adelaide* is a programme aiming to raise the awareness of water consumption and reach the goal of saving 37 GL of water per year and 33 GL through the recycling and refining of storm water (Australia, 1999).

1.2.2 Brisbane and South-East Queensland

Four large dams are the source of water in south-east Queensland (Australia, 1999). These are Somerest with 380 gallon (gal), Wivenhoe with 1165 gal, North Pine with 215 gal and Hinze Dam with 161 gal (Australia, 1999). South-east Queensland is experiencing its longest drought period in 100 years (Verdon-Kidd and Kiem, 2009). In response, restrictions have been implemented and further plans have been developed, combining a range of options for the safe and effective use of recycle water (Forever, 2005).

1.2.3 Canberra

The Australian Capital Territory's water supplier (ACTEW) has estimated water efficiency and future options for obtaining additional water (Hensher et al., 2005). The consideration of water efficiency measurements elsewhere were found exactly the same to those in Canberra, also with restriction on consumption of water and promotion of water efficient devices (Hensher et al., 2005).

1.2.4 Melbourne

Dams have provided Melbourne with water since its first dam (Yan Yean Reservoir) was built in 1857 (Abbott et al., 2011). Currently, there are 10 dams in service, the largest of which (Thomson Reservoir) was constructed in 1984 (Water, 2004). Melbourne takes most of its water supply from the Thomson River and from reservoirs in the east of the city (Viggers et al., 2013). Currently, construction of new dams is considered the last resort. In the 1960s, it was the policy of the state's Bolte Government that no water should be transferred between the Murray Basin and coastal areas of the state (Quiggin, 2006). However, it would be feasible to transfer water from irrigation users in Melbourne and in the Thomson River catchment by using existing infrastructure. Transferring water from the Goulburn catchment to the Murray–Darling Basin might be possible with modest additional investment (Quiggin, 2006).

Melbourne's water restrictions began in November 2002 following concern over the depletion of water in storage due to a drought that began several years previously (Low et al., 2015). However, the Victorian government has since revealed an overall assessment of Victoria's water future, with green and white papers prepared on water

(Edwards, 2006). Residential water users are now under permanent restrictions in various forms of water use. The most important aspects are creating a variety of incentives and penalties to encourage individuals to make efficiency improvements and discourage those who use water extravagantly. Moreover, there is a three-part rising block tariff (Edwards, 2006). Edwards (2006) described these policies as inequitable and inefficient and doubted the commitments of individuals to the right way of using water.

1.2.5 Perth and Sydney

Perth is the Australian city most affected by the water supply dilemma (Troy, 1995). Its unfavourable location and declining rainfall have kept Perth in permanent water shortage. The annual stream flow of Perth catchments from 1991 to 2003 was 285 billion L (Young, 2005). The committee revealed that Perth and Sydney in particular may face the dangers of significant water shortages (Roseth, 2006). As a consequence, the Western Australian government has been determined to examine solutions to the shortage, either in technological or political terms. Dr John Marsden discussed these two cities at a Sydney hearing and mentioned that they may share the same challenges; however, they may not have received the same response (Brown and Farrelly, 2007). A desalination plant has been constructed at Kwinana in Western Australia (Sanz and Stover, 2007) and is expected to produce 45 GL per year. The estimated cost of the delivered water is almost $1.50 per kL (Sanz and Stover, 2007). The plant uses reverse osmosis (RO), making it the first of its kind in Australia. This could provide up to 17% of Perth's water demand. Additionally, the Western Australian government covered the demand for water by purchasing water from irrigators near Perth and recharging underground storage plants (Sanz and Stover, 2007).

1.3 History of Desalination

For more than 50 years, Desalination of water provides the main source of fresh water to some countries in the Middle East and other parts of the world (El Saliby et al., 2008). Australian desalination plants could be established in areas with lower rainfall and where the main source of available water is saline bodies or seawater (Gerofi and Fenton, 1981). In the past, fresh water from natural sources was sufficient to supply residents of major cities, with the exception of Adelaide and Perth where desalination

plants were needed the most. Nowadays, with climate change and population growth in Australia, water availability is becoming a public concern for each state (El Saliby et al., 2008). In 1903, the first desalination plant was built in the goldfields of Western Australia at Kalgoorlie (El Saliby et al., 2008). Wood-fire was used to generate energy for treating saline groundwater. Since then, small-scale desalination plants have been built to cover the needs for fresh water, irrigation and industrial water requirements in remote communities (Timbal, 2004). Agriculture, Fisheries and Forestry Australia classified desalination technology in Australia into two operations: (1) major process and (2) alternative processes (Australia's Agriculture, 2012). The major processes include electrodialysis (ED), membrane (RO), multiple effect distillation (MED), distillation (multi-stage flash distillation [MSF]) and vapour compression distillation (VC) (Australia's Agriculture, 2012). Further details are provided below.

1.3.1 The Situation of Australian Desalination Plants

Australian large-scale desalination plants are in early stage in comparison with other plants in the world (Roberts et al., 2010). Desalination of water worldwide is considered an expensive alternative compared with the price of existing metropolitan water (Roberts et al., 2010). The price of desalinating water is driven by available mainstream technologies; however, by 2020 this could change if new alternative technologies are employed at industrial scale in Australia (Roberts et al., 2010). Desalination is highly attractive for governments in Australia as they are in a current water crisis (El Saliby et al., 2008). Former Prime Minster Kevin Rudd mentioned in one of his interviews that 'different states and Territories have different responses to recycling and desalination. It depends, I imagine, very much on local circumstances, local engineering possibilities, as well as the financial feasibility of various projects' (El Saliby et al., 2008).

In Australia, government approvals and project contract requirements for desalination plants may differ from state to state. For instance, the project timelines for the Kurnell (Sydney) and Kwinana (Perth) desalination plants were each ~4–5 years (El Saliby et al., 2008). Community consultation, initial concept plans, legal procedure plans and proposal amendments play an important role in determining the project timeline (El Saliby et al., 2008). On 16 November 2005, two of the parliament suggested submitting a concept plan for the development of the Kurnell desalination plant (Wright and Cox,

2006) . After a year the plan was approved with some modifications and the contract was signed on 17 August 2007 (El Saliby et al., 2008).

According to the Western Australia Water Corporation (2006), the establishment of new desalination plants has many prerequisites (Knights et al., 2007). For example, the need for a large area for the plant's construction, discharge of brine to the marine environment and energy consumption to operate the plant must all be considered. Therefore, the ultimate effects of these prerequisites should be determined. The most important is the environmental impact assessment for any project including a desalination plant. In 1979, the New South Wales *Environmental Planning and Assessment Act* (EP&A Act) included the concept of a plan to declare any project and define its environmental impact (Momtaz and Gladstone, 2008). Often, water recycling and desalination plants have high energy consumptions, which will increase their gas emissions (Momtaz and Gladstone, 2008). This needs to be minimised, but bigger desalination plants (Raluy et al., 2006) mean higher gas emissions. Some reports have pointed out that reduction in CO_2 emissions by desalination plants could be achieved by fixing their energy consumption (Omer, 2008). Other suggestions include coupling renewable energy with desalination plants as environment impacts are certain with energy consumption (Raluy et al., 2006). Cleaning effluent and brine discharged during water treatment influence both the environmental and economic impacts of desalination (Lattemann and Höpner, 2008). In the RO process, treated water will contain a large amount of salt and contaminants. Unfortunately, the high concentrations of salt from brine discharged from seawater desalination are sufficient to destroy large areas of ocean floor as a result of a high thickness of waste (McKinnon, 1982). In the main, desalination plants discharge large volumes of iron, which can discolour the ocean floor and destroy the region (Lattemann and Höpner, 2008). Chemicals such as coagulants, antifouling agents, disinfectants and pH buffers added to discharged brine could worsen these effects (Raluy et al., 2006). Worryingly, the effect of these components remains unpredictable (Von Medeazza, 2005). Lake and Bond (2007) suggested that at a local scale, the impacts include noise, altered land use and the need to move recreation facilities; broader environmental issues included soil salinity, groundwater intrusion and expansion of invasive species. Further, if business continues without the restoration of restrictions and no conversation, efforts will get hard with following the regulations occurred by past legacies (Lake and Bond, 2007).

1.3.2 A Brief Summary of Desalination Technologies

Technologies used in desalination can be divided into three categories. The first is processes that depend on a physical change in water appearance such as freezing or distillation. The second category is processes that operate using membranes; for example, ED and RO. The third group comprises processes that affect chemical bonds, such as ion exchange (Mezher et al., 2011). Processes based on ion exchange are mostly used to produce water at high quality for industrial purposes; therefore, they are not appropriate for treating seawater (Grasshoff et al., 2009). However, the other two processes, which are based on the physical appearance of water and filtering by membranes, have been commonly used for treating seawater for several decades and have been continually developed for commercial applications. These processes can be divided into major and alternative processes as in Table 1.1 (Australia, 2002).

Table 1.1: Commonly used processes in desalination plants (Australia, 2002).

Major Processes	**Alternative processes**
Membrane	***Solar Humidified***
Reverse Osmosis (RO)	Freezing
Electrodialysis (ED)	Membrane Distillation
Distillation	Renewable Energy power
Multi-Stage Flash Distillation	
Multiple Effect Distillation	
Vapour compression distillation	

RO and ED mainly use membranes to differentiate and selectively isolate salts and water (Sonune and Ghate, 2004). However, the membranes are differently used in each of these processes (Australia, 2002). For instance, RO is a pressure process in which the water is forced to pass through a membrane; the remaining salts are trapped and discharged. ED uses electrical potential to selectively remove salts through membranes and leave water behind (see Figure 1.10; Australia, 2002).

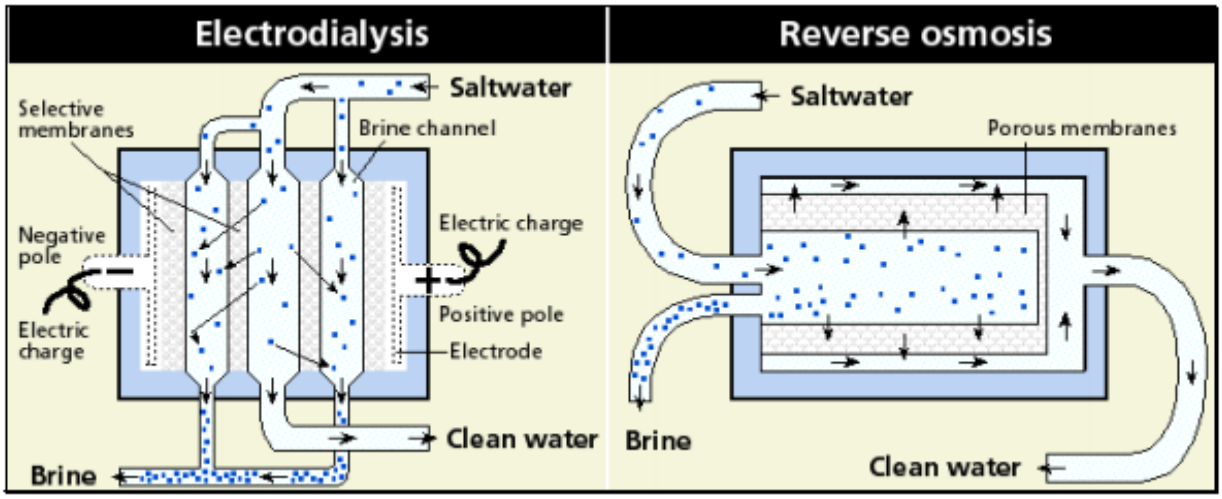

Figure 1.10: Explanation of membrane layers used in the electrodialysis and reverse osmosis processes (Australia, 2002).

1.3.3 Major Processes

1.3.3.1 Reverse Osmosis

RO membrane was developed more than 40 years ago and it remains a leading technology in recently established plants (Greenlee et al., 2009). Eighty % of desalination plants worldwide use RO in their system (Greenlee et al., 2009). Recently, two branches of RO desalination have emerged: brackish water RO and seawater RO (Greenlee et al., 2009). The contrasts between these two water resources, which include waste brine, salinity, foulants, plant location and disposal options, produce significant variation in process development and application (Greenlee et al., 2009). The foundation of osmosis is the transfer of water through semi-permeable membranes influenced by a concentration gradient. The chamber has two compartments; one holding pure water and the other saline water. The process occurs when water flows towards the saline solution through the semi-permeable membrane (Australia, 2002). The quantity of water transmitted by osmosis will decrease in parallel with the influence

of high pressure. The applied pressure stops when there is no flow of water crossing the membrane. This balance is called osmotic pressure of the saline solution (Australia, 2002). RO is conducted by increasing the pressure on the saline solution beyond the osmotic pressure, which pushes the flow of water in the opposite way to the osmotic flow (Australia, 2002).

1.3.3.2 Electrodialysis

Using a similar technique to RO, ED involves the movement of water over a filtering membrane. Pre-treated water is pumped through ED cells under the influence of a low-voltage direct current electrical field (Australia, 2002). The fed water is pumped into ED cells containing many narrow compartments. These compartments are segregated by membranes that are permeable to either negative ion (anion) controls or positive ions (cations). Under the influence of a direct current, anions and cations migrate through the appropriate membrane, creating a compartment of low-electrolyte product water and high-electrolyte waste water (Australia, 2002). Non-ionic particles, residual turbidity and bacteria can pass through the cells into the product water, and therefore the water should be subjected to further treatment to meet expected drinking water standards (Australia, 2002).

1.4 Nanoparticle-based Membranes

In membrane separation technologies, development of low-fouling membranes is an important research area (Kim and Van der Bruggen, 2010). Membranes have been widely used for the removal of many contaminants from wastewater (Kim and Van der Bruggen, 2010). However, the most significant limitation of ceramic and polymeric membranes is that they can become corrupted easily. The consequences of membranes fouling due to rejected colloids, microbes and chemicals are higher energy consumption and higher cost of membrane cleaning and replacement (Kim and Van der Bruggen, 2010). Although many investigations have been carried out to improve membrane surfaces using chemical modification, the effect is still insufficient to satisfactorily reduce membrane corruption (Kim and Van der Bruggen, 2010). The revolution of nanotechnology applications has expanded to include synthesising membrane technologies for use in water and wastewater treatment (Kim and Van der Bruggen, 2010). After using NP-based membranes, beneficial effects have been observed in

mitigation of membrane fouling (Kim and Van der Bruggen, 2010). Nanoparticle-based membranes provide the membrane with a high degree of consistency so it can reach optimal functional ability as well as the desired structure (Kim and Van der Bruggen, 2010). Nanoparticle-based membranes are mainly developed by compiling engineered NPs inside porous membranes or blending them with inorganic or polymeric membranes (Li et al., 2009). Researchers have created membranes with carbon nanotubes or metal oxides to optimise the novelty of permeability, membrane materials and fouling resistance (Cortalezzi et al., 2002). Due to the catalytic properties of several metal oxide NPs, integrating chemical oxidation with NP-based membranes reduces membrane fouling and reduce functionality corruption (Kim and Van der Bruggen, 2010).

1.4.1 Manufacturing of Nanoparticle-based Membranes

1.4.1.1 Nanoparticles in Polymeric Membranes

In recent years, the manufacturing process for polymeric membranes using NPs has received attention with respect to fouling reduction and flux enhancement. Hybrid membranes containing inorganic fillers are well known. Some of the common fillers are oxides such as zeolites and SiO_2 (Luo and Wan, 2011). Thus, the concentration of the filler may be very high, but this will not influence the physical properties of the polymeric membranes. Such membranes are known as mixed polymeric membranes (Kim and Van der Bruggen, 2010). Two phases are present with equal influence (Luo and Wan, 2011). The filler used for separation improvement can be zeolites and for flux enhancement, metal oxides (Luo and Wan, 2011). When using mixed-matrix membranes, inorganic materials are mainly used in accumulation. The principle of this approach is related to the interaction between the two phases having similar distributed particles. This could lead to enhanced flux and fouling mitigation (Luo and Wan, 2011). The second phase is detailed extensive research for several polymer/NP combinations. The manufacturing process is the most challenging step in the development of NP-enhanced membranes (Kim and Van der Bruggen, 2010). It is done by adding a carefully chosen amount of NPs to a casting solution. For instance, poly(ether) sulfone (PES) and titanium dioxide (TiO_2) composite membranes are prepared using a vapour-induced phase separation and immersion precipitation process. The casting solution contains 15% by weight PES dissolved in an identical amount of N,N

dimethylacetamide and diethlyene glycol; and 0–15% of TiO_2 is added (Kim and Van der Bruggen, 2010).

1.4.2 Nanoparticles as Potential Aquatic Pollutants

Industrial products and waste seem to reach waterways despite safeguards (Moore, 2006). The rise of the nanotechnology industry's scale of production inevitably will increase the chance of nanoscale particles reaching waterways. Thus, it is imperative to have a risk assessment procedure to deal with potential hazards (Moore, 2006). It is well known that NPs play an important role in water quality and treatment. Nanoparticle size and functionalisation for several applications is a crucial factor in wastewater reclamation (Brar et al., 2010). Functionalisation of NPs is a method of connecting organic/surfactant molecules to keep them in a dispersed state (Kim et al., 2010). This changes the behaviour of the dissolved contaminant and micron-sized particles during water treatment. In the meantime, particles in the wastewater will reach the wastewater sludge, more so through aggregation and/or agglomeration and settling mechanisms (see Figure 1.11; Brar et al., 2010). Unfortunately, wastewater sludge contamination is completely neglected, which has led to the spread of wastewater sludge to agricultural fields, increasing the potential for leachability of NPs into the sub-surface water and ground water (Kim et al., 2010; Santiago-Martín et al., 2015).

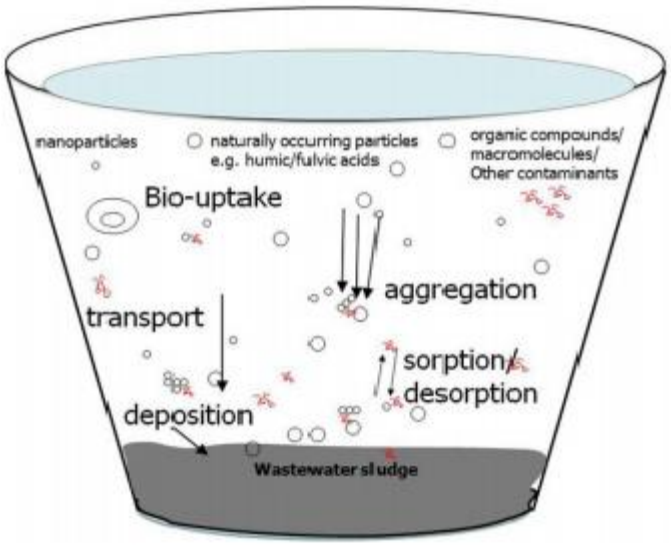

Figure 1.11: Pictorial explanation of steps used in wastewater treatment plants (Brar et al., 2010).

1.4.3 *N*-Nitrosodimethylamine as a Water Contaminant

N-nitrosodimethylamine (NDMA) is a nitrogen-containing organic compound that is well known for its carcinogenic properties. For decades, NDMA was commonly used as a fire retardant, antioxidant and additive for lubricants. Therefore, this compound has been a health concern for some industries including the international water industry after it was used as a disinfectant in drinking water and wastewater with chlorine or chloramines. Most of the focus has been on NDMA as a water contaminant; however, other nitrosamines can enter recycled and drinking water systems by similar mechanisms and they are considered toxic. For decades, NDMA has been identified as a probable human carcinogen. The eight possible types of nitrosamines that might be found in recycled and drinking water are:

- *N*-nitrosodiethylamine (NDEA)
- *N*-nitrosodi-n-propylamine (NDPA)
- *N*-nitrosodi-n-butylamine (NDBA)
- *N*-nitrosomethylethylamine (NMEA)
- *N*-nitrosomorpholine (NMor)
- *N*-nitrosopiperidine (NPip)
- *N*-nitrosopyrrolidine (NPyr)
- *N*-nitrosodiphenylamine (NDPhA).

1.4.3.1 Existence of N-Nitrosodimethylamine in Water

The occurrence of nitrosamines in drinking water and wastewater is not only a result of disinfection but can also be due to chemical and biological reactions. However, the most dominant factor in nitrosamines reaching waterways is industrial waste streams. For example, NMor is commonly used in wastewater plants for disinfection and has been used in rubber industry waste and in some hydraulic fluids. Another way of NMor reaching the waterways is by bacterial nitrosation of a secondary amine, known as morpholine. In a similar way, NDMA can reach waterways through run off from agriculture because farmers use pesticides contaminated with the compound.

1.4.3.2 N-Nitrosodimethylamine Attracting International Attention

NDMA is the most well-studied of the nitrosamine precursors due to publicity around its commercial use; most published data demonstrate its risk to ecosystem (Newcombe et al., 2012). In Japan, samples of drinking water were examined for NDMA and most samples contained 10 ng/L (Newcombe et al., 2012). A survey of 41 drinking water providers in the United Kingdom during December 2006 and November 2007 detected that 10% of samples contained 1 ng/L NDMA (Templeton and Chen, 2010). In China, a survey conducted on 12 drinking water plants to detect the eight types of nitrosamine discovered six of them (NDMA, NDEA, NMor, NDBA, NMEA and NDPhA) (Wang et al., 2011). The total concentration of nitrosamines found in samples was up to 42 ng/L for source water and 26 ng/L for finished water. In South Australia, chloramination is a common practice; therefore, the South Australian Water Corporation accomplished a routine monitoring scheme for NDMA in four systems in 2007 (Newcombe et al., 2012). They found that the levels of NDMA in distribution system changed considerably with time due to variation in retention time, which is controlled by demand. From 2007 to 2012, the average concentration of NDMA taken from more than 750 samples around South Australia was 20 ng/L; in south-east Queensland, nitrosamine was found in five drinking water treatment plants (Newcombe et al., 2012). Three of these plants practiced chloramination and the other used a combination of chlorine and ozone. A one-year survey was conducted on drinking water that was chlorinated and chloraminated, and on a chlorinated recycled system. NDMA, NDEA and NMor was detected in 130 samples (Newcombe et al., 2012). NDEA was not found in any sample; however, NMor was detected in 42% of the chlorinated recycled water. Ten ng/L was the detection limit for both compounds. NDMA was found in 75% of samples, including some chlorinated drinking water samples.

The existence of nitrosamines in effluent of drinking and wastewater treatment plants can occur via three pathways (Nawrocki and Andrzejewski, 2011; Newcombe et al., 2012). First, they might form during the treatment process. Second, they might enter as contaminants during treatment or distribution. Third, they may not be removed during treatment and may then reach the influent to the plant. It seems that NDMA and other nitrosamines are found in drinking and recycled water regardless of the treatment process and source (Newcombe et al., 2012). Most samples with 10 ng/L or less have

disinfection by-products; concentrations over 100 ng/L are regularly reported and drinking water suppliers consider that the levels may be different seasonally due to water quality and operational changes (Newcombe et al., 2012).

1.5 Scope and Aims of the Thesis

The overall aim of this study was to investigate the toxicity of synthetic NPs to human cell lines. This study used two cell lines as *in vitro* models: the HaCaT cell line and human colon carcinoma cell line (Caco-2). One of the main issues affecting the assessment of NP toxicity to humans and the environment is the use of biochemical assays that could be affected by the NPs themselves and provide false data or subsequent incongruent predictions of toxicity. Inconsistent and/or inaccurate data will make it difficult to establish guidelines for the safe use and production of nanomaterials (NMs). Therefore, this study examined the interference of eight NPs with two cell viability assays (3-(4,5-dimethylthiazol-2-yl)-2,5-diphenyltetrazolium bromide [MTT] and crystal violet) (see Chapter 2).

Occupational exposure to amorphous silica is associated with an increased risk of pulmonary diseases such as silicosis, chronic bronchitis, COPD and lung cancer. Moreover, the skin penetration and cellular uptake of amorphous silica particles poses a risk to industrial workers. In Chapter 3, I tested the toxicity of silica NPs (12 nm in diameter) to the HaCaT cell line. The particles were purchased from Sigma Aldrich and tested using MTT and crystal violet assays for 4, 24 and 48-h exposures. The estimated exposure of *in vitro* concentrations for workers were 0.05, 0.1, 0.5, 1.0, 1.5, 2.0, 4, 5, 7, 9 and 10 mg/mL.

Desalination plays a crucial role in producing pure water from brackish water. RO is the most efficient way to remove colloidal and dissolved silica, which can be found in high concentrations in brackish water. The existence of silica and its ability to foul membranes limits the use of silica-bearing waters for desalination and when used, it has many economic risks. In Chapter 4, I tested the toxicity of SiO_2 NPs (200 nm in diameter) synthesised using the Stöber method and NDMA as potent known carcinogens formed during chlorination on HaCaT and Caco-2 cell lines for 4, 24 and 48 h using MTT and lactate dehydrogenase (LDH) assays, as well as the morphology

and size of SiO_2 determined by scanning electron microscopy (SEM). The concentrations tested were 0.05–2 mg/mL, chosen based on the results from Chapter 3.

Recent advances in the synthesis of silica NPs with controlled size, morphology and chemical stability has made silica NPs attractive for use in a wide variety of nano-technological applications including adsorption, catalysis and separation. In addition, functionalising the surface of silica NPs can reduce their toxicity and enhance the probability of cellular uptake. These new advancements provide the possibility of designing a new generation of drug/gene delivery systems and biosensors. In Chapter 5, thiolated silica NPs (SiO_2) were synthesised using the Stöber method and then coated with low-fouling zwitterionic sulfobetaine methacrylate (SBMA) with thiol-ene addition. The morphology of the particle was examined by SEM and size dynamic light scattering (DLS). Toxicity of the SiO_2-SBMA NPs (concentrations of 0.05–2.00 mg/mL) to Caco-2 and HaCaT cell lines was investigated using MTT, LDH and crystal violet assays for 4, 24 and 48 h. Also, particles were exposed to UV light for 1 h and photodegradation was determined by zeta potential measurements.

Chapter 2: The MTT and Crystal Violet Assays—Potential Confounders in Nanoparticle Toxicity Testing

Abdulmajeed G. Almutary[1], Barbara J. S. Sanderson [2]

Authors Contribution

AA carried out the experimental work, analysed the data and drafted the manuscript. BJSS participated in the design of the study and reviewed the manuscript and gave her intellectual input. All authors read and approved the final manuscript.

Abstract

The toxicological effects of NPs on humans, animals and the environment are largely unknown. Assessment of NP cytotoxicity depends on the choice of test system. Due to NPs' optical activity and absorption values, they can influence classical cytotoxicity assays. Eight NPs were spiked in MTT and crystal violet assays and tested with HaCaT human skin cells. The MTT assay standard curve optical density (OD) measurements were altered by the presence of trisilanol phenyl and trisilanol isooctyl polyhedral oligomeric silsesquioxane particles. The crystal violet standard curve OD measurements were significantly shifted by AuNPs, but they did not affect the MTT assay. Carbon black decreased ODs in the MTT and crystal violet assays and was localised in the cell cytoplasm. These findings strongly indicate that careful choice of *in vitro* viability systems is required to avoid flawed measurements of NPs toxicity.

2.1 Introduction

The wide use of nanomaterials in many areas including chemistry, medicine and biology, as well as incomplete characterisation of the toxicity of many NPs. heightens the demand for related occupational health and safety guidelines (Langer and Tirrell, 2004; Salata, 2004). The creation of these guidelines relies on experimental investigation to characterise the framework for hazards and identification of the risk of exposure to newly synthesised NPs (Amoabediny et al., 2009; Chen et al., 2000; Hoyt

and Mason, 2008; Schmid and Riediker, 2008). Industrial workers are at daily risk from occupational exposure (Bhabra et al., 2009; Davis and Shin, 2008; Hoet et al., 2004; Trouiller et al., 2009). Therefore, it is essential to identify the cytotoxicity of newly developed NPs (Brunner et al., 2006; Chang et al., 2006; Kirchner et al., 2005; Lam et al., 2004; Lin et al., 2006). Research has identified the interference of some NPs with some assays, including Alamar Blue™ (AB), Neutral Red (NR), MTT and 2-(4-iodophenyl)-3-(4-nitrophenyl)-5-(2,4-disulfophenyl)-2H-tetrazolium (WST-1) (Casey et al., 2007a, b; Dobrovolskaia et al., 2008; Fotakis and Timbrell, 2006; Hurt et al., 2006; Isobe et al., 2006; Monteiro-Riviere and Inman, 2006; Zhang et al., 2008).

Tetrazolium salts are extensively used in the measurement of metabolic activity of cells due to the ease of carrying out the assays (Altman, 1976; Mattson et al., 1947; Nineham, 1955; Novikoff et al., 1961). An MTT assay is a versatile and popular assay to assess mitochondrial activity (Gerlier and Thomasset, 1986; Pieters et al., 1990). Metabolically active cells reduce water-soluble MTT salts to the form of MTT formazan crystals (Berridge and Tan, 1993). This creates insoluble MTT formazan, which is found in the cytoplasm, mitochondria and some parts of the plasma membrane (Bernas and Dobrucki, 2002). The decrease of MTT activity in cells is considered an indicator of cell redox activity (Berridge et al., 2005; Goodwin et al., 1995; Mosmann, 1983).

The current study examined the interference of eight NPs with two classical cytotoxicity assays. I selected commonly used cytotoxicity assays with two different cytotoxic end-points: metabolic activity (MTT) and cell death (crystal violet). The NPs studied were four novel POSS particles: carbon black, CdS QDs, SiO_2 and AuNPs.

2.2 Materials and Methods

2.2.1 Particles Used for Testing

Table 2.1 illustrates the physical and chemical characteristics of POSS particles, SiO_2 and carbon black. POSS, CdS QDs and AuNPs were provided by the department of Chemical and Physical Sciences, Flinders University in South Australia. SiO_2 and carbon black were purchased from Sigma Aldrich.

Table 2.1: Physical and chemical characteristics of nanoparticles tested.

Particles	Trisilanol isooctyl POSS	Trisilanol cyclohexyl POSS	Trisilanol phenyl POSS	Trisilanol cyclopentyl POSS	SiO_2	Carbon black	CdS QDs	AuNPs
Appearance	Oil	Solid powder	Powder	Powder	Powder	Powder	Powder	Powder
Boiling point	N/A	N/A	N/A	N/A	2230°C	4827°C	N/A	N/A
Colour	Clear to pale yellow	White	White	White	White	Black	White	White
Evaporation rate	N/A	N/A	N/A	N/A	N/A	N/A	N/A	N/A
Molecular weight	1184.16	973.69	~931.34	875,5100	N/A	N/A	N/A	N/A
Odour	N/A	N/A	None	N/A	N/A	N/A	N/A	N/A
Odour threshold	N/A	N/A	N/A	N/A	N/A	N/A	N/A	N/A
Physical state	Viscous liquid	Solid	N/A	N/A	N/A	N/A	N/A	N/A
Reactivity in water	Insoluble	N/A	Insoluble	N/A	Soluble	Insoluble	N/A	N/A
Solubility in water	Insoluble	N/A	Insoluble	N/A	Soluble	Insoluble	Insoluble	Soluble
Density	N/A	N/A	N/A	N/A	2.648 g/cm	0.056 g/cm^3	N/A	N/A
Vapour density	N/A	N/A	N/A	N/A	N/A	N/A	N/A	N/A
Molecular /chemical formula	C56H122O12Si7	C42H80O12Si7	C42H38O12Si7	C35H66O12Si7	SiO2	CH4	CdS	Au
Size	100 nm	100 nm	100 nm	100 nm	20 nm	500 nm	8 nm	13 nm

SiO_2 (CAS number: 7631-86-9) and carbon black (CAS number: 1333-86-4) were purchased from Sigma Aldrich; N/A = not available

2.2.2 Cell Culture

The HaCaT cell line originated from the American Type Culture Collection (ATCC). Cells were grown in Roswell Park Memorial Institute (RPMI) medium with 10% foetal bovine serum (FBS) and incubated at 37°C with 5% CO_2 in a humidified incubator. Cells were established at 2×10^6 cells/mL and sub-cultured every 2–3 days when confluence reached 60–70% (Altenburger and Kissel, 1999; Schoop et al., 1999).

2.2.3 Cell Exposure to Carbon Black for Transmission Electron Microscopy

HaCaT cells were seeded and a cell suspension of 2×10^6 cells/mL was exposed for 24 h to 10 mg/mL carbon black. The cells were fixed in 1% glutaraldehyde and 4% formaldehyde in 0.1 M Phosphate buffered saline (PBS) (pH 7.4) by mixing equal volumes of fixative and cell suspension (Peters et al., 2004; Warheit et al., 2004). Cells were transferred to a centrifuge tube and spun for 10 minutes at 1200 revolutions per minute (RPM), and then the fixative was removed. Fresh fixative was added for approximately 2 h and then also removed. Three washes of 15 minutes in 8% (0.2 M) sucrose in 0.1 M PBS at 4°C were done, followed by 1 h post-fix with 1% osmium tetroxide ($OsO_{4)}$ in 0.1 M PBS. Finally, OsO_4 was aspirated and the pellet rinsed in 0.1 M PBS three times for 10 minutes each time.

Dehydration of the cell suspension was carried out once using each of 50%, 70% and 95% ethanol for 15 minutes; twice with 100% ethanol for 15 minutes; and then twice with 100% propylene oxide for 15 minutes. The cell suspension was embedded in beam capsules and baked in a 60°C oven for 48 h. Finally, the cell suspension was sectioned (0.5–2 µm) and stained with uranyl acetate and lead citrate.

2.2.4 MTT Assay Standard Curve Procedure

MTT assay standard curves were carried out in 96-well, flat-bottomed microplates (Price and McMillan, 1990). The standard curves were prepared by halving serial dilutions of cells in four technical replicate wells, from 40,000 cells per well to 78 cells per well (Toi et al., 1992). The final volume of cell suspension in each well was 100 µL. The plates were incubated at 37°C with 5% CO_2 in a humidified incubator for 18 h. Media was then removed and 0.5 mg/mL of MTT solution was added to each well (200 µL/well). The plates were incubated for 4 h at 37°C with 5% CO_2 in a humidified incubator. Sodium dodecyl sulphate (SDS) (80 µL of 20% solution) was added and the plates were incubated in the dark at room temperature overnight. Absorbance was read at a primary wavelength of 570 nm and a reference wavelength of 630 nm. In addition, the absorbance of the dilutions of specific NPs in RPMI was determined at the primary and reference wavelength.

2.2.5 MTT Assay Particle Interference Experimental Procedure

Four replicate standard curve plates were prepared for each interference assay. Replicate 1 was the media control plate. Replicate 2 was the solvent control plate if required when the particle was suspended in other than media. Replicate 3 had NPs added at the same time as the MTT. Replicate 4 had NPs added with the SDS solubilising solution. The doses tested for each NP are shown in Table 2.2.

Table 2.2: Particle toxicity and interference doses tested.

Particle type	Interference dose	Solvent
Trisilanol isooctyl POSS	10 mg/mL	DMSO
Trisilanol cyclopentyl POSS	0.1 mg/mL	Ethanol
Trisilanol cyclohexyl POSS	0.1 mg/mL	DMSO
Trisilanol phenyl POSS	0.1 mg/mL	DMSO
CdS QDs	1 mg/mL	Sodium phosphate buffer (SPB)
SiO_2	1.5 mg/mL	Water
AuNPs	0.017 nM	Water
Carbon black	10 mg/mL	DMSO

Doses are those predicted to be approximately one in a thousand dilution of the maximum solubility for each NP (Holder et al., 2012) because this was predicted to be the maximum residual dose after performing a treatment experiment and then washing three times; DMSO = dimethyl sulfoxide

2.2.6 Crystal Violet Assay Standard Curve Procedure

Crystal violet standard curve plates were set up identically to the MTT standard curve plates except that six technique replicate wells were used per number of cells/well. After overnight incubation, media was aspirated and replaced by 50 µL of crystal violet stain, followed by incubation at room temperature for 15 minutes. The stain was washed off with demineralised water and plates left to dry overnight. A 33% (v/v) acetic acid solution was then added and the ODs read using a spectrophotometer at 570 nm (Chiba et al., 1998).

2.2.7 Crystal Violet Assay Experimental Procedure Particle Interference

Three standard curve replicate plates were used. Replicate 1 was the media control; replicate 2 was the solvent control (solvent added with the stain) and replicate 3 had the test particle added with the stain.

2.2.8 Statistical Analysis

The data were analysed as mean ± SE (standard error of the mean) of at least three independent experiments using one-way analysis of variance (ANOVA) and Tukey–Kramer multiple comparisons tests using SPSS (version x8) software to compare exposure groups.

All comparisons were considered significant at $p < 0.05$.

2.3 Results

For the analysis of NP interference with popular *in vitro* toxicity test systems, eight NPs were tested on HaCaT skin cells for two classical bioassays. POSS particles and carbon black with significant interference were also tested with RPMI media only in a dose response to verify any OD properties of those particles in the absence of cells (see Table 2.3).

Table 2.3: Optical densities for dilutions in media of nanoparticles that showed significant interference with MTT standard curves (see Figure 2.1).

Dose	Trisilanol phenyl POSS	Trisilanol isooctyl POSS	Carbon black
0	0.0980	0.1000	0.0943
0.01	ND	0.1015	0.1033
0.05	0.0995	ND	ND
0.1	0.0983	0.1023	0.0998
0.5	0.1000	ND	ND
1	0.0980	0.1043	0.1030
10	ND	0.1013	0.1025

n = 1; four technical replicates; ND = not done

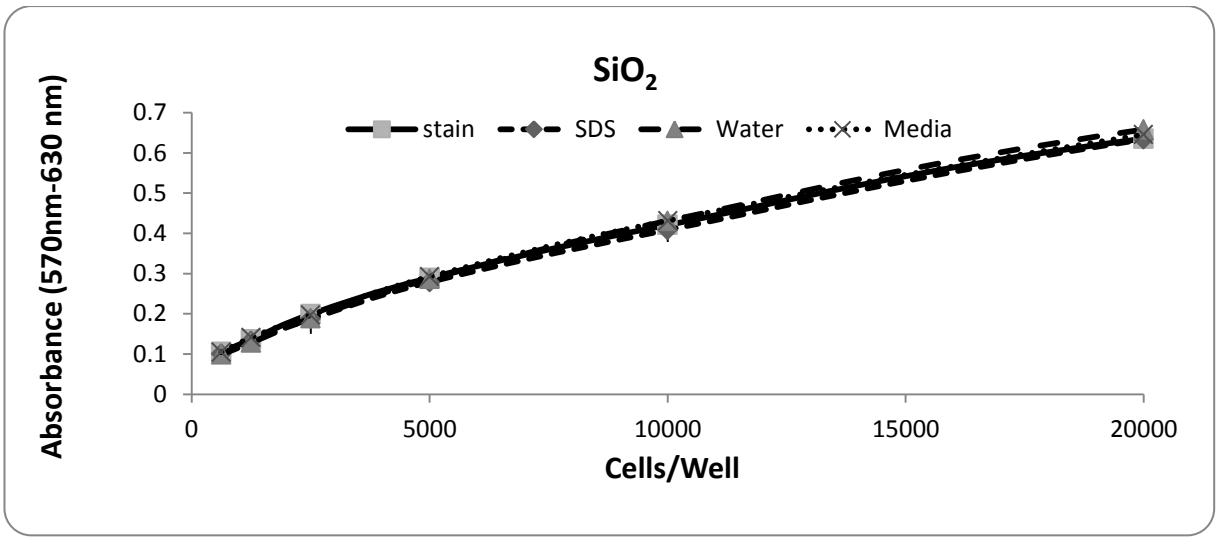
SiO2
stain
SDS
Water
Media
Absorbance (570nm-630 nm)
0.7
0.6
0.5
0.4
0.3
0.2
0.1
0
0
5000
10000
15000
20000
Cells/Well

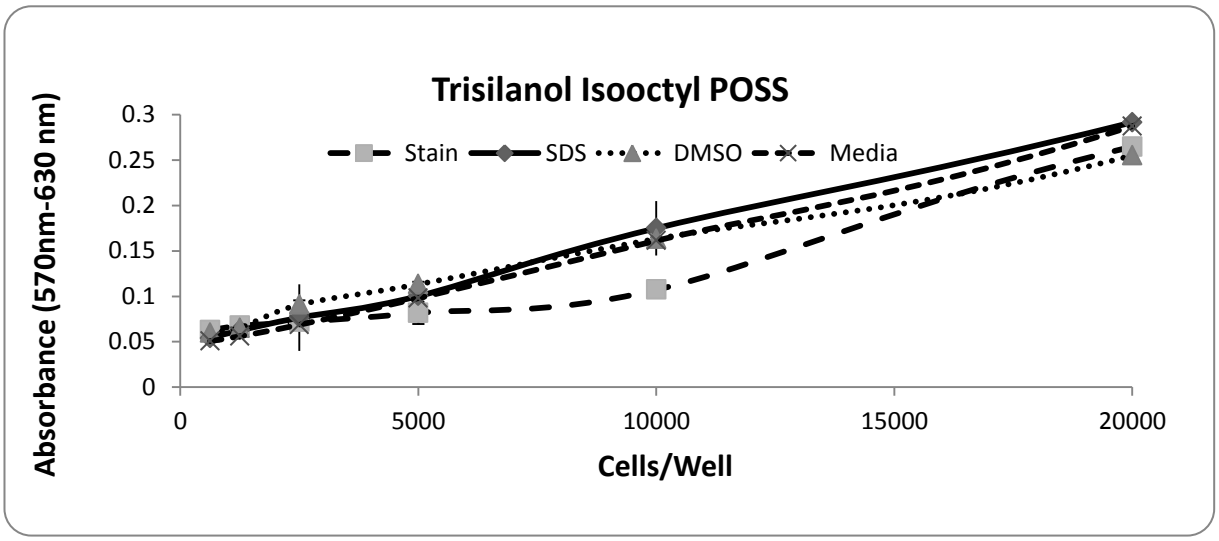
Trisilanol Isooctyl POSS
Stain
SDS
DMSO
Media
Absorbance (570nm-630 nm)
0.3
0.25
0.2
0.15
0.1
0.05
0
0
5000
10000
15000
20000
Cells/Well

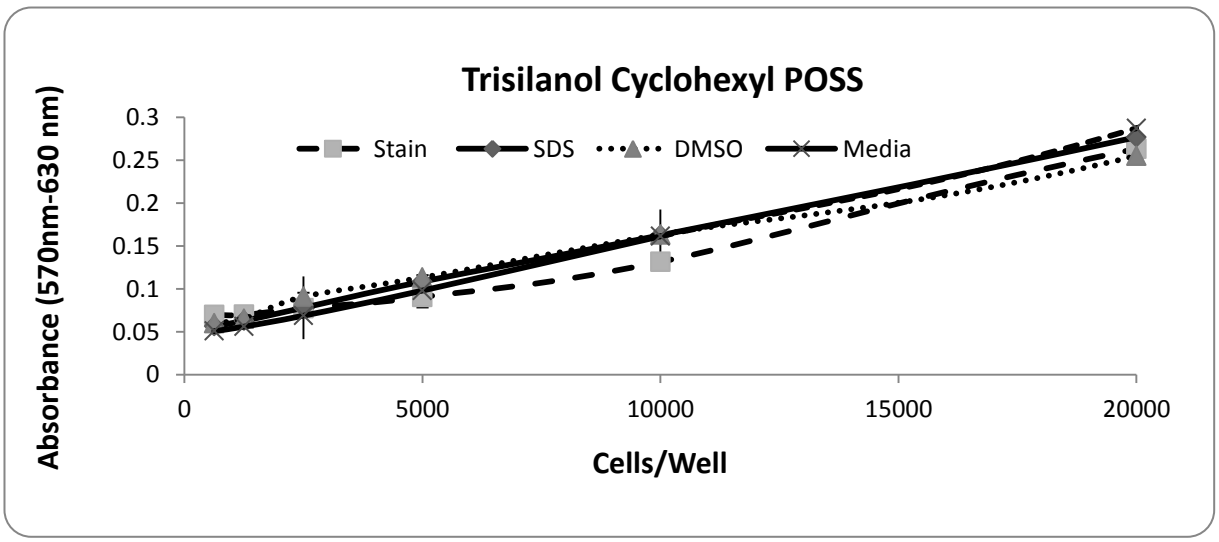
Trisilanol Cyclohexyl POSS
Stain
SDS
DMSO
Media
Absorbance (570nm-630 nm)
0.3
0.25
0.2
0.15
0.1
0.05
0
0
5000
10000
15000
20000
Cells/Well

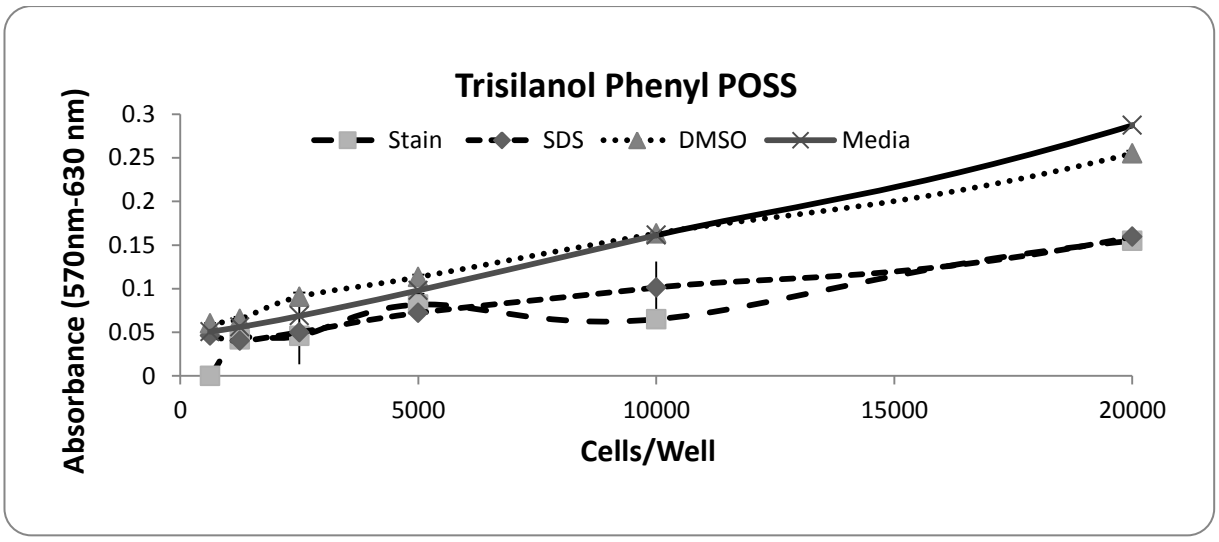
Trisilanol Phenyl POSS
Stain
SDS
DMSO
Media
Absorbance (570nm-630 nm)
0.3
0.25
0.2
0.15
0.1
0.05
0
0
5000
10000
15000
20000
Cells/Well

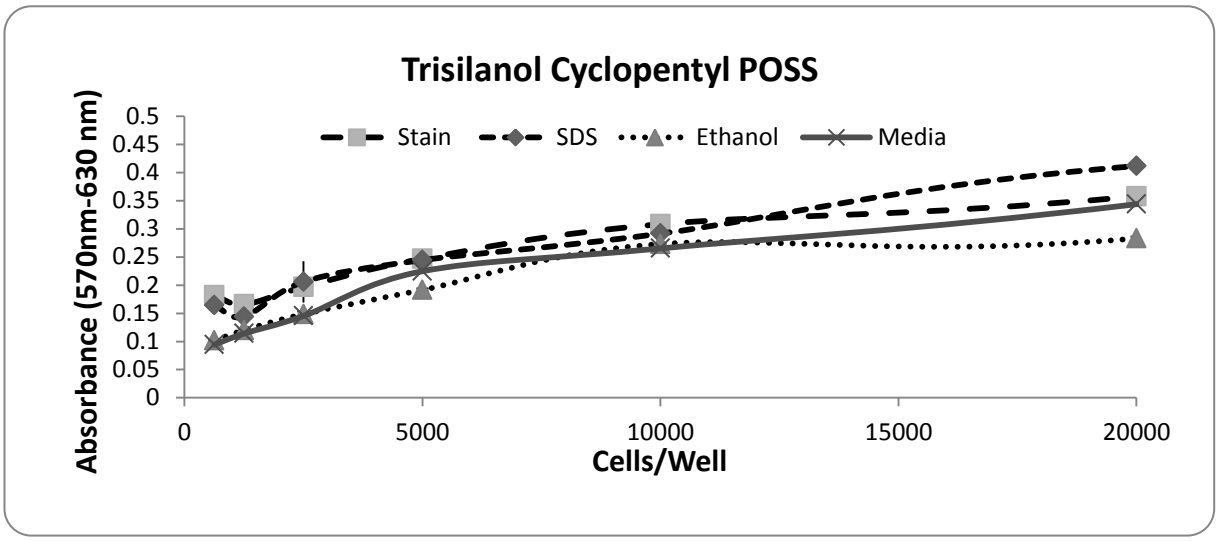
Trisilanol Cyclopentyl POSS
Stain
SDS
Ethanol
Media
Absorbance (570nm-630 nm)
0.5
0.45
0.4
0.35
0.3
0.25
0.2
0.15
0.1
0.05
0
0
5000
10000
15000
20000
Cells/Well

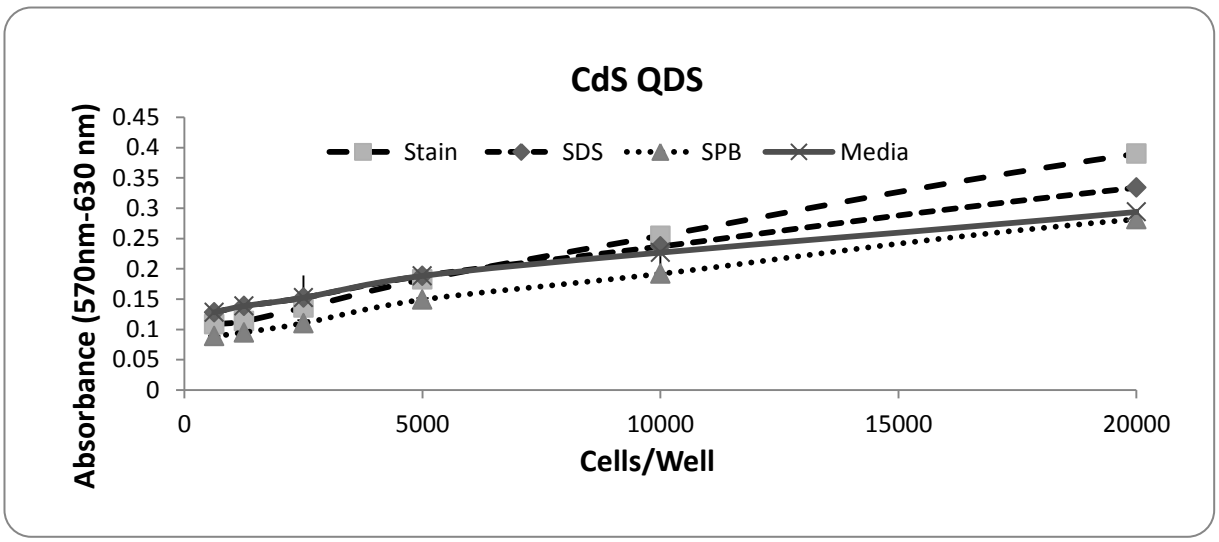
CdS QDS
Stain
SDS
SPB
Media
Absorbance (570nm-630 nm)
0.45
0.4
0.35
0.3
0.25
0.2
0.15
0.1
0.05
0
0
5000
10000
15000
20000
Cells/Well

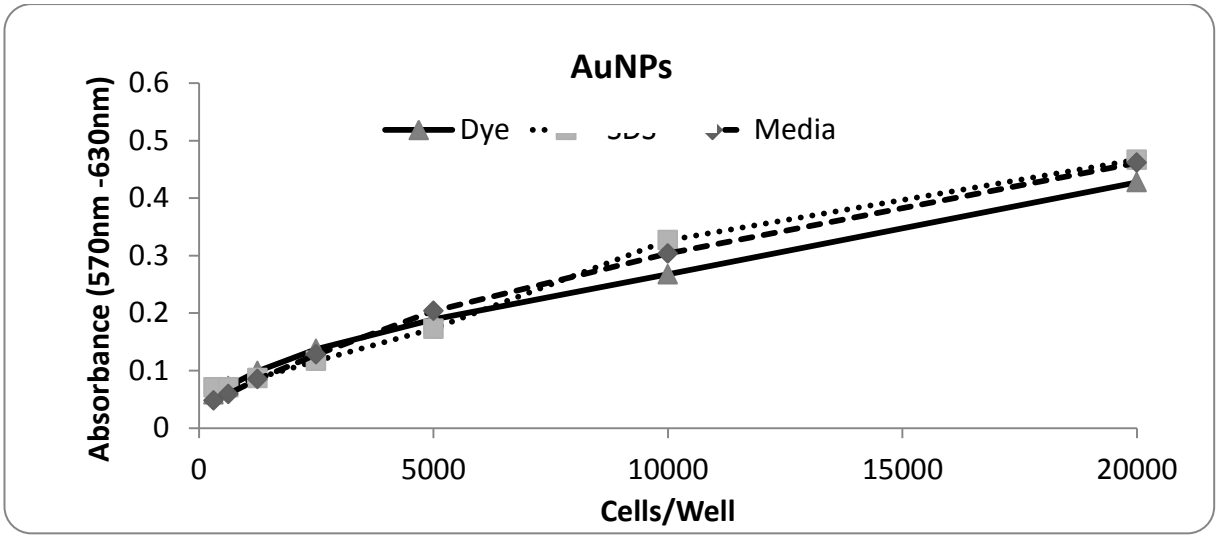

Figure 2.1: MTT standard curves generated using HaCaT cells in the absence and presence of nanoparticles (NPs), and the relevant solvents indicated. Media = untreated standard curve; MTT = NP added concurrently with MTT; SDS = NP added concurrently with SDS; water, DMSO, ethanol and SPB = solvent controls with no particles added.

2.3.1 Particle Interference-MTT Assay

Of the eight NPs examined for potential interference with the components of the MTT assay, trisilanol phenyl POSS and trisilanol isooctyl POSS resulted in a significant alteration in the MTT standard curve (Figure 2.1). There were decreases in OD for ≥10,000 cells/well when the particles were added with either MTT or SDS. These changes were significant ($p \leq 0.05$). As can been seen in Figure 2.1, there were smaller non-significant changes for ethanol and trisilanol cyclopentyl POSS when added with SDS in MTT.

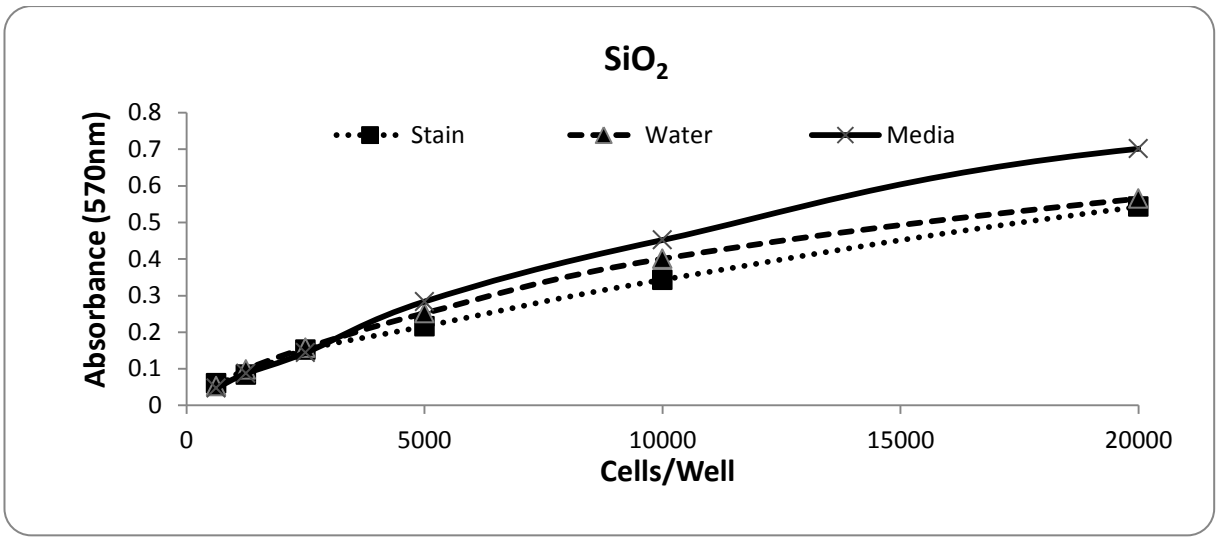
SiO2
Absorbance (570nm)
0.8
0.7
0.6
0.5
0.4
0.3
0.2
0.1
0
Stain
Water
Media
0
5000
10000
15000
20000
Cells/Well

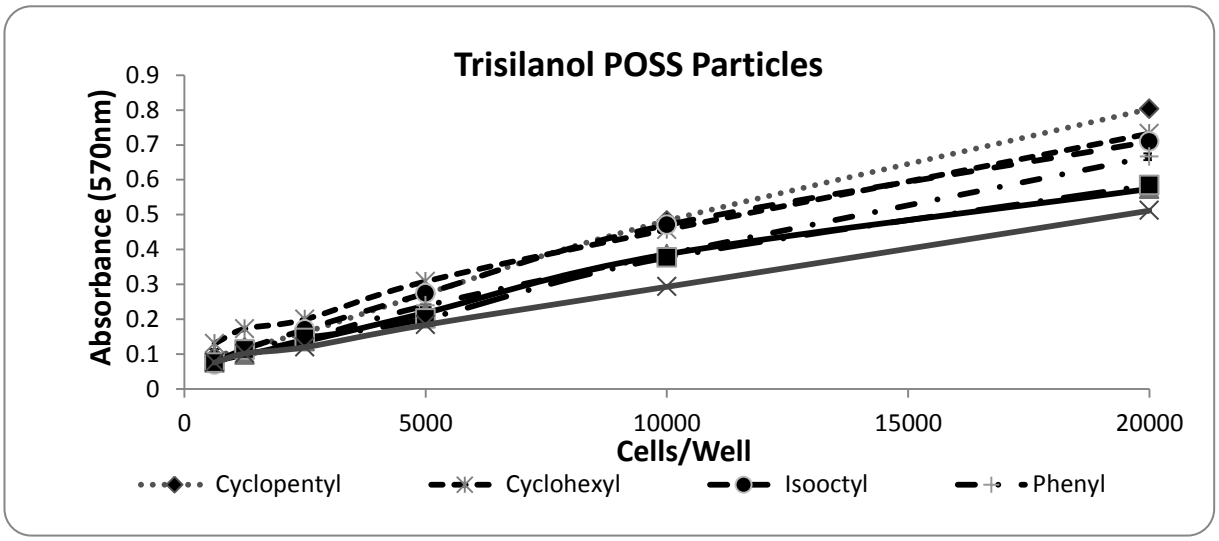
Trisilanol POSS Particles
Absorbance (570nm)
0.9
0.8
0.7
0.6
0.5
0.4
0.3
0.2
0.1
0
0
5000
10000
15000
20000
Cells/Well
Cyclopentyl
Cyclohexyl
Isooctyl
Phenyl

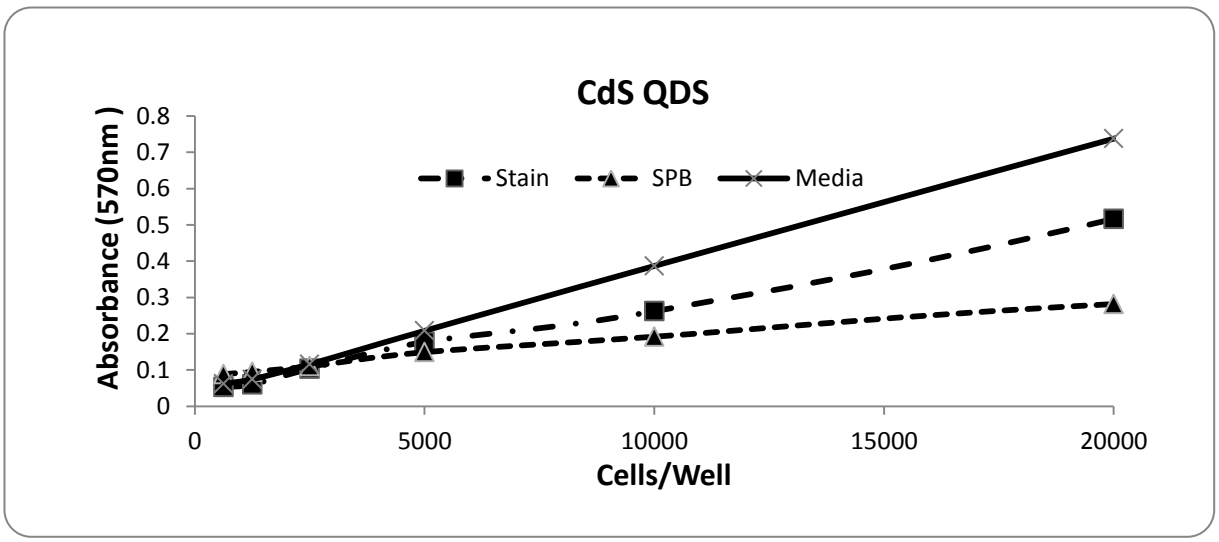
CdS QDS
Absorbance (570nm)
0.8
0.7
0.6
0.5
0.4
0.3
0.2
0.1
0
Stain
SPB
Media
0
5000
10000
15000
20000
Cells/Well

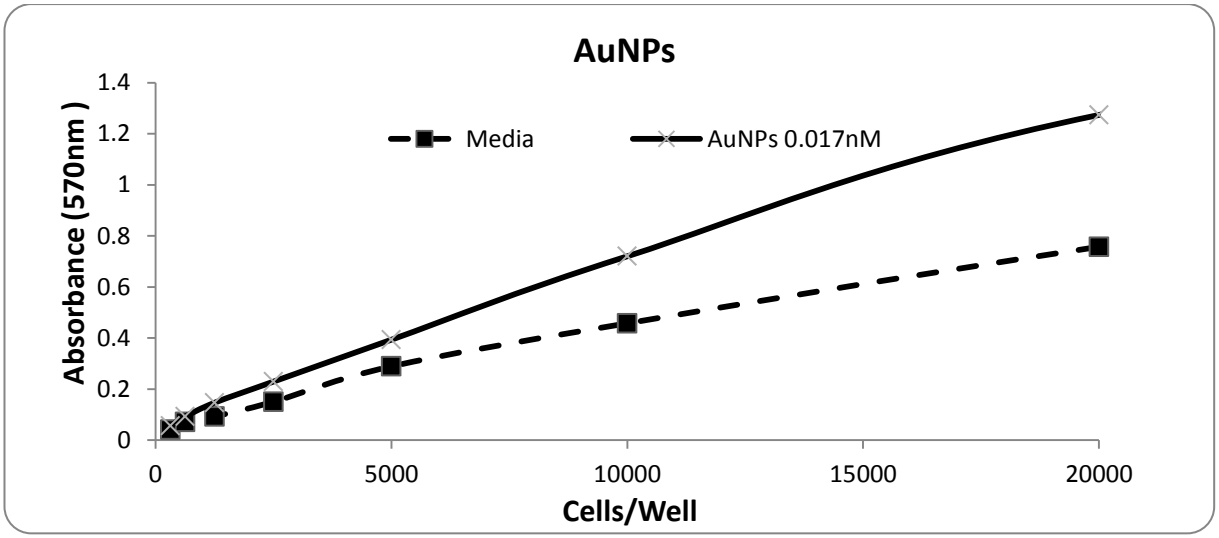

Figure 2.2: Crystal violet standard curves generated using HaCaT cells in the absence and presence of nanoparticles (NPs), and the relevant solvents indicated. Media = untreated standard curve; stain = NP added concurrently with crystal violet; SDS = NP added concurrently with SDS; water, DMSO, ethanol and SPB = solvent controls with no particles added.

2.3.2 Particle Interference-Crystal Violet Assay

Altered OD values in the crystal violet assay standard curves were observed when NPs and solvents were added to the assay plates. Standard curves for the solvent controls of SiO_2, trisilanol isooctyl, cyclohexyl and phenyl showed similar OD readings to the NPs (see Figure 2.2). For all particles, the differences between control standard curve media OD values and the OD values with NPs increased as cell densities (cells/well) increased. AuNPs significantly shifted the crystal violet standard ODs. In contrast, for sio_2 and trisilanol cyclopentyl POSS there was no significant change in the shape of the crystal violet standard curve when the particles of the negative solvent were present ($p \leq 0.05$).

2.3.3 Carbon Black Interference Assay (Positive Control)

In the current study, 10 mg/mL reduced the absorption values of the MTT and crystal violet assay standard curves (Figure 2.3). In the MTT assay, for the solvent control dimethyl sulfoxide (DMSO), there was no effect; when carbon black was added with the MTT or SDS there was a small non-significant decrease in the OD between 20^3 and 10^3 cells/well. In contrast, the effect of the solvent control in the crystal violet assay was

a significant decrease in the ODs for all values ≥5000 cells/well. The standard curve in the presence of carbon black was the same as that for DMSO. After 1-h exposure to carbon black, the particle was not seen in the cytoplasm of HaCaT cells; however, it was seen after 24-h exposure (Figure 2.4).

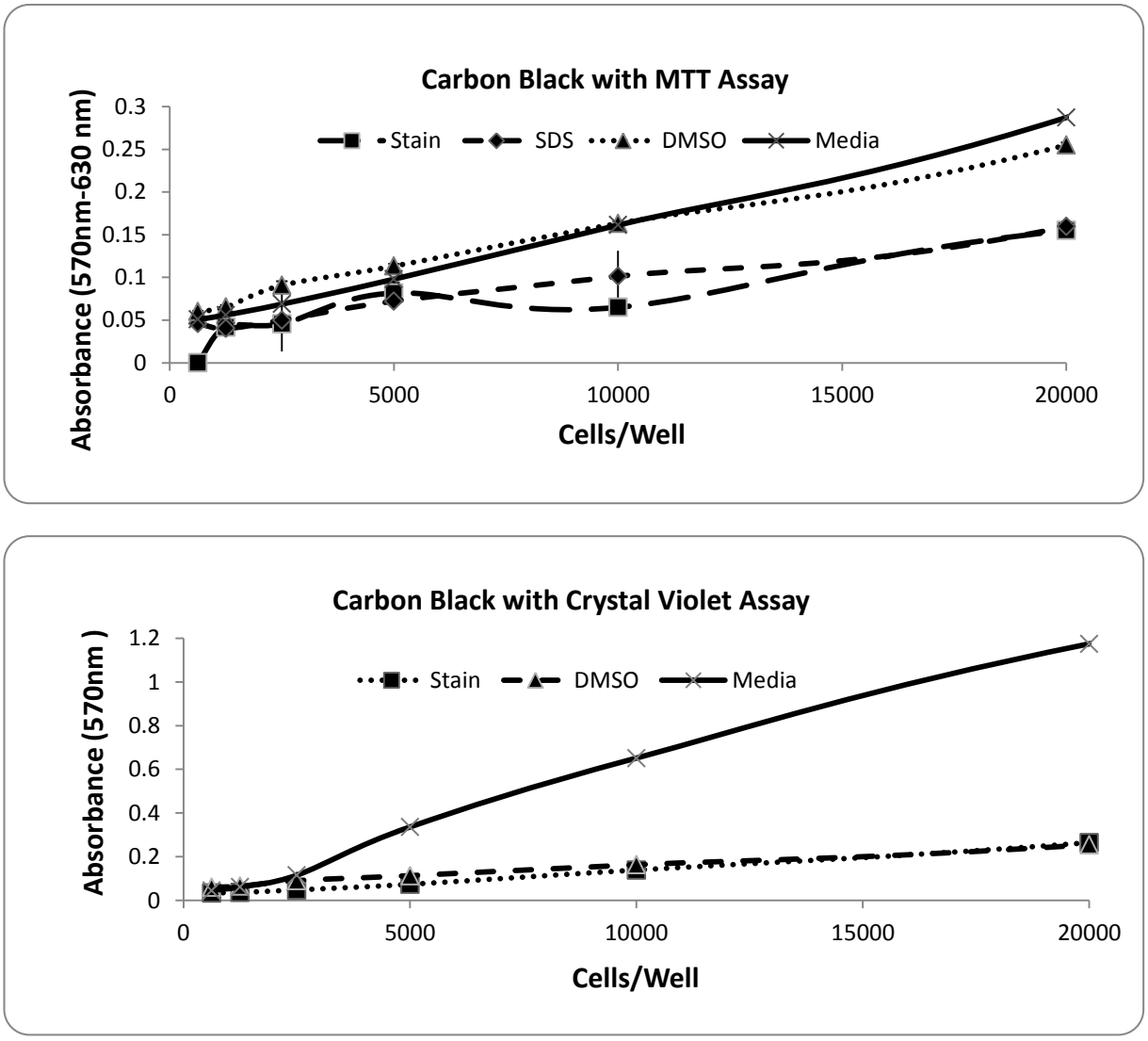

Figure 2.3: Absorbance (optical density) versus cells/well obtained from the MTT and crystal violet assay using HaCaT cells. Media = no changes to standard curve; DMSO = DMSO added with MTT or crystal violet stain; dye and stain = carbon black at 10 mg/mL added with MTT and crystal violet; SDS = added with media and carbon black.

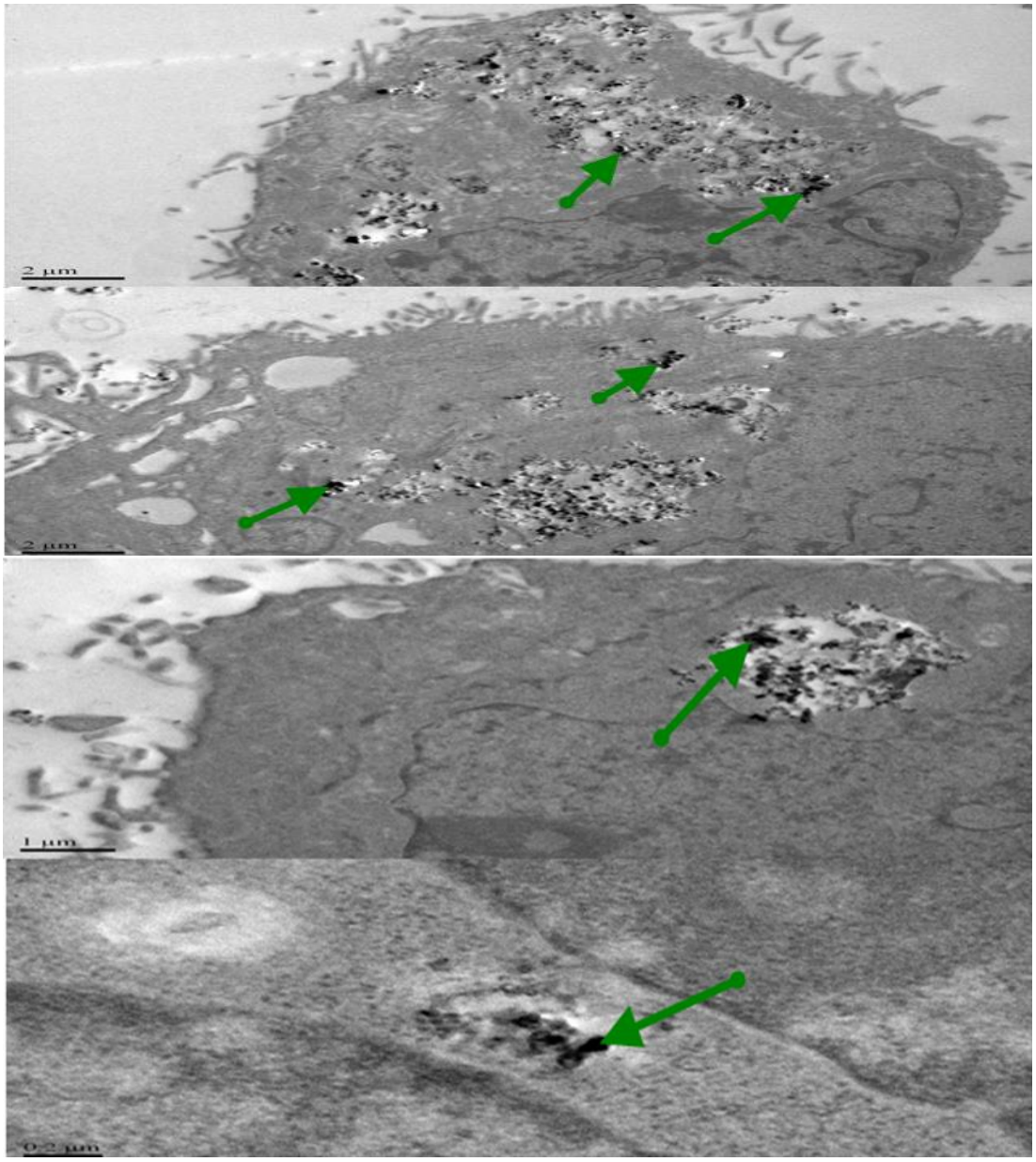

Figure 2.4. Carbon black as can be seen primarily in the cytoplasm of the cells after 24 h using transmission electron microscopy. Green arrows indicate particle accumulation in the cytoplasm. Bar = 2, 1, 0.2 µm.

2.4 Discussion

Single-walled carbon nanotubes (SWCNTs) and a variety of carbon-based nanomaterials interact in common cytotoxicity assays, such as MTT and crystal violet assays, and could interfere with fluorescence/absorption data used to evaluate the cytotoxicity level (Wörle-Knirsch et al., 2006). There are few data on the effect of NPs on cell proliferation and viability as evaluated using *in vitro* assays (Rajapakse et al.,

2013; Suresh et al., 2012). Thus, this study related the detection of NP interference principally with previous research on SWCNTs and metal oxide NPs (see section 2.1).

Wörle-Knirsch et al. (2006) reported that when human bronchoalveolar carcinoma A549 cells were exposed to SWCNTs, there was a false strong cytotoxic effect within the MTT assay after 24 h that reached approximately 50%; however, the same treatment with SWCNTs, but with the cell proliferation reagent WST-1, did not reveal cytotoxicity. Thus, SWCNTs appear to interfere with some tetrazolium salts such as MTT but not with others such as WST-1. The effect of these NPs does not seem to be on the enzymatic reaction but due to the insoluble nature of MTT formazan.

Despite substantial research effort, the cellular responses to nanomaterials are often variable and even contradictory (Sohaebuddin et al., 2010). Additionally, the relationships between nanomaterial properties and responding cell types are not well understood (Sohaebuddin et al., 2010). These effects were studied in an *in vitro* study using three cell lines of different origins (RAW 264.7 murine peritoneal macrophages, human telomerase reverse transcriptase [hTERT] and 3T3 fibroblasts) and comparing nanomaterials of various compositions (multi-wall carbon nanotubes [MWCNTs], SiO_2 and TiO_2) and size (MWCNTs of diameter <8 nm, 50 nm, 20–30 nm; but constant length of 0.5–2 μm) to detect the influence of size and composition on toxicity assessment (Sohaebuddin et al., 2010). Nanomaterial composition and size showed a distinct role in the cellular response. Additionally, the response varied between cell types and was more likely to be attributed to the physiological function of the type of cell origin Moreover, depending on the exposed cell type, the same materials caused different intracellular responses and had potentially different mechanisms of toxicity. These findings both emphasise the priority of analysing the effects of NPs in the most related exposure model and uphold the idea that NP engineering methods should be focussed on the cell types that are likely to be exposed to the particles.

Applications *in vitro* and inhalation studies *in vivo* have been known to yield divergent results. The aim is to discover why some particles yield strong positive cytotoxicity results in some *in vitro* assays but not others. Such conflicting data are the subject of investigation in the current research on the presence of particles and their potential interference with the MTT and crystal violet assays. Four trisilanol POSS particles with similar compositions, shape and diameter were synthesised to compare with CdS QDs,

SiO_2, AuNPs and the control carbon black at different composition size, shape and diameters. Interactions of trisilanol cyclopentyl POSS, trisilanol cyclohexyl POSS, SiO_2, CdS and QDs particles were clearly observed not to interfere with standard curves via the MTT dye as compared with carbon black (Figures 2.1 and 2.3). However, trisilanol phenyl POSS, trisilanol isooctyl POSS and AuNPs gave similar results with carbon black (Figures 2.1–2.3).

In a recent study, the influence of structure, surface and polymer compatibility on composite morphology and bulk properties of POSS particles was examined. Nylon 6-clay hybrid (NCH) was chosen as the matrix polymer (Sohaebuddin et al., 2010). Two POSS structures—one being a fully condense nonpolar octan-substituted octaisobutyl-POSS cage and the other an open cage polar trisilanol phenyl POSS—were scattered over the nylon matrix at different concentrations (Sohaebuddin et al., 2010). Variation was observed in the dispersion, surface characteristics, bulk (thermomechanical) properties and solubility in the polymer. The variation in POSS particle interference may be attributed to the alteration of POSS particles after being dispersed in suitable matrices; therefore, the results for POSS with the MTT assay highlight the potential to clearly design POSS nanocomposites with particular surface enhancement capabilities via the control of the POSS chemical structure.

The crystal violet stain assay gave different results from the MTT assay, with the exception of carbon black, which interfered with both assays (Figures 2.2 and 2.3). The differences may be due to particle interaction with the stains or with the HaCaT cells. HeLa cells were used as a bioindicator of cell viability in an *in vitro* assay method that combined dyes WST-1, NR and crystal violet (Wang et al., 2005). The joined cell viability assay using WST-1, NR and crystal violet presented an absorbance that correlated linearly with the number of cells over the range 1,000–50,000 cells/well (Ishiyama et al., 1996). This suggests that human cell lines interact linearly with crystal violet and that HaCaT cells are not causing the reduction in OD values with crystal violet as seen in our study.

Due to their small size and SA, insoluble NPs are minimally affected by gravitational forces; therefore, cells may not be exposed to the majority of NPs in suspension (Jiang et al., 2009; Lison et al., 2008). In contrast, particles may aggregate at the bottom of a culture vessel, preventing staining of cells by crystal violet (Kendall et al., 2011).

Carbonaceous material and several metal oxide particles interrupt light through spectral regions, which could affect the outcome of the assay (Ju-Nam and Lead, 2008). Mass concentration and composition are the main cause of spectral absorbance (Jang et al., 2001). Carbon black and single-wall nanotubes decrease the tetrazolium compound in XTT (2,3-bis-(2-methoxy-4-nitro-5-sulfophenyl)-2h-tetrazolium-5-carboxanilide) and MTT assays even in the absence of cells. Further, silver NPs (AgNPs) interfere with the LDH enzyme, leading to false vaiablity assessment (Belyanskaya et al., 2007; Monteiro-Riviere et al., 2009).

Monteiro-Riviere and Inman (2006) examined the effect of carbon black of different sizes on adult human epidermal keratinocytes (HEKa) using the NR (Wang et al., 2005) and MTT assays (Chang et al., 2006). Four types of carbon black particles were examined. Conflicting results were reported across the cytotoxicity end-points at 0.1–0.4 mg/mL, suggesting the adsorbing properties of carbon were interfering with the components of the assays. This could be due to particle dispersion or agglomeration (Pegel et al., 2008). Variation in particle dispersion has recently been demonstrated to have an important role in nanomaterial toxicity (Pegel et al., 2008). Sohaebuddin et al. (2010) assessed the size distribution of nanomaterials using DLS. Apparent particles increased in both media and PBS. For example, MWCNT >50 nm at 10 µg/mL increased to 100 µg/mL after dispersal in both media and PBS. Compared with similar particle composition, SiO_2 did not show a reduction in formazan and solubilising solution while CdS QDs informed overlap with MTT and SDS. Binding of particles with crystal violet stain was observed to reduce the OD readings for most of the particles tested, except AuNPS. This could be due to the particle composition, size and SA. In this study, particle interruption was tested with cells using TEM. The 24-h exposure of carbon black at 10 mg/mL revealed aggregation in the cytoplasm but not in the nucleus of HaCaT cells (Figure 2.4).

In conclusion, the interference of particles does not seem to affect enzymatic reactions of HaCaT cells but does interrupt the insoluble nature of MTT formazan and crystal violet. These findings strongly suggest that verifying cytotoxicity data with independent test systems is necessary for this new class of materials (nanomaterials). TEM was chosen to verify disruption of cells by particles. Clear reference material was needed to evaluate the interference with fluorescence/absorption in *in vitro* assays; therefore,

carbon black was chosen. Nanomaterial cytotoxicity could produce artefacts if they are not tested in combination with screening for interruption of insoluble formazan and crystal violet dyes. This study demonstrates that interference assays need to be included as an important part of any screening of novel NPs for potential cytotoxic hazard.

Chapter 3: Amorphous Silica Nanoparticles Show Concentration and Time-dependent Toxicity on Human HaCaT Cells

Abdulmajeed G. Almutary [1], Barbara J. S. Sanderson [1], Amanda V. Ellis [2]

Authors Contribution

AA carried out the experimental work, analysed the data and drafted the manuscript. BJSS participated in data analysis, design etc. AE participated in the design of the study and reviewed the manuscript and gave her intellectual input. All authors read and approved the final manuscript.

Abstract

The wide use of nanomaterials in medicine and biology and the unknown cytotoxicity of some nanoparticles heighten the demand for health and safety guidelines. The creation of these guidelines relies on experimental investigation to inform guidelines to eliminate the risk of exposure from newly synthesized nanoparticles. Skin contact of nanoparticles can cause skin cancer; therefore, the focus of this study was to identify the cytotoxicity of these particles to skin cells in an in vitro model. The toxicity of 12-nm amorphous silica (SiO2) nanoparticles following 4, 24 and 48h exposure was investigated using a human keratinocyte cell line (HaCaT) with [3-(4,5-dimethylthiazol-2yl)-diphenyltetrazolium bromide] (MTT) and crystal violet assays. Eleven concentrationsof 12-nm SiO2 ranging between 0.05-10 mg/mL were tested. At 4, 24 and 48h exposure, a dose dependent increase in cell killing with increasing concentration were observed when screened with the MTT assay. At 24h for concentrations ≥ 2 mg/mL, relative survival decreased when assayed by the MTT assay and relative cell number decreased when assayed with the crystal violet assay. After 48htreatment, cytotoxicity was observed at every treatment concentration assessed with the MTT and crystal violet assays. The level of cytotoxicity was also time dependent (4, 24, 48h)at every concentration. The level of cytotoxicity after 48h treatment was equal to or less than that of cell population streated for 24h. Silica nanoparticles are toxic to cultured human skin cells at a concentration as low as 0.05 mg/mL for 48h treatment

when screen by the crystal violet assay. When nanoparticles of consistent structure and surface area are used to treat human cells in culture, results varied between two well recognised colourimetric bioassays. However, with both assays, silica nanoparticles are toxic to human skin cells in vitro and toxicity is both concentration dependent and time dependent.

3.1 Background

The rapid development of nanotechnology has produced a myriad of engineered nanomaterials. Nanoscale particles have been used in many areas including chemical, medical research and related industries. The potential hazard arising from nanomaterials has led to the study of their toxicological effects on human health and the environment (Colvin, 2003; Donaldson et al., 2006; Hardman, 2006; Nel et al., 2006; Oberdörster et al., 2005). Although some nanomaterials such as QDs and carbon nanomaterials have been intensively studied toxicologically, other engineered nanomaterials have not been assessed in this way.

This study focussed on amorphous silica NPs. Exposure to silica is linked to the development of lung cancer, and in 1997, the International Agency for Research on Cancer (IARC) classified inhalation of crystalline silica at occupational sources as a group 1 human carcinogen (Linch et al., 1998; Murphy and Sethi, 2002; Schottenfeld and Beebe-Dimmer, 2006). The use of amorphous silica in nanotechnology has been an important part in bioanalysis and imaging, diagnostics, drug delivery and gene transfer (Barbe et al., 2004; Luo et al., 2004; Wang et al., 2005, 2006; Zhao et al., 2004). This adds to the increasing industrial exposure to silica NPs during production, transportation, storage and consumer use, through which human exposure and environmental burden are obviously increased. The National Institute of Occupation Safety and Health (NIOSH) recommended the limit of exposure to crystalline silica as 0.05 mg/m^3. However, miners are exposed at levels equal to or greater than this (Yassin et al., 2005). Therefore, it is conceivable that amorphous silica could enter the human body through all possible routes, including inhalation, oral, intravenous injection and transdermal delivery. In the current study, the HaCaT cell line was chosen as an ideal cell model for studying dermal toxicity (Boukamp et al., 1988). To govern the safe use of silica in the future, it is important to gather toxicity information by testing the *in vitro* and *in vivo* properties of amorphous silica (Zhang et al., 2010). Recently, two studies

revealed that amorphous silica may present toxicity concern at high doses in a number of organs (Chang et al., 2007; Lin et al., 2006). A549 cells were exposed to 15-nm or 46-nm SiO_2 NPs for 48h at dosage levels of 10–100 μg/mL and decreased cell viability was observed in a dose-dependent manner [26]. The concentrations chosen for this study were based on previously published *in vitro* and *in vivo* studies [26, 27]. This chapter investigates the response of the HaCaT cell line to 11 concentrations of amorphous silica NPs (0.05–10 mg/mL) using the thiazolyl blue tetrazolium bromide (MTT) and crystal violet assays.

3.2 Materials and Methods

3.2.1 Chemicals

Silica NPs (12 nm [TEM], nanopowder and 99.8% trace metals) were purchased from Sigma Aldrich (Matsusaki et al., 2005). The NP characteristics are shown in Table 3.1. Culture media was RPMI with 10% heat-inactivated FBS (HYQ®, HyClone Laboratories, UT, USA) containing penicillin–streptomycin, MTT and β-nicotinamide adenine dinucleotide (NADH) at the concentrations specified below. General reagents were obtained from Sigma Chemical Company (St. Louis, MO, USA). The HaCaT cell line originated from the ATCC.

Table 3.1: The physical and chemical properties of silica nanoparticles (Sigma Aldrich).

Characteristic	Value
Assay	99.8% trace metal basis
Colour	colourless
Form	nanopowder
Primary particle size	12 nm (TEM)
Surface area (SA)	Spec SA 175–225 m^2/g (Steenland et al., 2003)
Formula	SiO_2
Molecular weight	60.08 g/mol
Boiling point	2230°C (lit.)
Melting point	> 1600C (lit.)
Relative density	2.6 g/cm^3

3.2.2 Cell Culture

The cells were grown in RPMI medium, pH 7.4, with 10% heat-inactivated FBS and a 1% antibiotic mixture of penicillin (10,000 units/mL) and streptomycin (10,000 µg/mL). The treatment media was the same as the growth media. The cells were seeded in a T-75 flask at 1×10^6 cells/mL in a total volume of 25-mL fresh medium. When the cells reached 70–80% confluence, they were trypsinised and sub-cultured (Schoop et al., 1999). The cells were maintained in a humidified incubator with 5% CO_2 at 37°C (Boukamp et al., 1988). The number of viable cells after trypsinisation was determined by Trypan Blue staining and counting using a haemocytometer.

3.2.3 Trypan Blue Cell Counting

For the cell counting method, an aliquot of 50 µL of cell suspension was mixed with 50 µL of Trypan Blue, and the number of cells in the flask was counted by a haemocytometer after trypsinisation (Dein et al., 1994).

3.2.4 SiO_2 Treatment

For the bioassays, HaCaT cells were seeded at 10,000 cells/well in 96-well, flat-bottomed microplates and then incubated overnight to allow adherence. Cells were exposed to SiO_2 at 11 concentrations (0.05, 0.1 , 0.5, 1.0, 1.5, 2.0, 4, 5, 7, 9 and 10 mg/mL) for 4, 24 and 48 h. Amorphous silica NP was diluted in fresh medium (stock at 20 mg/mL) and then mixed by vortexing for 5 min, followed by dilution to the required concentration with media. After exposure of the cells for the appropriate time, the suspension was removed and the cells were washed twice with PBS to remove excess SiO_2.

3.2.5 Bioassays

3.2.5.1 Crystal Violet Assay (Screening for Cell Adherence Phenotype)

Cells were stained with crystal violet, and live cells remained adhered to the plate while dead cells were washed away. Plates for the crystal violet assay included six technical replicate wells per treatment. After treatment (see section 3.2.4), the plates were washed and 50 µL of crystal violet stain was added and incubated at room temperature for 15 minutes. The stain was washed off with demineralised water and the plates were

left to dry overnight. A 33% (v/v) acetic acid solution was then added and the OD at 570 nm was read within minutes using an ELISA reader. Three biological replicates were carried out for each treatment experiment. The results were expressed as percentage viability compared with the untreated control.

3.2.5.2 MTT Assay (Screening for Metabolic Functioning)

The cytotoxicity of silica NPs was determined using the MTT assay as described previously (Mosmann, 1983; Young et al., 2005). Cells (1×10^4) were seeded in a volume of 100 µL into 96-well, flat-bottomed microplates. MTT was added to each well at 0.5 mg/mL, and then plates were incubated at 37°C for 4 h, after which 80 µL of 20% SDS in 0.02 M HCl was added to each well. The plates were kept in the dark at room temperature overnight. The OD was read on an ELISA reader at 570 nm, with 630 nm as the reference wave length. For each experiment, a standard curve was run to convert the OD values to cells/well.

3.3 Statistical Analysis

The data were analysed as mean ± SE of at least three independent experiments using one-way ANOVA and Tukey–Kramer multiple comparisons tests using SPSS (version x8)) software to compare exposure groups.

All comparisons were considered significant at $p < 0.05$.

3.4 Results

The silica particle size was approximately 12 nm when measured by TEM (Sigma Aldrich). Interference assays were carried out for the MTT and crystal violet assays. No interference was observed (data not shown). HaCaT skin cells were exposed to silica NPs at increasing concentrations at three exposure time points. At each given time, there was no significant concentration-dependent cell death. For example, no significant difference in concentration dependency was observed for the 4-h treatment when assayed with the MTT assay or after crystal violet (Figures 3.1 and 3.2). Decreases in relative viability and relative cell numbers were observed with increasing concentrations after the 24-h and 48-h treatments; however, the decreases were not statistically significant (Figures 3.1 and 3.2). For a given exposure time, there was concentration-

dependent death. At 4-h exposure, there was a concentration-dependent increase in cell death only with MTT assays. At 24 h, cell death increased to 70% and was obvious with the crystal violet assay. At 48 h, cell death up to 80% was observed clearly in the crystal violet assay.

There was a time-dependent increase in cell death that was observed when assayed with the crystal violet assay only (Figure 3.1). This was significant when assay using the crystal violet assay cell number decreased to 75%. At each dose concentration, the change from 4 h to 24 h to 48 h was examined.

The 4-h treatment, when assayed for metabolic activity with the MTT assay, showed very little change with dose (Figure 3.1). However, for most concentrations following 4 h when assayed for adherence with the crystal violet assay there were increases in relative cell number (Figure 3.2). This was also observed for low concentrations at 24 h (0.05–2 mg/mL).

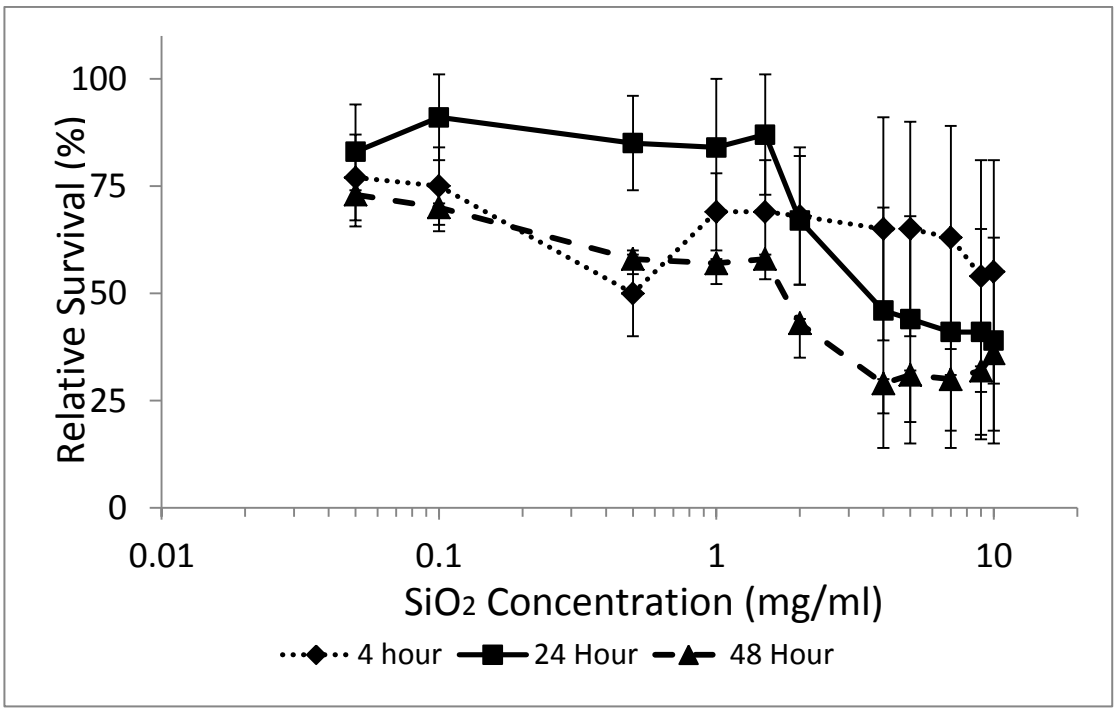

Figure 3.1: The effect of treatment of HaCaT cells with silica particles assessed using the MTT assay. Data are shown as relative survival (%) compared with the untreated control and are presented as mean ± SE; n = 3, except for 2 mg/mL where n = 6.

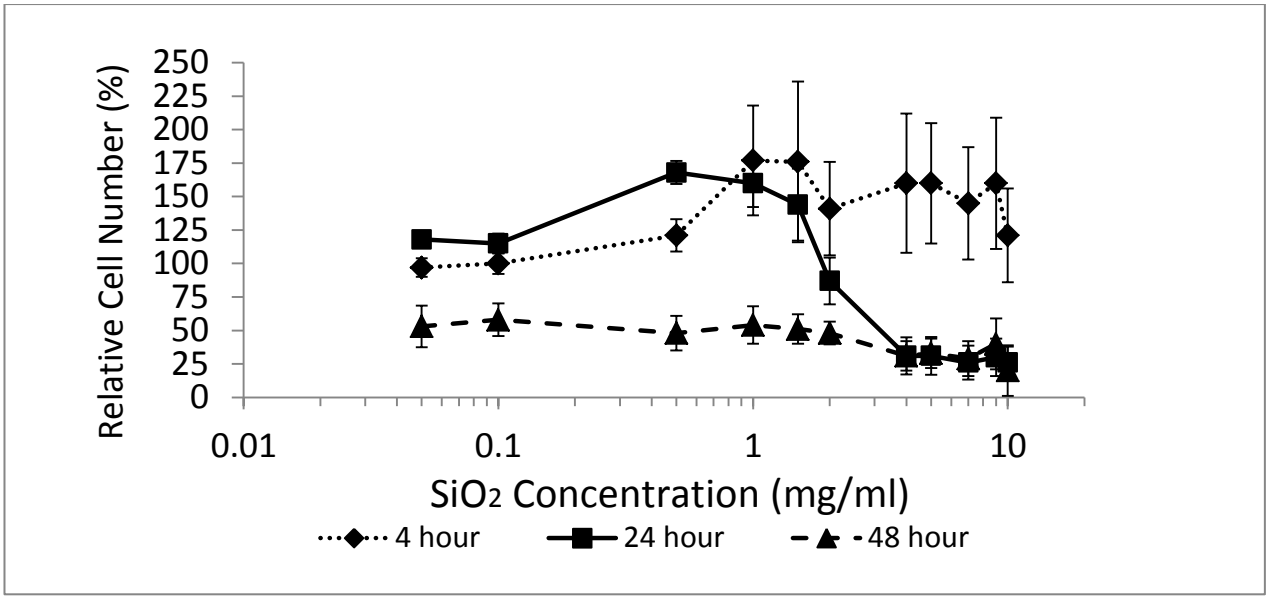

Figure 3.2: The effect of treatment of HaCaT cells with silica particles assessed using the crystal violet assay. Data are shown as relative cell number (%) compared with the untreated control and are presented as mean ± SE of three separate experiments, except for 2 mg/mL where $n = 6$. All treatments with the crystal violet assay were significantly different from the untreated control (100%) at $p < 0.05$, except 1.5 mg/mL.

3.5 Discussion

The immortal HaCaT cell line exhibits similar biological properties to those of normal human keratinocytes and is therefore a useful cell model for studying dermal toxicity (Yang et al., 2010). Particle size and concentration influence cytotoxicity assessment; also, different cell lines respond differently to the same particle at the same concentration (Zhu et al., 2008). A recent study on AgNPs (20, 80 and 113 nm) examined exposure to the RAW 264.7 cell line, L929 mouse fibroblasts, D3 murine embryonic stem cells and mouse embryonic fibroblasts (MEF-*LacZ*) (Park et al., 2011). The AgNPs at 20 nm were more toxic than the larger NPs. Further, not all cell lines were affected by the 20-nm NPs. Therefore, the ability of AgNPs to induce cell death is influenced by cell type and NP size.

A range of characteristics of NPs can influence their toxicity in *in vitro* biological systems, including cell culture systems (Brown et al., 2007; Brunner et al., 2006; Limbach et al., 2007; Pumera, 2011). The toxicity of NPs is also dependent on dose and duration of exposure (Lison et al., 2008; Napierska et al., 2009). Silica NPs, depending on their shape and dimension, are taken up by cells via different mechanisms of

endocytosis, and then undergo distinct intracellular processing until they are exocytosed (Park et al., 2011). Smaller particles are understood to be easier to internalise in cells than larger particles (Rothen-Rutishauser et al., 2006). This suggests that the 12-nm particles in the current study would have been internalised due to their small size. This warrants further investigation via such techniques as specialised microscopy.

A549 cells treated with 15 nm of silica NPs at doses of 10 and 100 μg/mL for 48 h showed dose-dependent decreased cell viability (Lin et al., 2006). Based on the MTT viability assay, a similar effect was observed for the 12-nm particle used in the current study (see Figure 3.1). It was observed that cytotoxicity was a function of (1) particle concentration and (2) duration of exposure. A similar result was observed with the crystal violet assay at higher doses and exposure times. At 4-h exposure, there was a dose-dependent increase in cell death, which was also seen at 24 h and at 48 h with an increased level of cell death (see Figure 3.2).

According to Drescher et al. (2011), silica particle cytotoxicity in the 3T3 fibroblast cell line was caused by silica concentration and the content of foetal calf serum (FCS). DLS revealed that the physical parameter of silica was affected by agglomeration (Drescher et al., 2011). Silica NPs induced less toxicity by decreasing relative viability in parallel with dosage concentration. In the current study, particle concentrations were altered across a wide range of exposure times. Silica particles at concentrations of 0.05–2 mg/mL produced gradual increased toxicity, which also increased with increasing time of exposure (Figure 3.1). A concentration of 2–10 mg/mL exhibited a further decrease in cell viability, which also increased with the duration of exposure. Chang et al. (2007) exposed WS1 and CCD-966sk human skin cell lines to silica for 48 h. The increase of particles mass concentration decreased the relative viability in both cell lines. At a concentration of 667 μM, cell viability decreased to approximately 80% of the control (Schoop et al., 1999).

In Figure 3.2, the relative cell number showed a gradual reduction over the time of exposure and concentration of treatment. Concentrations of 0.05–2 mg/mL decreased relative cell number at 48 h. Dosages of 2–10 mg/mL similarly had a toxic effect at 24 and 48 h. The cytotoxicity of silica in both assays showed variation in cell death but both confirmed that the mass concentration of silica particles will affect the cell population. The effect was most marked using the crystal violet assay as an end-point.

3.6 Conclusion

The MTT and crystal violet assay revealed that silica NPs become toxic to cultured human skin cells at the 11 concentrations tested here, and may also impede cell proliferation. The outcome of this study suggests that even with NPs of similar structure and dimensions, toxicity may vary even with the end-point measured in recognised colourimetric bioassays. This leads to the conclusion that toxicity is not dependent only on particle size and SA. Mass concentration and exposure time clearly influence the outcome. It is useful to carry out interference detection for colourimetric assays, as other work by my research group has suggested that other parameters may influence OD readings (data not shown).

Thus, the findings of this work demonstrate the importance of studying duration of exposure and NP concentration when studying additional cell lines for toxicity assessment of NPs.

Chapter 4: Toxicity of N-Nitrosodimethylamine and SiO_2 Nanoparticles Found in Wastewater Treatment to HaCaT and Caco-2 Cell Lines

Abdulmajeed G. Almutary[1], Barbara J. S. Sanderson [2]

Authors Contribution

AA carried out the experimental work, analysed the data and drafted the manuscript. BJSS participated in the design of the study and reviewed the manuscript and gave her intellectual input. All authors read and approved the final manuscript.

Abstract

NPs offer the possibility of safe removal of pollutants and microbes in water treatment and purification. Nowadays, NPs are used in the detection and purification of water from chemicals and biological substance such as metals (cadmium, copper, lead and zinc), nutrients (nitrate, nitrite ammonia and phosphate), bacteria, viruses, parasite and antibiotics. Metal-containing NPs are among the four classes of particles used commonly in water treatment. Membrane technologies such as ultrafiltration (UF), nanofiltration (NF) and RO have been widely used all over the world, especially for water treatment and desalination. NPs incorporated into membranes have gained attention due to their ability to enhance membrane permeability, mechanical properties and selectivity in some cases. However, these membranes are suspected to be subject to fouling, allowing NPs and other contaminants to reach waterways. This chapter examines the toxicity of SiO_2 NPs synthesised by the Stöber method and NDMA as a potent known carcinogen during chlorination on HaCaT and Caco-2 cell lines for 4, 24 and 48 h using MTT and LDH assays; further, the morphology and size of SiO_2 NPs was determined by SEM. After exposure to SiO_2 (concentrations of 0.05–2 mg/mL), 2 mg/mL of inactivated LDH was added to both cell lines; however, it did not reduce their metabolic activity in the MTT assay use. SEM revealed spherical and uniform SiO_2 particles of 200 nm in diameter. NDMA (concentrations of 0.1–1000 µg/mL) inactivated LDH leakage in HaCaT and Caco-2 as well as reducing the metabolic activity of HaCaT cells at 48-h exposure. The outcomes of this study suggest that a

concentration of SiO_2 <2 mg/mL used in water treatment can reduce the risk of nanomaterial toxicity to humans and possibly ecosystems. These results urge for more studies on the effect of nanomaterials in the aquatic environment and of human exposure to NPs.

4.1 Background

The rapid development of NP applications has resulted in enhanced processes of product manufacturing and development of products that reduce the concentrations of toxic compounds, and has assisted in the attainment of water quality standards and health advisories (Salata, 2004). Therefore, it is necessary to investigate the possible risks to humans related to these small particles during environmental exposure. Microfiltration (MF) and UF are some of the most effective methods for raw water treatment (Shen et al., 2011). The majority of UF membranes are formed by hydrophobic polymers such as polysulfone (PS), polyethersulfone (PES), polypropylene (PP), polyethylene (PE) and polyvinylidenefluoride (PVDF) (Shen et al., 2011). PES is the most commonly used polymer in UF membrane due to its excellent thermal and mechanical properties and chemical resistance. However, PES is hydrophobic in nature and is suspected to cause fouling (Darracq et al., 2015). The main interest in the clearing efficiency of NPs within sewage plants is to prevent nanomaterials from reaching the waterways (Dahle and Arai, 2015). Recently, the possible toxic effects of carbon nanotubes on aquatic species such as larval zebrafish (*Danio rerio*) and *Daphina magna* have been studied (Baun et al., 2008; Farré et al., 2009). Another study investigated the physiological changes and toxicity to *Daphina magna* exposed to TiO_2 NPs, which are one of the most important metal oxide NPs (Lovern et al., 2007). These studies urge clarification of the entrances of nanomaterials into the aquatic environment.

At this stage, little is known about nanomaterials reaching waterways (Lynch, 2016). Some studies have criticised standard wastewater treatment as it is poorly suited to capture nanomaterials (Lynch, 2016). Moreover, Wiesner et al. (2008) reported that waterways contaminated with nanomaterials from water desalination plants may become problematic (Wiesner et al., 2008). Due to the lack of experimental data, safe methods of nanomaterial disposal are not well understood (Thomas et al., 2006; Wiesner et al., 2008). Clearly, this will be problematic because there are insufficient data to explain the risk of inorganic NPs dispersed in the environment or public sewage

treatment plants. NDMA is well known for its carcinogenic properties (Halden, 2015; Sanagi et al., 2015). For many years, NDMA was used as a pesticide (nematicide), plasticiser for rubber, battery component, antioxidant, lubricant additive and in polymers (e.g. dimethylnitrosamine). Recently, studies have revealed that water treatment polymers such as poly(epichlorohydrin dimethylamine) and poly(diallyldimethylammonium chloride) may form NDMA if they come into contact with chloramine water (Zhang et al., 2008). In addition, NDMA is often used in research to induce cancer in mice (Bogovski and Bogovski, 1981). Thus, health concerns around this compound have been the focus for some industries after it was recognised in disinfection of drinking and wastewater containing chlorine and chloramines (Mitch et al., 2003). Recently, successful attempts have been made to add NPs to polymers in membrane synthesis for removing water contaminants (Kim and Van der Bruggen, 2010; Mahapatra and Karak, 2008).

Ceramic membranes have been made with catalytic NPs to produce synergistic effects on membrane enhancement (Kim and Van der Bruggen, 2010). However, other studies suggest that silica polymerisation in the presence of polyvalent cations and anions in RO systems are the cause of membrane fouling (Koo et al., 2001). RO is by far the most effective method of removing dissolved silica from brackish water. The present study investigates the toxicity of NDMA as a known water contaminant, and silica NPs as newly NPs used in membrane separation and found in high concentrations in brackish water (Patil et al., 2016). HaCaT and Caco-2 were exposed to NDMA and silica NPs; toxicity was determined using the MTT and LDH assays, and particle morphology was identified by SEM.

4.2 Materials and Methods

4.2.1 Reagents

All reagents were from Sigma Aldrich, Australia unless otherwise stated. These included MTT, NADH, β-nicotinamide adenine dinucleotide (NAD), phenazine methosulfate (PMS), trizma base, trizma HCl, lithium lactate and iodonitrotetrazolium chloride (INT). The culture mediums used were Dulbecco's Modified Eagle Medium (DMEM) for the Caco-2 cell line and RPMI for the HaCaT cell line with 10% heat-inactivated FBS, penicillin and streptomycin and Triton™ X-100 (positive control).

Millipore MQ water with resistivity = 18.2 MΩ.cm was used for all the experiments. NDMA solution was provided by Flinders University School of Chemical and Physical Sciences.

4.2.2 Preparation of SiO_2 Nanoparticles

Silica NPs were synthesised by the Stöber method (Ibrahim et al., 2010). One mL of the silica precursor tetraethyl orthosilicate (TEOS) at 98% concentration was added rapidly to a mixture of 95% ethyl alcohol (10 mL) and MQ water (3 mL). The reaction was allowed to proceed for 30 min with mild stirring at 50°C to obtain a homogeneous mixture. Subsequently, 1 mL ammonia solution (30%) was added drop-wise over an 8-min period with stirring. The mixture gradually changed from transparent to milky as the NPs formed. The mixture was then stirred for a further 2 h. The resultant precipitate was then centrifuged at 101,890 g and washed with MQ water four times. Finally, the silica particles were dried overnight at 75°C.

4.2.3 Nanoparticle Characterisation

SEM was performed on the silica NPs. The samples were sputter coated with a 10-nm layer of platinum using a Quorumtech K757X sputter coater (located at Flinders University, South Australia, Adelaide). Images of the sample were collected using CAMScan MX2500 SEM (located at Flinders University, South Australia, Adelaide) with a field emission source at an accelerating voltage of 10 kV.

4.2.4 Cell Culture

HaCaT and Caco-2 cell lines were obtained from the ATCC. HaCaT cells were grown in RPMI and Caco-2 cells in DMEM medium with 10% FBS and incubated at 37°C with 5% CO_2 in a humidified incubator. Cell growth started from 2×10^6 cells/mL and cells were sub-cultured every 2–3 days when confluence reached 60–70%.

4.2.5 Toxicity Assays

HaCaT and Caco-2 cells were seeded at 10,000 cells/well in a 96-well, flat-bottomed microplate and then incubated for 18 h to allow adherence. NDMA and SiO_2 were diluted in fresh medium. After incubation, cells were treated with six concentrations of silica NPs (0.05–2 mg/mL) and five concentrations of NDMA (0.1–1000 µg/mL) for 4,

24 and 48 h. The solution was removed and the cells were washed twice with PBS to remove excess SiO_2 residue.

4.2.5.1 MTT Experimental Procedure

The toxicity of SiO_2 and NDMA was determined by MTT assay as described in the literature (Mosmann, 1983; Young et al., 2005). Cells (1×10^4) were seeded in volume of 100 µL into 96-well, flat-bottomed microplates. MTT was added to each well at 0.5 mg/mL, and then plates were incubated at 37°C for 4 h, after which 80 µL of 20% SDS in 0.02 M HCl was added to each well. The plates were kept in the dark at room temperature overnight. Absorbance was read at a primary wavelength of 570 nm and a reference wavelength of 630 nm by an ELISA reader. In each experiment, a standard curve was run to convert the OD values to cells/well.

4.2.5.2 Lactate Dehydrogenase Leakage Assay

The leakage of LDH in HaCaT and Caco-2 cells was detected by LDH assay. Cells were plated into 96-well plates and exposed to concentrations of SiO_2 and NDMA as described in section 4.2.3. At the end of the exposure period, 50 µL of aliquoted cell medium was used for LDH activity analysis. The absorption was measured using an ELISA reader at a primary wavelength 490 nm and 630 nm as a reference wavelength. LDH assay experiments were performed in triplicate.

4.3 Statistical Analysis

The data were expressed as the mean ± standard deviation (SD) of at least three independent experiments using one-way ANOVA and Tukey–Kramer multiple comparisons test using SPSS (version x8) software to compare exposure groups. All comparisons were considered significant at $p < 0.05$.

4.4 Results and Discussion

Exposure of HaCaT and Caco-2 cell lines to monodisperse spherical SiO_2 (200 nm in diameter) for 4, 24 and 48 h did not interrupt cell growth. LDH leakage was clearly low at concentrations <2 mg/mL in both cell lines. Similarly, no tested concentrations reduced cell growth in either cell line according to the MTT assay compared with the positive control (Figure 4.1). Researchers have not been able to agree on dose and

physiochemical properties of NPs that could cause a biological response (Park et al., 2008). Some have related the toxicity of NPs to the particle's total weight; others to the number of particles per volume (Peyron et al., 2004). Recently, studies have suggested that the logical way to define particle toxicity is to calculate the dose based on the NP's total SA. Studies on SiO_2 NP_S have reported that the shape of the particle is the main cause of particle pathogenesis in lung disease (Bowman et al., 2012; Brown et al., 2007; Liu et al., 2014; Huang et al., 2012).

The ecotoxicological impact of SiO_2 NPs on freshwater fish is not completely understood (Priya et al., 2015). Therefore, the haematological, ionoregulatory and enzymological toxicity effect of silica NPs at concentrations of 1, 5 and 25 mg/L were evaluated on the freshwater teleost fish *Labeo rohita* (Priya et al., 2015). Exposure to silica NPs altered the values of haematological parameters such as haemoglobin (Hb) red blood cells, white blood cells and plasma electrolytes. Plasma electrolytes such as potassium, sodium and chloride levels, and Na^+/K^+ ATPase activity were shifted by all silica NP concentrations through all study exposure times. Moreover, the effect of the silica NPs was found to be time and concentration dependent (Priya et al., 2015). In another study, 12 fish cell lines taken from six species (rainbow trout, zebrafish, fathead minnow, haddock and American eel) were tested for metabolic activity using the AB assay (Vo et al., 2014). The toxicity of SiO_2 NPs (16, 24 and 44 nm in diameter) was related to physiochemical properties such as the size and temperature; it was also dose dependent and tissue specific. SiO_2 NPs (44 nm in diameter) at concentrations >100 µg/mL for 24-h exposure reduced the fish cell lines' viability by 50% (Vo et al., 2014). Smaller NPs (16 nm) were found to be more toxic than larger NPs. In addition to size-related toxicity, cells derived from external lining epithelial tissues (skin and gills) were more effected by SiO_2 NPs than were cells taken from internal tissues (brain, liver, intestine and gonads) (Vo et al., 2014). SEM images of the SiO_2 synthesised by the Stöber method showed a monodispersed spherical silica particle with a size of 200 nm in diameter (Figure 4.2).

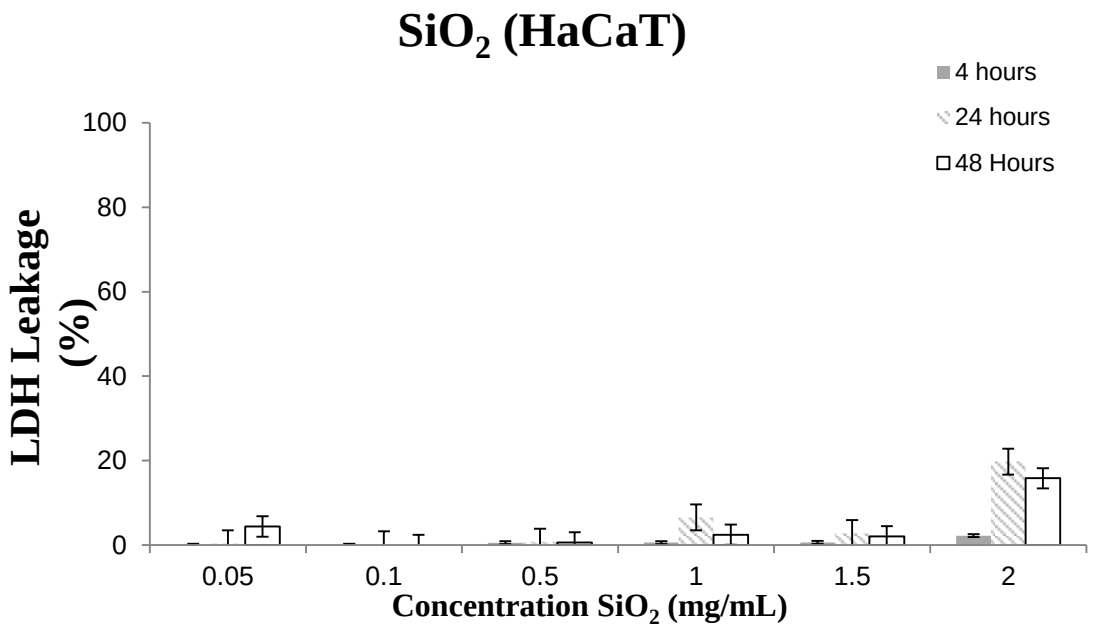
SiO2 (HaCaT)
4 hours
24 hours
48 Hours
LDH Leakage (%)
100
80
60
40
20
0
0.05
0.1
0.5
1
1.5
2
Concentration SiO2 (mg/mL)

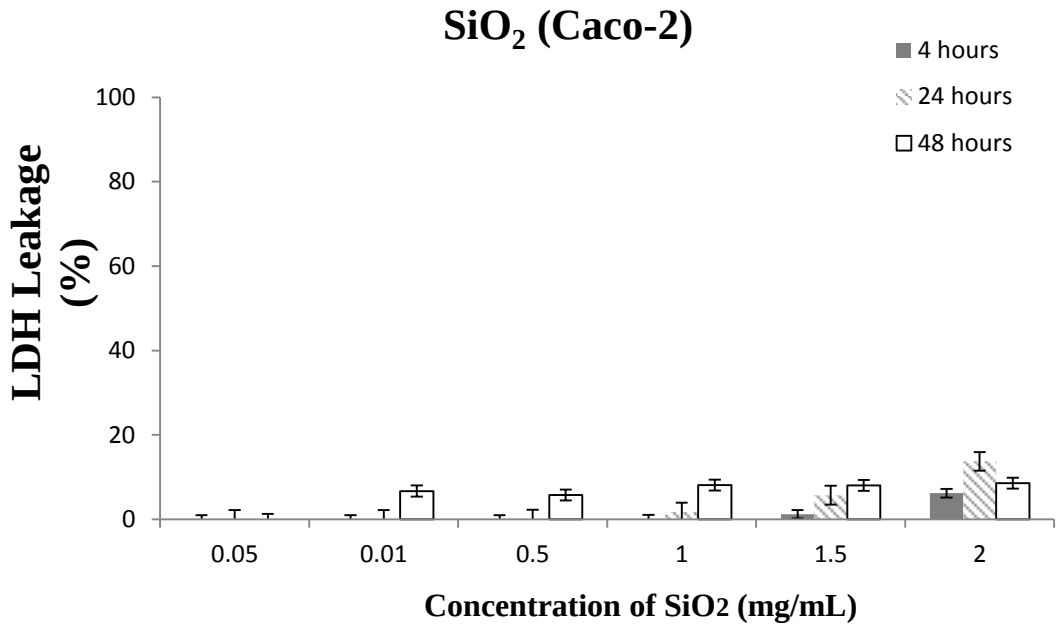
SiO2 (Caco-2)
4 hours
24 hours
48 hours
LDH Leakage (%)
100
80
60
40
20
0
0.05
0.01
0.5
1
1.5
2
Concentration of SiO2 (mg/mL)

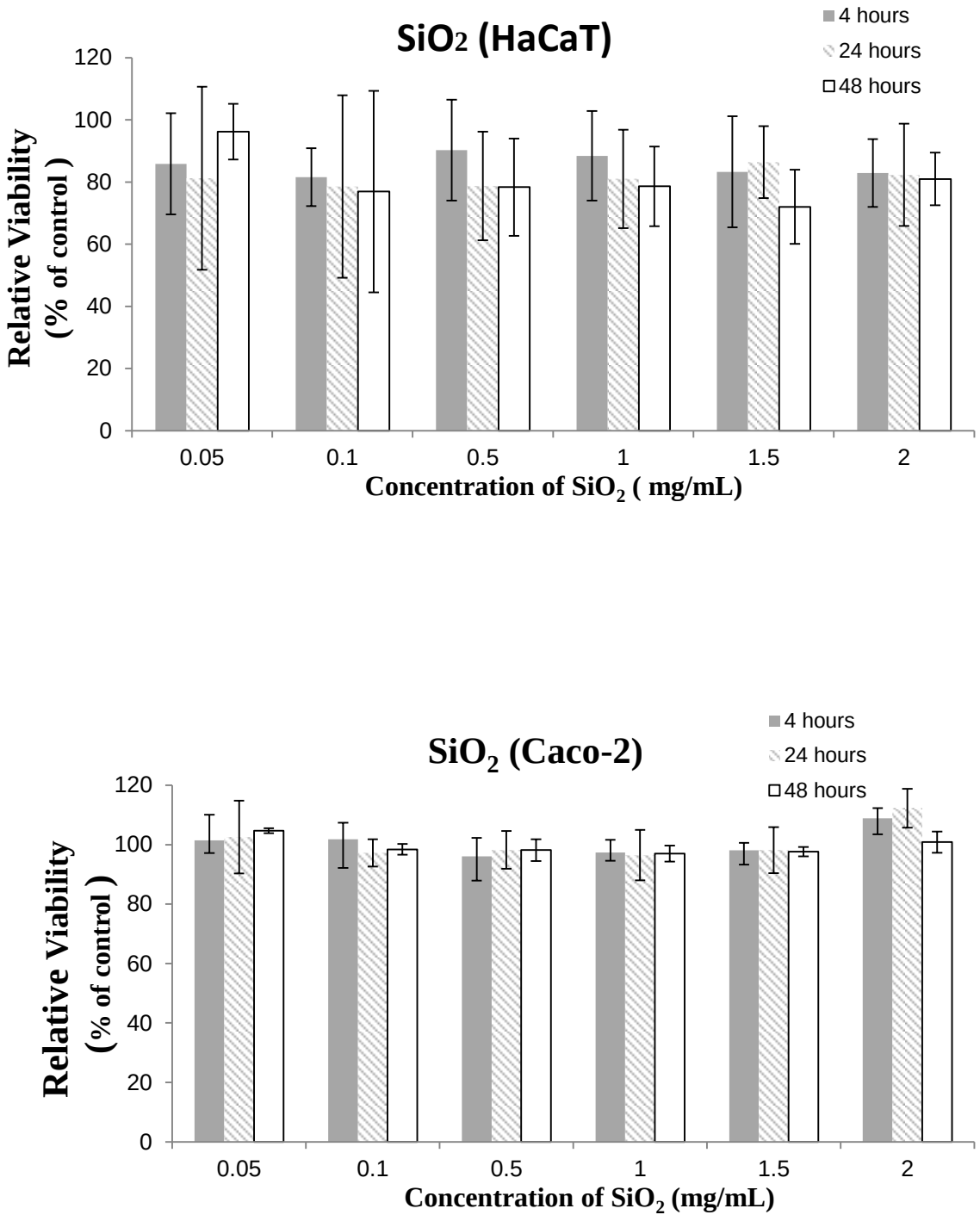

Figure 4.1: The effect of SiO_2 nanoparticles on HaCaT and Caco-2 cell viability using the MTT assay, and LDH leakage assessed by the LDH assay. HaCaT and Caco-2 cells were exposed to six concentrations of SiO_2. Data are expressed as means ± SD from three independent experiments. $p < 0.05$ compared with control group.

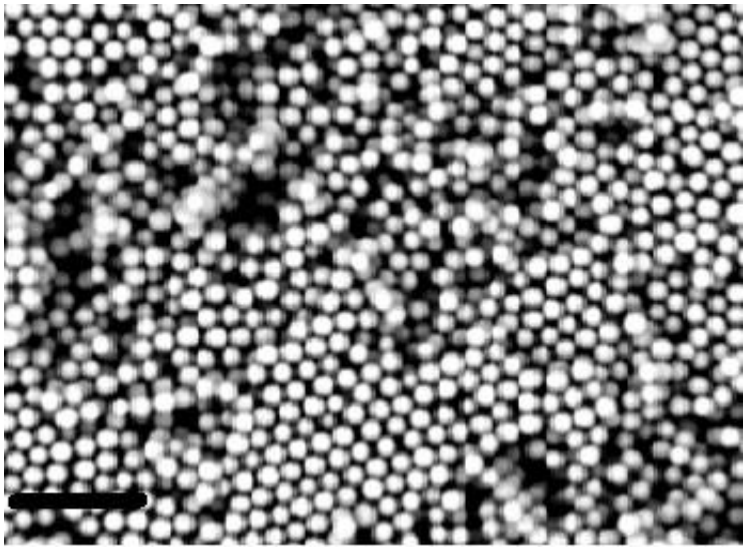

Figure 4.2: Scanning electron microscopy image of monodispersed SiO_2 nanoparticles (NPs); the scale bar represents 200 nm in diameter; the final formed NPs were spherical and uniform.

However, exposure to NDMA (concentrations 0.1–1000 µg/mL) activated LDH leakage in HaCaT and Caco-2 cell lines at all concentrations, and was most apparent at 4-h exposure. The LDH leakage due to NDMA reduced after 24 h and was only 5% at 48 h. In contrast, NDMA interacted with the metabolic activity of HaCaT cell lines at concentrations of 1µg/mL and higher after 48-h exposure, which clearly demonstrates toxic impact (Figure 4.3).

The NDMA formation potential (FP) test is a rapid and simple method to detect NDMA precursor concentrations in wastewater (Farré et al., 2011). This method was applied in tertiary wastewater treatment plants using UF–RO membranes. The results showed that the NDMA FP from a variety of water samples were in the range 350–1020 ± 20 ng/L (Farré et al., 2011). The fate of NDMA precursors was also investigated at two different points of advanced water treatment plants. The final results showed that more than 98.5 ± 0.5% of NDMA precursors were removed by RO (Farré et al., 2011). In California, one of the most commonly used herbicides is the phenylurea herbicide Diuron, which has been consistently found in the state's water sources, and its structure might make it an NDMA precursor. NDMA precursors were found consistently even in the absence of added ammonia, which is a cause of nitro-nitrogen formation during chloramination. This is due to both nitrogen atoms being donated by Diuron during chlorination, even when there is no ammonia present.

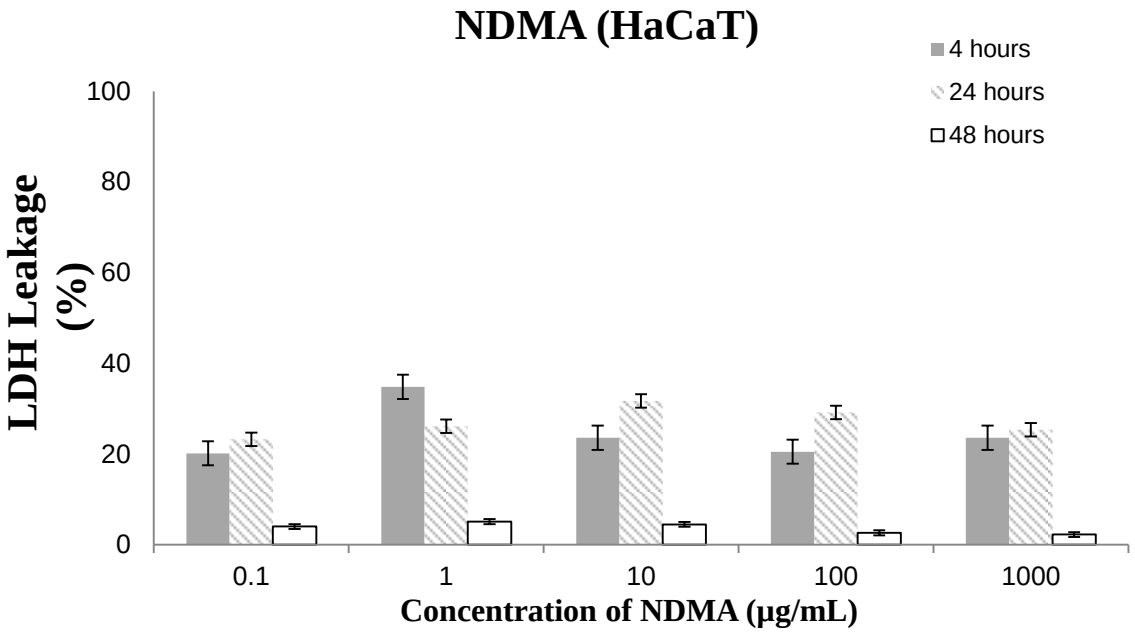
NDMA (HaCaT)
4 hours
24 hours
48 hours
LDH Leakage (%)
100
80
60
40
20
0
0.1
1
10
100
1000
Concentration of NDMA (µg/mL)

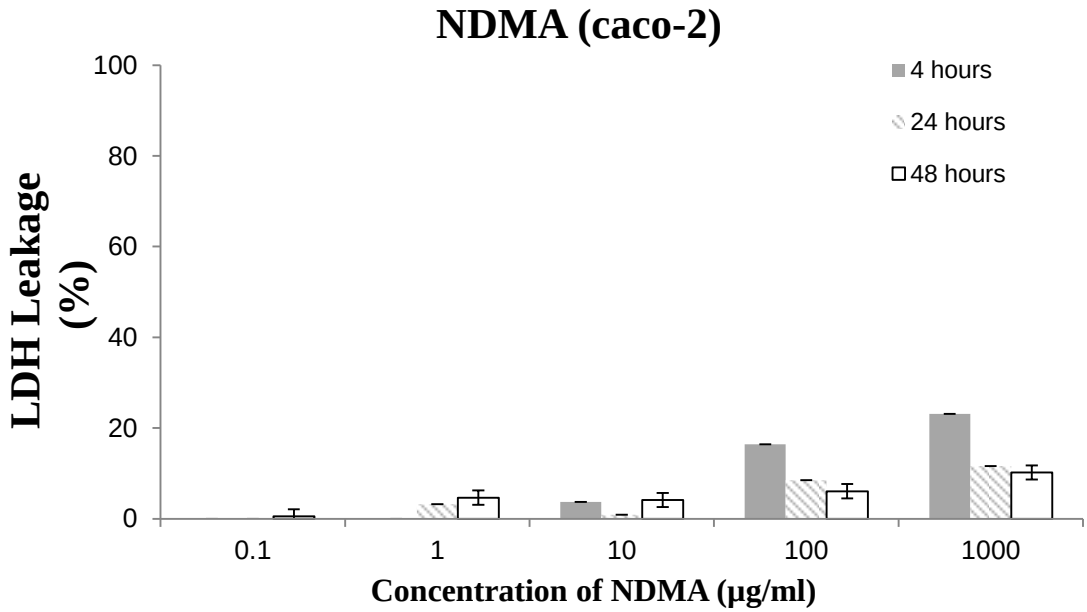
NDMA (caco-2)
4 hours
24 hours
48 hours
LDH Leakage (%)
100
80
60
40
20
0
0.1
1
10
100
1000
Concentration of NDMA (µg/ml)

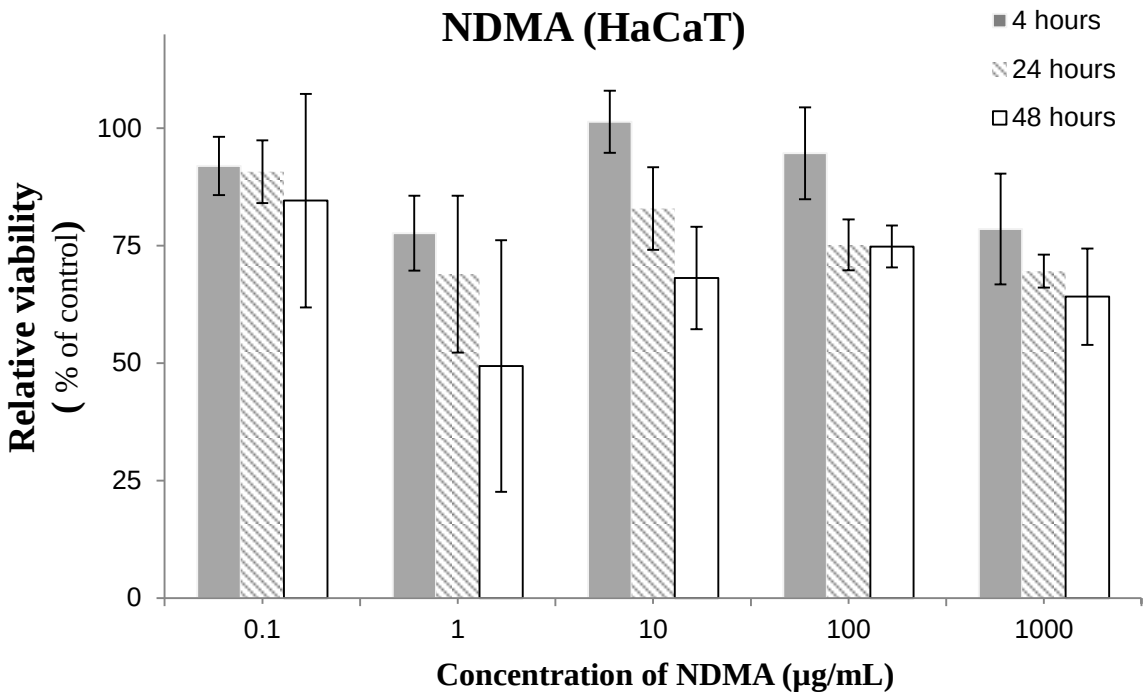

Figure 4.3: Toxic effect of *N*-nitrosodimethylamine (NDMA) on HaCaT and Caco-2 cell lines assessed by MTT and LDH assays. Both assays showed reduction in cell viability and increase in LDH leakage compared with the positive control. Data are expressed as means ± SD from three independent experiments. $p < 0.05$ compared with the control group.

4.5 Conclusion

In summary, SiO_2 NPs synthesised by the Stöber method resulted in a monodispersed spherical particle with size 200 nm in diameter as analysed by SEM. Due to multiple factors, membranes can foul and NPs can reach waterways, with adverse effects on ecosystems. This study tested the toxicity of SiO_2 NPs used in water filtration and NDMA as a member of a family of extremely potent carcinogens found in drinking water as contaminants resulting from reactions occurring during chlorination. After 4, 24 and 48-h exposure to SiO_2 (concentrations 0.05–2 mg/mL), HaCaT and Caco-2 cell lines showed increased LDH leakage compared with the positive control for only 2 mg/mL SiO_2, using MTT and LDH assays. NDMA activated LDH leakage in both cell lines and interrupted the metabolic activity of the HaCaT cell line at most

concentrations. These findings suggest that SiO_2 imposes less environmental risk to humans and animals at the tested concentrations.

Chapter 5: Toxicity of Thiolated Silica Nanoparticles Modified with Sulfobetaine Methacrylate for Potential Use in Chemotherapy Drug Conjugation

Abdulmajeed G. Almutary [1], Barbara J. S. Sanderson [3], Zahra Alhalili [2], Amanda V. Ellis [1]

Authors Contribution

AGA and AVE are equal contributors. AGA carried out the experiment work, contributed to acquisition, analysis, or interpretation of data, drafted the manuscript, and critically revised the manuscript for important intellectual content. AVE and BJSS contributed to conception and design, acquisition, drafted the manuscript, and critically revised the manuscript. Alhalili Z prepared the nanoparticles and partly revised the manuscript.

Abstract

NPs are promising substrates for the delivery of chemotherapy drugs to solid tumours. However, following injection these foreign bodies are often eliminated by the reticuloendothelial system (RES) within seconds or minutes. Previous studies have overcome this issue by coating nano-drug carriers with a surfactant that extends the circulatory half-life of the NPs and prevents opsonisation. In the current study, thiolated silica (SiO_2) NPs were synthesised using the Stöber method and then coated with low-fouling zwitterionic SBMA using thiol-ene addition. SEM revealed monodispersed spherical particles with DLS showing a small increase in nanoparticle average diameter after modification with SBMA. Toxicity of the SiO_2-SBMA NPs (concentrations of 0.05–2.00mg/mL) was investigated using the MTT, LDH and crystal violet assays on the Caco-2 and HaCaT cell lines for 4, 24 and 48 h. The particles were also exposed to UV light to identify any possible degradation effects; zeta potential measurements revealed strongly anionic particles after 1-h UV light exposure. The SiO_2-SBMA NPs did not decrease the mitochondrial activity of Caco-2 or HaCaT cells according to the MTT assays; however, LDH leakage increased and relative cell number decreased at 2.00 mg/mL, as clearly observed after the particles were exposed to UV light. These results indicate that concentrations ≤1.50 mg/mL of SiO_2-SBMA are of low toxicity, are biocompatible and show potential as a chemotherapy drug conjugate.

5.1 Introduction

Chemotherapy is necessary for the treatment of most solid tumours; however, adverse side effects often limit its benefits and affect the patient's quality of life (Nowak et al., 2003; Sutradhar and Amin, 2014). Repeated cycles of chemotherapy can cause MDR (Peer and Margalit, 2006, Kuo et al., 2011). To address these issues, there is a need to develop new methods of transporting medicines without causing damage to other tissues or organs (Farokhzad and Langer, 2009; Jin and Ye, 2007; Prausnitz et al., 2004).

NPs promote drug release and drug accumulation in tumours and can have more favourable pharmacokinetics than the free drug (Amoozgar and Yeo, 2012). NP delivery to tumours depends on the physiological and anatomical features of the tumour and its environment (Amoozgar and Yeo, 2012). As the tumour spreads, the higher demand for gas exchange, nutrients and waste removal leads to the formation of new blood vessels (Flier et al., 1995; Rak and Joanne, 2004). This happens by the extension of vasculature towards the tumour and the mobility of the progenitor endothelial cells (Narang and Mahato, 2006). Factors such as fibroblast growth and endothelial growth stimulate the extension of tumour vasculature (Folkman, 1971; Gao et al., 2008). However, anti-angiogenic factors can cause incompatible expansion and defects in the architecture of tumour vasculature (Fukumura and Jain, 2007; Hanahan and Folkman, 1996).

Studies using transplanted rodent tumours have revealed that the pore size of tumour micro-vessels ranges from 100 nm to 780 nm in diameter; therefore, this is an important feature in the extravasation of NPs (Hobbs et al., 1998; Li and Huang, 2010). Additionally, tumours commonly have poor lymphatic drainage, which can reduce the removal of NPs (Maeda et al., 2000). This is the EPR phenomenon (Aliabadi et al., 2008; Canelas et al., 2009; Matsumura and Maeda, 1986; Sutradhar and Amin, 2014). To realise the optimal benefits of the EPR effect, NPs must circulate for a long period, but the RES, which protects the body from extraneous particles, is a major obstacle to the retention of NPs (Hsu and Juliano, 1982; Senior, 1986). The clearance of foreign bodies such as NPs is initiated by phagocytic cells in the tissue and blood (Bartneck et al., 2009; Pratten and Lloyd, 1986) and mediated (labelling the surface of NPs as a foreign body) by plasma proteins or complement fragments (Moghimi and Patel, 1998). Many studies have shown that if the NP surface is not protected from opsonisation it

will be cleared from the blood within minutes by the RES (Mohanraj and Chen, 2006; Moghimi and Szebeni, 2003; Semple et al., 1998). Some surface coatings can prevent NP opsonisation and aggregation, improve cellular uptake, increase wettability and affect degradation rates (Khung and Narducci, 2015). These include polySBMA, PEG, dextran, chitosan, pullulan, sodium oleate, dodecylamine, polysorbate 80, poloxamer 188, polyvinyl alcohol, poly-2-methyl-2-oxazoline, polyvinylpyrrolidone and α-tocopherol PEG-1000 succinate (Izquierdo-Barba et al., 2016; Liu et al., 2014).

The circulatory half-life of NPs is greatly affected by their shape, size, surface chemistry, SA and multi-composition (Longmire et al., 2011; Pistone et al., 2016; Sheng et al., 2009; Yamamoto et al., 2001). Charged and hydrophobic NPs have shorter circulatory half-lives because of significant opsonisation (Amoozgar and Yeo, 2012). The method of opsonisation is one of the most important biological barriers to control the delivery of drugs into organs. Almost all NPs that are administrated systematically are coated with electrically neutral hydrophobic surface layers referred to as a 'stealth coating', which extends the half-life of NPs to >40 h (Moghimi et al., 2001). Administration of NPs via intradermal or subcutaneous injection showed a different distribution depending on the absence or presence of coatings (Hirai et al., 2012; Liu et al., 2014). The degree of NP coating plays an important factor in reaching targeted tissues (Liu et al., 2014). For instance, PEG-coated NPs reach lymphatic vessels and the circulatory system faster than do free injected NPs (Iannazzo et al., 2017; Liu et al., 2014).

Most surface stabilisation of NPs is accomplished either by surfactants or non-ionic hydrophilic polymers. PEG is often applied in the process known as PEGylation; however, it forms a flexible layer on the surface of the NP that can hinder the adsorption of opsonins via steric hindrance and phagocytic effects (Amoozgar and Yeo, 2012; Gref et al., 2000; Heald et al., 2002; Huang et al., 2001; Moffatt and Cristiano, 2006). The effect of PEGylation on the extension of NP circulatory half-life is well recognised (Verrecchia et al., 1995). Verrechia et al. (1995) identified that PEGylated NPs were more concentrated in the plasma and lived longer than non-PEGylated NPs. Significantly, in one study the uptake of PEGylated polylactic acid (PLA) NPs by the liver was 9% less than that of non-PEGylated PLA NPs (Amoozgar and Yeo, 2012).

Although the PEG stealth coating method has demonstrated successful protection for a variety of NPs, other studies have reported its disadvantages (Gref et al., 1994; Poon et al., 2011; Suh et al., 2007; Zhang et al., 2008). The delivery of the drug to targeted cells often involves the uptake of the NPs, especially when the drug depends on the NPs to enter or exit from the cells. NPs pass through five stages: (1) transport to the extracellular matrix, (2) bonding to the cell membrane by receptors, (3) internalisation into the cells, (4) drug release and exit from intracellular vesicles to cytosol, and (5) transfer to the targeted organelles. Therefore, a method for coating surfaces to prevent protein adsorption is to use zwitterionic molecules (Du et al., 1997; Gupta et al., 2003; Khalil et al., 2006). Estephan et al. (2011) compared the efficacy of protein adsorption between PEGylated and zwitterion-coated silica particles. PEGylation formed three-dimensional coatings whereas the zwitterion formed monolayer-type coverage with lower thicknesses (Estephan et al., 2011). The silica-modified NPs were challenged with serum, salt, lysozyme and albumin at 25 and 37°C. Both methods were effective at preventing protein adsorption and aggregation of particles. The mechanism for adsorption resistance was thought to be based on preventing ion pairing between protein and surface charges, which releases counter-ions and water molecules, an entropic driving force enough to overcome a disfavoured enthalpy of adsorption.

There is an assumption that NPs can use a mechanism to pass through gastrointestinal barriers by (1) paracellular crossing through the intestinal epithelial cells as a result of their small size (<50 nm); (2) uptake by intestinal enterocytes via endocytosis (size <500 nm); and (3) lymphatic absorption by Microfold cells (M cells size in diameter <5 µm). Also, coating NPs with a suitable bio-adhesive material can increase their ability to fight MDR proteins (Win and Feng, 2005). However, these NPs may be engulfed by macrophages in the liver, which is the organ most likely to be influenced regardless of the method of preparation (Owens and Peppas, 2006). NPs can also accumulate in the lungs, spleen, bone marrow, lymph nodes, colon and brain, causing severe toxicity (Garnett and Kallinteri, 2006; Hagens et al., 2007).

Silica NPs are broadly used in biomedical applications as drug carriers and vehicles for gene delivery (Csőgör et al., 2003; Roy et al., 2005). This study describes the synthesis of thiolated silica NPs coated with a zwitterionic SBMA coating using a thiol-ene

addition reaction. The toxicity of these NPs to Caco-2 and HaCaT cell lines was then determined using MTT and LDH assays.

5.2 Materials and Methods

5.2.1 Reagents and Nanoparticles

All reagents were from Sigma Aldrich, Australia unless otherwise stated. These included MTT, NADH, NAD, PMS, trizma base, trizma HCl, lithium lactate, INT, Triton X-100, 98% TEOS, (3-mercaptopropyl)trimethoxysilane (MPTMS), [3-(methacryloylamino)propyl] dimethyl(3-sulfopropyl) ammonium hydroxide inner salt and SBMA. The culture media used was DMEM and RPMI with 10% heat-inactivated FBS, penicillin and streptomycin. Millipore MQ water with resistivity = 18.2 MΩ.cm was used for all the experiments.

5.2.2 Preparation of SiO2 Nanoparticles

Silica NPs and thiolated silica NPs were synthesised by a modified Stöber method (Figure 5.1) (Ibrahim et al., 2010). One mL of a silica precursor of TEOS was added rapidly to a mixture of 95% ethyl alcohol (10 mL) and MQ water (3 mL). The reaction was allowed to proceed for 30 min with mild stirring at 50°C to obtain a homogeneous mixture. Subsequently, ammonia solution (30%) (1 mL) was added drop-wise over an 8-min period with stirring. The mixture gradually changed from transparent to milky as the NPs formed. The mixture was then stirred for a further 2 h. The resultant precipitate was then centrifuged at 101,890 g and washed with MQ water four times. Finally, the silica particles were dried overnight at 75°C.

5.2.3 Preparation of Thiolated SiO2 Nanoparticles

A mixture of 1mL TEOS and 0.25 mL MPTMS was stirred for 2 min and then added to a mixture of 10 mL ethyl alcohol and 3 mL MQ water. The reaction mixture was stirred for 30 min at 50°C, and then 1 mL ammonia solution (30%) was added drop-wise over an 8-min period with stirring. The mixture was then stirred for a further 2 h. The resulting gel was centrifuged at 101,890 g and washed with MQ water four times before being dried overnight in an oven at 80°C. After drying, the gel became a white powder.

5.2.4 Synthesis of Zwitterionic Sulfobetaine Methacrylate-coated Silica Nanoparticles by Thiol-ene Addition

SBMA (5 g) was dissolved in 25 mL MQ water and then stirred in a two-necked, round-bottomed flask under nitrogen (N_2) for 30 min. The synthesised thiolated SiO_2 NPs (1.32 g) were then added to the solution and the temperature was increased gradually to 70°C. Subsequently, 50 mg V50 initiator dissolved in 2.5 mL MQ water was added, and the reaction mixture was stirred for approximately 17 h at 70°C. The resulting suspension was centrifuged at 101,890 g and washed four times with acetone. The resultant powder (SiO_2-SBMA NPs) was dried under N_2 and protected from light by storing it in a brown sealed vial.

5.2.5 Nanoparticle Characterisation

SEM was performed on the thiolated SiO2-SBMA NPs. The samples were sputter coated with a 10-nm layer of platinum using a Quorumtech K757X sputter coater. Images of the sample were collected via SEM using a CAMScan MX2500 with a field emission source at an accelerating voltage of 10 kV. The hydrodynamic diameter (determined in RPMI medium) and the zeta potential were measured by DLS using a Malvern High-performance Particle Sizer. Data were acquired with a scattering angle close to 180° at a temperature of 25°C.

5.2.6 Cell Culture

Caco-2 and HaCaT cell lines were obtained from the ATCC. Caco-2 cells were grown in DMEM and HaCaT in RPMI at pH 7.4, with 10% FBS and a 1% antibiotic mixture of penicillin (10,000 units/mL) and streptomycin (10,000 µg/mL). The cells were maintained in T-75 flasks at 1×10^6 cells/mL. When the cells reached 80% confluence they were trypsinised and sub-cultured (Sambuy et al., 2005). The cells were maintained in a humidified incubator with 5% CO_2 at 37°C. The cell density after trypsinisation was determined by TB counting (Sambuy et al., 2005).

5.2.7 Cell Exposure to Nanoparticles

SiO_2-SBMA NPs were diluted in deionised water (stock at 20 mg/mL) and then mixed by vortexing for 5 min, followed by dilution to the required concentration with media.

Caco-2 and HaCaT cells were seeded at 10,000 cells/well in 96-well, flat-bottomed microplates, then incubated overnight to allow adherence. Cells were exposed to SiO_2-SBMA NPs at six concentrations (0.05, 0.1, 0.5, 1.0, 1.5 and 2.0 mg/mL) and the control was Triton X-100 for 4, 24 and 48 h. After exposure, the solution was removed, and the cells were washed twice with PBS at pH 7.4 to remove any excess NPs.

5.2.8 UV Light Exposure of SiO2-Sulfobetaine Methacrylate Nanoparticles

SiO_2-SBMA NPs were exposed to UV light at 365 nm with a peak irradiance of 13.05 mW/cm^2 for 1 h.

5.2.9 MTT Assay

The MTT assay was used as an indicator of metabolic viability where the yellow MTT is enzymatically changed to insoluble purple formazan for visualisation. Each concentration was examined in four technical replicates and the experiment was repeated three times ($n = 3$). Media containing MTT tetrazolium salt (5 mg/mL) was added to exposed cells for 4 h. The purple formazan formed inside the cells was dissolved with 10% SDS in 0.1 M HCl. Absorbance was read using a spectrophotometer at a primary wavelength of 570 nm and a reference wavelength of 630 nm.

5.2.10 Lactate Dehydrogenase Assay

Caco-2 and HaCaT cells were seeded in triplicate wells at 1×10^4 viable cells/100 µL DMEM in 96-well, flat-bottomed microplates. The cells were cultured for 16 h to allow adherence and then media was replaced with six different concentrations of NPs, plus controls, for 4, 24 and 48 h. After exposure, the plate was spun at 1200 RPM and 50-µL aliquots of cell lysate from each well were transferred to a new 96-well, flat-bottomed microplate containing 150 µL of LDH stain per well. Cells were incubated at room temperature for 5 min and then the absorbance was read at 590 nm using a spectrophotometer.

5.2.11 Crystal Violet Assay (Screening for Cell Adherence Phenotype)

After the HaCaT cells were exposed to SiO_2-SBMA NPs, the plates were washed with PBS and 50 µL of crystal violet stain was added and incubated at room temperature for 15 minutes. The stain was washed off with demineralised water and the plates were left

to dry overnight. A 33% (v/v) acetic acid solution was then added and the OD at 570 nm was read within minutes using an ELISA reader. Six technical replicate wells per treatment and three biological replicates were carried out for each treatment experiment. The results were expressed as percentage viability compared with the untreated control.

5.2.12 Statistical Analysis

The data were expressed as the mean ± (SD) of at least three independent experiments using one-way ANOVA and Tukey–Kramer multiple comparisons test using the SPSS (version x8) software to compare exposure groups. All comparisons were considered significant at $p < 0.05$.

5.3 Results and Discussion

The formation of thiolated silica particles is depicted in Figure 5.1, Steps 1 and 2. During hydrolysis reactions, an intermediate compound $[Si(OC_2H_5)_{4-X}\ (OH)X]$ containing silanol groups is formed by nucleophilic substitution reactions between water molecules and ethoxy groups of TEOS. These silanol groups then undergo condensation reactions to form siloxane bridges, resulting in silica NPs. However, when MPTMS is present, the silanol groups can also undergo condensation reactions with the methoxy groups of the MPTMS. In this manner, silica NPs containing both siloxane bridges and thiol functionalisation can be achieved (Figure 5.1, Step 1). Step 2 shows the synthetic pathway for the formation of SBMA-functionalised SiO_2 NPs. This relies on a thiol-ene addition reaction between the thiol-modified SiO_2 NPs and the alkene moiety on the SBMA. The reaction typically results in an anti-Markovnikov addition to the alkene. The reaction is stereoselective and occurs rapidly with high yields (Yang and Rioux, 2014).

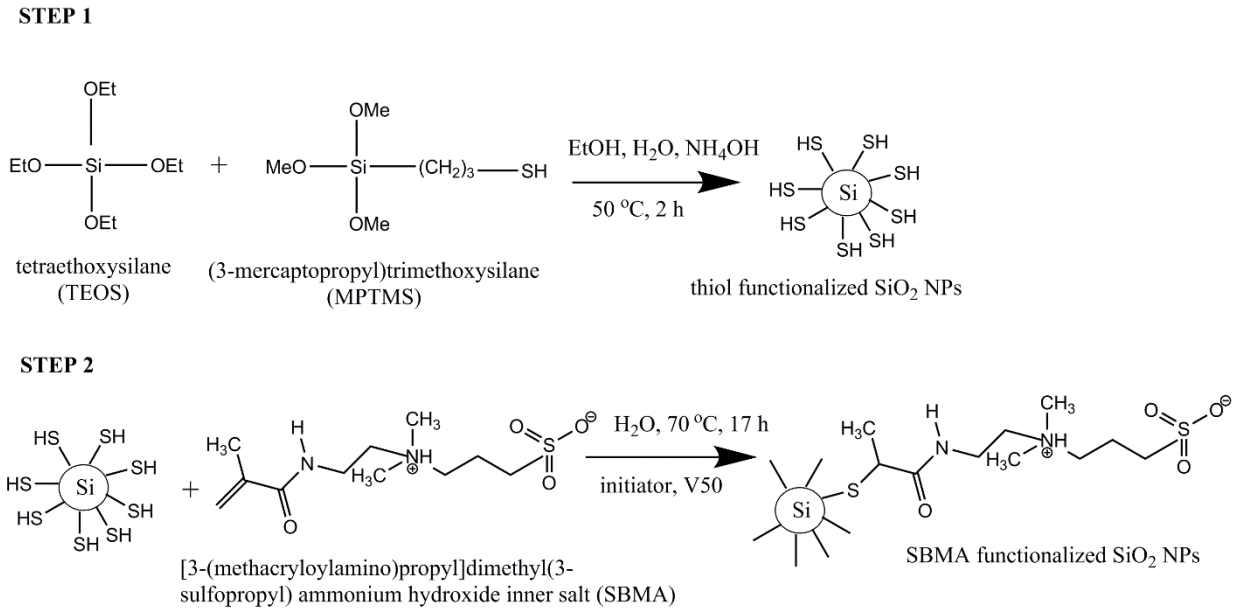

Figure 5.1: Synthesis of thiolated silica nanoparticles and subsequent thiol-ene reaction to produce SiO_2-SBMA nanoparticles

Figure 5.2 shows the size distribution of the particles both before and after the reaction of the thiolated SiO_2 NPs with SBMA measured using DLS. SBMA functionalisation is shown as an increase in the average size of particles by approximately 8 nm, from 87 nm to 95 nm after functionalisation. This increase in hydrodynamic radius is larger than the length scale of the attached moiety but is a result of the shielding attraction between the zwitterions, giving rise to an increase in the hydrodynamic volume.

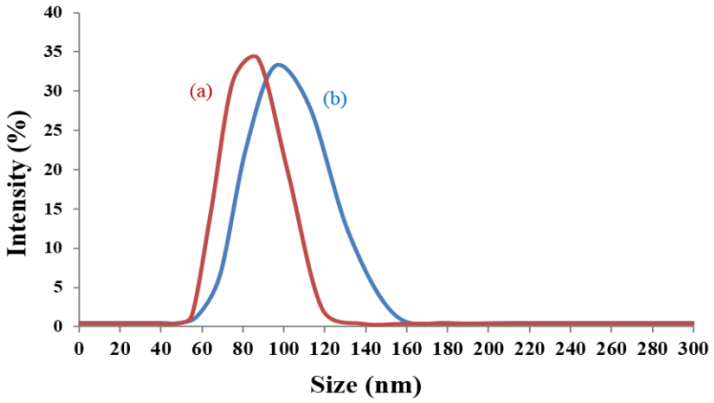

Figure 5.2: Analysis of nanoparticles using DLS. (a) SiO_2 nanoparticles (average size = 87 nm) and (b) after coating with SBMA (average size = 95 nm).

SEM images of the thiolated and subsequently SBMA-modified SiO_2 NPs are shown in Figures 5.3a and b, respectively. The images show that both before and after SBMA

modification, the particles are monodispersed and spherical, indicating the thiol-ene addition has not damaged the NPs. The average dry particle size is ≤20 nm.

Caco-2 and HaCaT cell viability studies were then carried out on the SiO_2-SBMA NPs (concentrations 0.05–2.00 mg/mL) using the MTT assay. At all concentrations, the relative viability of the cells did not decrease (Figure 5.4, left). However, SiO_2-SBMA that was photodegraded by exposure to UV light significantly decreased the cell viability of both Caco-2 and HaCaT at concentrations of 0.10–2.00 mg/mL (Figure 5.4, right). The UV light-exposed NPs (1.5 mg/mL), when exposed to Caco-2 cells for 4 h, resulted in an approximately 30% decrease in cell viability compared with the control. This was also observed with HaCaT cells at 48 h. The toxicity towards both cell lines is most likely due to the strongly anionic NPs after irradiation with UV light.

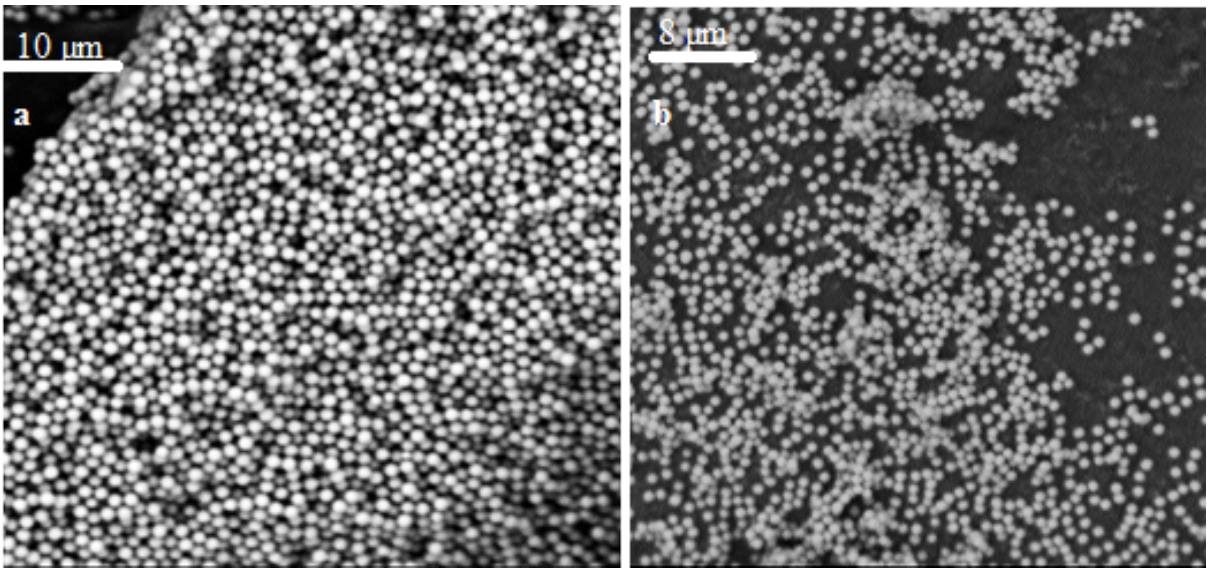

Figure 5.3: Scanning electron microscopy images of (a) monodispersed spherical thiolated SiO_2 and (b) SiO_2-SBMA nanoparticles (NPs); the final NPs formed were spherical and uniform.

Figure 5.5 shows the results from the LDH assays, which revealed that the highest concentration of SiO_2-SBMA NPs (2.00 mg/mL) significantly increased LDH leakage, by almost 25% at all time exposures. This was not seen in the MTT assay, which may be related to particle interference from the MTT formazan. These results indicate that both LDH release and MTT reduction accurately determine the toxic effect of SiO_2-

SBMA. However, the MTT assay does not always correctly quantify NP toxicity; this likely reflects differences in the point of death pathway (Smith et al., 2011). The assessment of NP cytotoxicity depends on the choice of the test system. Due to NPs' optical activity and absorption values, they can influence the classical cytotoxicity assay. In a previous study from our laboratory, SiO_2 NPs (20 nm in diameter) did not alter the MTT standard curve with or without the presence of HaCaT cells (Almutary and Sanderson, 2016). Cell death detected by crystal violet assay increased 20% at 2 mg/mL for 4 and 24-h exposure to SiO_2-SBMA (Figure 5.6). LDH leakage increased substantially, by nearly 90%, after UV light exposure. Yin et al. (2012) reported the cytotoxicity to HaCaT cell lines of four UV light-exposed (15 mW) TiO_2 NPs with size range 25–325 nm and with two different crystal forms. Upon UV irradiation, all TiO_2 NPs induced photocytotoxicity and cell membrane damage, in a dose-dependent manner. In the current study, photodegradation of SiO_2-SBMA after 1-h exposure to UV light caused LDH leakage of Caco-2 cells.

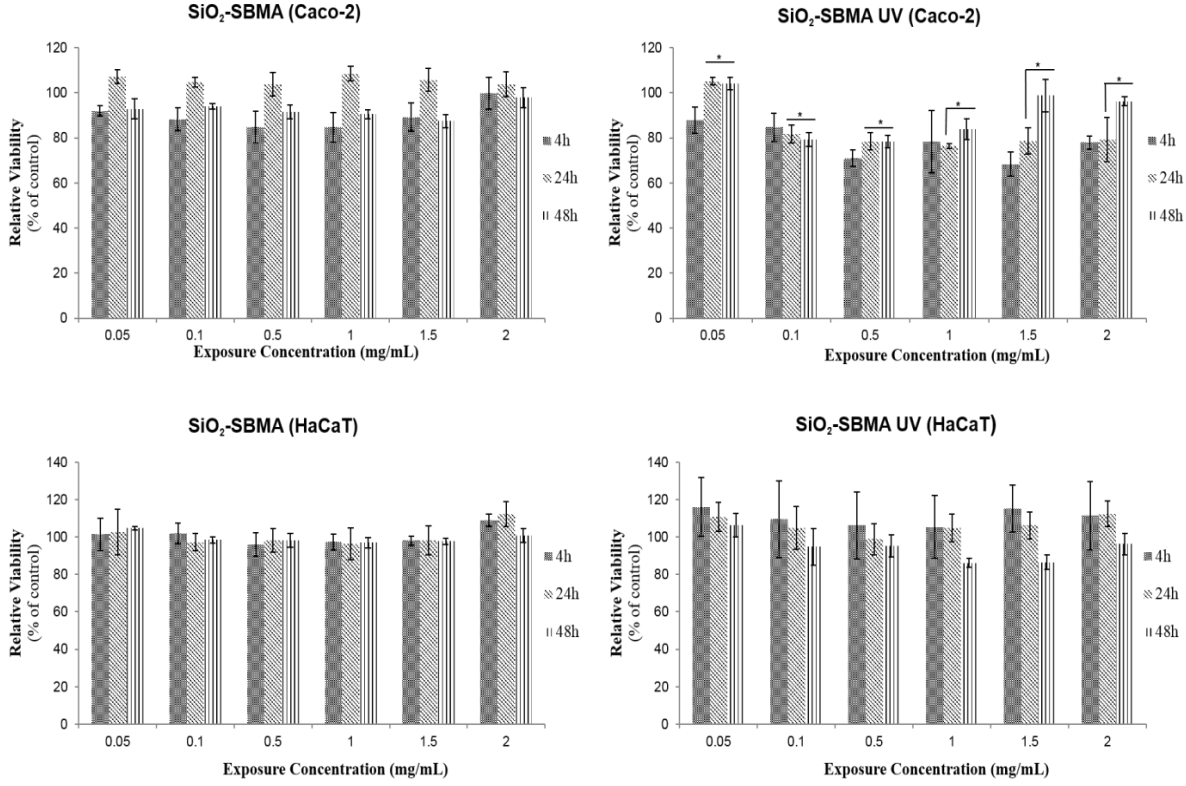

Figure 5.4: Effect of SiO_2-SBMA (left) and UV-exposed nanoparticles (right) on Caco-2 and HaCaT cell viability using the MTT assay. Caco-2 and HaCaT cells were exposed to different concentrations of SiO_2-SBMA. Data are expressed as means ± SD from three independent experiments. *$p < 0.05$ compared with control group.

Based on the literature, it was assumed that similar effects would be observed for the HaCaT cells in this study (results not shown). NPs with zeta potentials in the range of –10 to +10 mV are neutral and those between –30 and +30 mV are anionic and cationic (Clogston and Patri, 2011). Characteristics of NPs such as size, surface charge and agglomeration are crucial parameters in the determination of particle toxicity (Jiang et al., 2009). Cationic surfactants are used to protect NP size, agglomeration and photophysical properties. In this study, the zeta potential measurements of SiO_2-SBMA were –30 mV prior to and –70 mV after UV light exposure. This shows an increase in anionic particle activity. Some cationic particles are moderately toxic, whereas anionic particles are often nontoxic (Janát-Amsbury et al., 2011). Therefore, it may be expected that SiO_2-SBMA NPs are rendered less toxic after UV treatment.

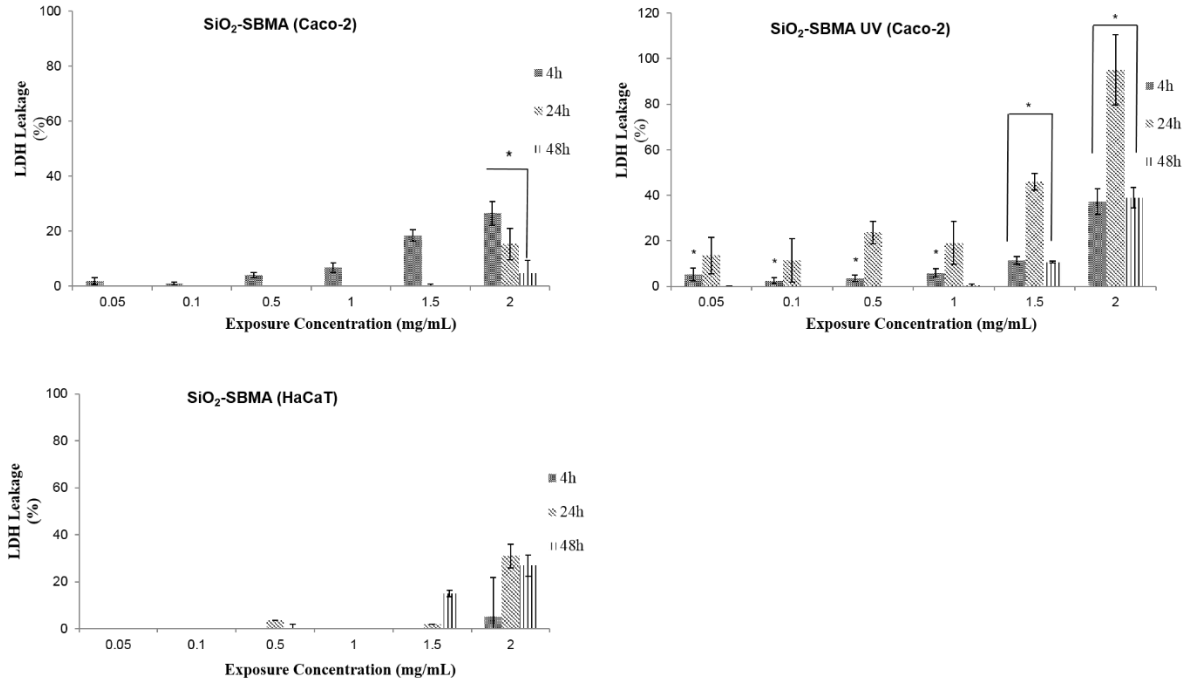

Figure 5.5: Effect of SiO_2-SBMA (left) and UV-exposed nanoparticles (right) on LDH leakage levels. Caco-2 and HaCaT cells were exposed to different concentrations of SiO_2-SBMA. LDH levels increased at 2.00 mg/mL after 4, 24 and 48-h exposure. Data are expressed as means ± SD from three independent experiments. *$p < 0.05$ compared with control group.

Napierska et al. (2009) examined the effect of monodispersed spherical SiO_2 NPs of different sizes on the growth of an endothelial cell line (EAHY926). The cytotoxic

damage indicated by LDH release and the decrease in cell survival determined by the MTT assays differed according to SiO_2 diameter. Concentrations led to a 50% decrease in cell viability for the smallest SiO_2 (14–60 nm) compared with less cytotoxicity from the largest SiO_2 NPs (104 and 335 nm). In addition, the smaller SiO_2 was shown to affect the exposed cells and cause cell death faster than for the larger particles, within just a few hours (Napierska et al., 2009).

Here, the SiO_2 NP concentrations were carefully chosen from previous work in our group on silica toxicity that showed that when HaCaT cell lines were exposed to SiO_2 NP concentrations of 0.05–10 mg/mL, there was a dose-dependent increase in cell death with increasing concentration when screened with the MTT assay (Almutary and Sanderson, 2016). In this work, at SiO_2 concentrations ≥2 mg/mL (24 h) there was decreased relative survival when assayed using MTT, and relative cell number was shown to decrease when assayed using the crystal violet assay. At 48-h treatment, cytotoxicity was observed at every treatment concentration. Moreover, the level of cytotoxicity was time dependent (4, 24, 48 h) at every concentration.

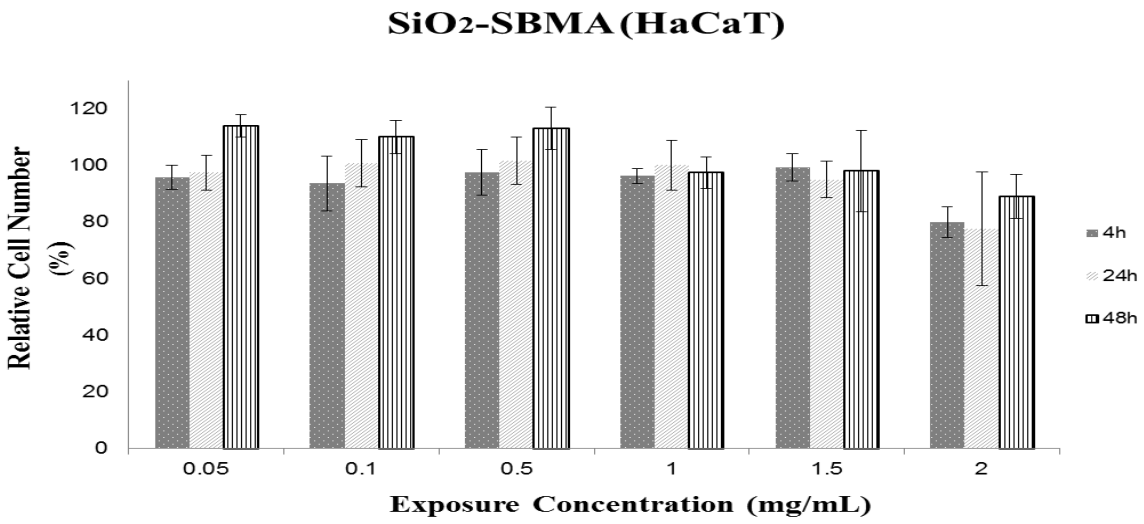

Figure 5.6: Effect of SiO_2-SBMA-exposed nanoparticles on relative cell number. HaCaT cell death increased at 2.00 mg/mL. Data are expressed as means ± SD from three independent experiments. $p < 0.05$ compared with control group.

5.4 Conclusion

In summary, thiolated SiO_2 NPs produced via a modified Stöber process were coated with a novel biocompatible zwitterionic SBMA via thiol-ene addition. The SEM images of both the thiol- and SBMA-modified SiO_2 NPs showed spherical and monodispersed particles. DLS showed that there was an increase in NP size after modification with SBMA, arising from an increase in hydrodynamic radius caused by a shielding interaction of the zwitterions. The toxicity of SiO_2-SBMA NPs was detected by MTT, LDH and crystal violet assays over 4, 24 and 48 h. The particles did not affect mitochondrial activity, even after 48-h exposure. Proliferation assays such as MTT have two main limitations: they can give false positive results in which a specific aspect of cellular metabolism is affected; and they are unable to differentiate cell cycle inhibition from cellular death. Activated LDH enzyme and a decrease in relative cell number were found at 2.00 mg/mL, predominantly after 4 and 24-h exposure. The SiO_2-SBMA zeta potential measurements were –30 mV before and –70 mV after UV light exposure. The SiO_2-SBMA NPs were exposed to UV light irradiation at 365 nm wavelength for 1 h. A significant increase in LDH leakage in the Caco-2 cell line was detected. Photodegradation of the strongly anionic NPs caused by UV light could be avoided by reducing the exposure time to less than 1 h at the same wavelength. Further investigation is needed on the drug release and SiO_2-SBMA cellular uptake.

Chapter 6: General Discussion and Conclusion (Partly of this chapter was published as short review article)

6.1 Challenges for Assessing Nanomaterial Toxicity

The overall aim of this study was to investigate the risks associated with NP exposure for human cell lines. The use of NMs in medicine, biology and industry applications has increased rapidly in the past decade (Pandit et al., 2016). NMs have been a crucial substance in the production of many therapeutic agents. However, the safe use of NMs has been a concern for many scientists (Teow et al., 2011). Many conflicting reports on the potential toxicity of NMs have complicated the estimation of their biological effect (Kroll et al., 2009, 2012). One of the main issues affecting the assessment of NM toxicity to humans and the environment is the use of biochemical assays that could be affected by the NMs themselves and provide false data or subsequent incongruent prediction of toxicity (Ong et al., 2014). Inconsistent and/or inaccurate data will make it difficult to establish guidelines for the safe use and production of NMs.

Common assays used in the detection of NM toxicity are the LDH cytotoxicity assay, AB, tetrazolium-based assays such as 3-(4,5-dimethylthiazol-2-yl)-5-(3-carboxymethoxyphenyl)-2-(4- sulfophenyl)-2Htetrazolium (MTS) , MTT and crystal violet assay (Almutary and Sanderson, 2016; Malvindi et al., 2014). These assays have been reported to be affected by NM artefacts. In addition, more *in vivo* and *in vitro* nanotoxicology assays have provided false positive data in the presence of a variety of NMs (Hartung, 2014). Studies have reported the interference to be from NMs binding to the proteins or dyes and then altering their structure or function; this could be a common factor in every toxicity assay (MacCormack et al., 2012; Stone et al., 2009). Other studies have reported that the presence of NMs in toxicity detection assays may interrupt cellular reactions and cause significant changes in enzymatic activity, fluorescence and absorbance values of indicator molecules (Stueker et al., 2014).

NP parameter investigation has been a research focus to avoid interference with common toxicity assays *in vitro* and *in vivo* (Mahmoudi et al., 2011). These parameters include NP morphology, crystal structure, purity, mass concentration, size and size distribution, SA/charge, chemical composition, surface stability under experiment

conditions and degree of aggregation. These characterisations are of particular importance not only for *in vivo* studies, but more for the correct interpretation of NM behaviour under realistic environmental conditions (Kumar et al., 2012). Toxicity studies under environmental conditions will be influenced by the dispersion and adsorption of various molecules on the surface of NPs and additional toxicity may be due to a change in the accumulation of heavy metals in the presence of metal oxide NPs (Fabrega et al., 2011). After this, research has focussed on achieving a well-dispersed suspension by the addition of surfactants or additives to control NP agglomeration (Djurišić et al., 2015). A recent study investigated whether the interference of NPs is based on the surface characteristics of metallic NPs, by studying the effect of different surface coatings on AgNPs and maghemite NPs (γ-Fe_2O_3NPs) on classical *in vitro* assays targeting two of the main cytotoxic endpoints—cell viability and oxidative stress response (Vrček et al., 2015). The cell viability assays were MTT, MTS and WST-8 and the assays utilised fluorescent dyes as markers for the production of ROS including DCFH-DA, DHE and glutathione levels. The results showed that the NPs affected all of the investigated assays, leading to false interpretation of the data obtained (Vrček et al., 2015). The range and type of interference were dependent on the surface coating of the NPs, their stability in biological media, their concentration, and the particle and assay (Vrček et al., 2015).

More stringent control for nanotoxicological studies to minimise the potential of NP interactions with assays is needed. Concentrations ≥10 mg/mL have been shown to interfere with assay function yet the use of such concentrations is not rare in nanotoxicological studies (Guadagnini et al., 2015). Thus, NP concentrations after treatment should be limited, knowing that even with multiple washes and/or centrifugation NPs are able to remain within the cells or attached to membranes (Kroll et al., 2012). Centrifugation insufficient if the NPs bounded to the assay components, which lead to removal of dyes and protein important in obtaining an accurate reading (Lynch and Dawson, 2008). Thus, each *in vitro* test system has to be evaluated for every NP type to avoid flaws and give an accurate assessment of the NP's toxicity.

One of the promising applications of NMs is the use of zerovalent iron (nZVI), which is becoming the most important example of fast-emerging technology with potential benefits; however, uncertainties and misconceptions regarding the basics of this technology have meant this application has not reached it maximum performance (Stefaniuk et al., 2016).

There are currently three major areas of uncertainty associated with the use of nZVI: (1) high concentrations of nZVI aggregate and lead to production of micron-sized clusters that do not exhibit the true nanosize effect; (2) under the same conditions, the mobility of the bare or uncoated nZVI will be less than a few metres and (3) the risk to humans and animals remain unknown (Stefaniuk et al., 2016). NPs present their risk in terms of (1) dispersal, which is the transport in the environment enabling them to travel long distances; (2) ecotoxicity, which could have many effects on organisms in the environment; (3) persistence, which is the ability to remain longer in the environment; (4) bioaccumulation, or the ability to bioconcentrate in many organisms; and (5) reversibility, which is the ability to reverse their original introduction into the environment (Stefaniuk et al., 2016). Although nanotechnology can provide a beneficial replacement for any site remediation, further investigation of NPs' health and environmental effects are demanded. Large studies on dermal toxicity caused by NP exposure have been a public concern (Lewinski et al., 2017). The *ex vivo* and *in vivo* human skin studies investigated the extent of NP penetration to skin after sunscreen application (Lewinski et al., 2017). There was little evidence that NPs can cross the stratum corneum into the epidermis and dermis. However, the lack of penetration could be due to the small size of the NPs (Lewinski et al., 2017). Some studies have reported it is unlikely that NPs would penetrate living skin tissue; they suggested removal of NPs from the skin surface by thorough washing with soap.

6.2 Engineered Nanomaterial Fate and Transport

To understand ENM mobility, bioavailability and final fate, there are many processes that must first be considered (Cornelis et al., 2014). These processes include ENM emissions to air, water and soil; diffusive transport, volatilisation to air and transformation into other ENMs; and aggregation, sedimentation, dissolution and filtration (Quik et al., 2011). Some of these processes are necessary to ENMs that may not be closely connected to the environment behaviour (Garner and Keller, 2014). These processes are the degree of aggregation, deposition, dissolution and attachment, as determined by ENM size, surface properties and the surrounding environmental characteristics (Garner and Keller, 2014). Moreover, several ENMs dissolve over time; therefore, exposure can be from both suspended NPs and dissolved ions (Stebounova et al., 2011). Aggregation of ENMs can alter the state of NPs to make them behave in unexpected ways. For instance, aggregated NPs will interact at different levels with the environment compared with individual NPs or dissolved

ions (Zhang et al., 2008). The majority of ENMs will undergo transformation processes that will alter their properties, such as coatings that could change their chemical properties and environmental behaviour (Lowry et al., 2012). To achieve a complete understanding of the fate and transformation processes of ENMs, complex factors such as NP emission into the environment, surface coatings, interaction with colloids and environment properties surrounding the ENM are important to gain a complete picture of an ENM's fate and transport patterns (Gottschalk et al., 2011).

The release of ENMs to the atmosphere is through indirect or disuse sources and they will eventually be deposited on land and in surface water (Keller and Lazareva, 2013). Recent studies have pointed out that the release of ENMs to the atmosphere is quite low, even with 8,300 metric tons of ENMs released annually around the world (Keller and Lazareva, 2013). Although this amount is small compared with the release and the resistance time in the atmosphere, the fate on ENMS in the atmosphere must not be neglected. The location of release of ENMs such as those used in pesticides could lead to temporarily high concentrations of ENMs in the atmosphere; thus, we need to understand their resistance time and eventual fate in the atmosphere (Tiwari and Marr, 2010). Moreover, ENMs in the atmosphere will be subjected to physical and chemical alterations that will change their fate and environmental concentrations (Tiwari and Marr, 2010).

A major obstacle for current measurement devices is their inability to differentiate background particles from ENMs (Kuhlbusch et al., 2011). The only instrument that is capable of sizing and analysing nanoscale particles is the aerosol mass spectrometer (Kuhlbusch et al., 2011). The device cannot measure metal and metal oxides, although this aspect is under development (Kuhlbusch et al., 2011). Other available devices are only able to discriminate particles according to their size, rather than both size and density (Washington, 2005). Research to date has produced insufficient data to determine significant patterns in the fate and transport process of ENMs in air; therefore, more research is needed (Brouwer et al., 2009).

After ENMs are released into the atmosphere, their size and aggregation will increase due to condensation of organic and inorganic vapours on the particles (Meesters et al., 2013). In condensation, water and semi-volatile substances concentrate on a particle and then form a shell around it; whereas in coagulation, the particles move by

Brownian motion and collide with each other, and then aggregate, increase in size and reduce in number (Kuhlbusch et al., 2011). Environmental factors such as humidity, temperature and atmospheric turbulence will influence the size and concentration of ENMs in the atmosphere (Navarro et al., 2008). A few studies have investigated the fate of ENMs in the workplace by focussing on the release of ENMs in indoor air during the production of ENMs or any product that includes NPs. Although these studies were not aiming to estimate ENMs in the atmosphere, they nonetheless have helped in explaining processes and rates. Current statistics estimate that around 66,000 metric tons of ENMs are release into surface water every year (Garner and Keller, 2014). The transport and fate of ENMs depends closely on the chemical properties of the water (Garner and Keller, 2014). ENMs can be precipitated to sediment compartments by gravitational settling of aggregates or precipitated ENMs with other suspended particles (Westerhoff et al., 2013). There is a strong relationship between aggregation and sedimentation due to the importance of particle size in the rate of sedimentation; particle buoyancy is another important factor (Westerhoff et al., 2013).

6.3 Engineered Nanomaterial Toxicity to Aquatic Ecosystems

The ecotoxicology of ENMs hazard assessment reported that ENMs differ in two significant ways from conventional pollutants such as organic pollutants or traces of metals (von Moos, 2014). First, ENMs can reach aquatic environments as colloids, and then may physically and chemically transform to a new species (Nowack et al., 2015). Second, ENMs are known to have a high surface reactivity as a result of their high SA to weight/volume ratio; due to their electrically charged surface, ENMs also have high redox activity (Nowack et al., 2015). The main focus with respect to the ecotoxicity of ENMs is their potential to physically interact with cellular and subcellular organelles, which will cause harm to exposed organisms. It is believed that the interaction and harm caused by ENMs to living organisms is related to their very high reactivity (Mueller and Nowack, 2010). Their small size possibly facilitates their access to subcellular compartments, unlike conventional bulk contaminants (Mueller and Nowack, 2010, Zhu et al., 2012). In addition, their unique high SA, potentially enhanced reactivity and physicochemical nanoscale properties are involved in their interactions with ocean-living organisms (Klaine et al., 2008).

A large number of studies have focussed on the toxicity of ENMs to the marine ecosystem. Most studies on zinc oxide (ZnO) NPs have been conducted on freshwater fish, mammalian cell lines and bacteria (Bondarenko et al., 2013). Toxicological data in marine fish are still few for the majority of sensitive early life stages (Novelli et al., 2002). A study on the toxic effects of ZnO NPs on aquatic plants attributed their effect to the dissolved Zn+ ions that resulted from particle accumulation and translocation (Ma et al., 2013). Moreover, a high concentration of ionic and pH of seawater can change the physicochemical properties of ZnO NPs, thus, this explains the NPs toxicity (Misra et al., 2012). ZnO NPs are listed extremely toxic and aquatic environmental hazards as a cause from it adverse effect on variety of aquatic organisms such as bacteria, algae, ciliates and fish (Fabrega et al., 2011). For example, the exposure of ZnO NPs to freshwater zebrafish resulted in mortality, tissue injuries, hatching inhibition, hindered growth and abnormalities in both embryos and larvae (Zhu et al., 2009). Exposure of marine echinoderms to ZnO NPs has been shown to cause malformation in developing sea urchin embryos, which involves delayed/arrested development (gastrula stage), skeletal abnormalities and radoalised plutei (Burić et al., 2015). Also ZnO NPs were discovered to significantly decrease the growth rate of marine phytoplankton (*Skeletonema marinol*, *Dunnaliella tertiolecta*, *Isochrysis galbana* and *Thalassiosira pseudonan*) (Miller et al., 2010). Moreover, ZnO NPs can cause damage at subcellular levels in zebrafish via shrinkage or loss of cell cytoplasm, alterations in the shape of nuclei and oxidative effects (Xiong et al., 2011). Beside the harmful effects of ZnO NPs on marine creatures, AgNPs were discovered to have several toxicity impacts including cytotoxicity and genotoxicity, tissue accumulation, alteration of gene expression and histopathological disorders (Kruszewski et al., 2011). In addition, TiO_2 NPs are one of the most commonly used ENMs and can reach critical concentrations in surface water that could pose threat to ecosystems (MacCormack et al., 2013). TiO_2 NPs are mainly phototoxic to human cell lines, although they have been used as anti-cancer agents and in wastewater disinfection (Miller et al., 2012).

6.4 Engineered Nanomaterial Toxicity to Humans

When NPs are inhaled they are deposited throughout the entire respiratory tract, from the nose and pharynx to the lungs (Oberdörster et al., 2004). The lung is composed of airways that transport air in and out, as well as alveoli, where gas exchange occurs (Yeh

and Schum, 1980). The internal SA of human lungs is ~75–140 m^2 and they contain ~300 × 10^6 alveoli (Salata, 2004). As a result of this large SA, the lung is the primary portal for inhaled particles. Spherically shaped materials with diameters <10 μm are able to reach the gas exchange surfaces (Oberdörster, 2000; Salata, 2004,). Particles with larger diameters tend to be deposited further up in the respiratory tract due to gravitational settling, interception and impaction (Lippmann, 1990). Larger diameter particles are found to be deposited in the branching respiratory tree in a saddle shape; whereas smaller particles are mainly affected by diffusion and thus gather in the smaller airways and alveoli (Lippmann, 1990).

Insoluble particle loads in the lungs can induce several toxicological responses that differ from those due to soluble particles (Kovacic and Somanathan, 2009). Soluble or partly soluble particles will dissolve in the aqueous fluid surrounding the epithelium and then pass into the circulatory and lymphatic systems; insoluble particles must be removed by other mechanisms such as the mucociliary escalator (Kovacic and Somanathan, 2009). Particles that are degradable or insoluble in the lungs will accumulate upon continued exposure (Kovacic and Somanathan, 2009). Therefore, when macrophage clearance capacity is exceeded, the lung defence mechanisms are overwhelmed, which results in injury to the lung tissue (Muller et al., 2005). The harmful effect of inhaled NPs on the lungs relies on the lung burden, which is determined by the rate of particle deposition and clearance as well as the residence time in the lungs (Muller et al., 2005). For instance, carbon nanotubes are not completely removed, or are only slowly removed: 81% were found in rat lungs 60 days after exposure (Muller et al., 2005).

NPs, like nanoorganisms, can enter cells and interact with subcellular structures. The cellular uptake, subcellular localisation and catalysing products of NPs rely on their size, shape and chemistry (Xia et al., 2006). Their mechanism of penetrating cells without specific receptors is presumed to be passive uptake or adhesive influence. The uptake probably begins by van der Waals forces, steric interactions, electrostatic charges or interfacial tension, but not from vesicle formation. Steric interactions occur when NPs are of the right size and geometry, and have bonding and charges optimised for interaction with receptors. After this type of uptake, NPs are not necessarily located within a phagosome, which offers some protection to other cellular organelles from

chemical interactions with the NP. C_{60} molecules can be found along the nuclear membrane and in the nucleus; this free movement within cells is very dangerous due to immediate interruptions to the cytoplasm proteins and organelles.

The exact mechanism for NP induction of pro-inflammatory effects are no understood; however, it has been proposed that they create ROS, which result in modulated intracellular calcium concentrations, and induce cytokine production and active transcription factors (Brown et al., 2004). *In vitro* and *in vivo* studies have shown that NPs of different compositions including fullerenes, QDs, carbon nanotubes and automobiles can lead to creation of ROS (Oberdörster et al., 2005). ROS have been shown to damage cells by altering proteins, disrupting DNA and preventing signalling functions (Risom et al., 2005). Oxidative stress is a consequence of cell injury and also occurs as an effect of metabolism ischaemia/reperfusion, cell respiration, inflammation and metabolism of foreign compounds (Risom et al., 2005). Oxidative stress caused by NPs can originate from the following factors (Risom et al., 2005). First, it can be generated on the surface of particles when free radicals and oxidants are present. Second, transition metals such as iron, copper, vanadium, chromium and lead to ROS act as catalysts in Fenton-type reactions. Third, altered functions of the mitochondrion are caused by smaller NPs. Finally, activation of inflammatory cells can lead to reactive oxygen/nitrogen species (Risom et al., 2005).

Many diseases are linked to dysfunction of basic cellular processes such as cell proliferation, metabolism and death. For instance, cancer results from uncoordinated cell proliferation, while neurodegenerative diseases are associated with premature cell death (Antonini et al., 2006). Oxidative stress has been involved in many diseases such as cardiovascular and neurological diseases, cancer and pancreatitis (Risom et al., 2005). Some studies have suggested that the initiation and development of neurodegenerative diseases such as Parkinson's, Pick's and Alzheimer's are linked to oxidative stress and accumulation of metals such as zinc, aluminium, copper and iron in the brain (Miu and Benga, 2006). Iron is crucial in many cellular functions where it takes part in many neuronal processes. However, excess iron is toxic to brain cells and the brain frequently accumulates iron, which results in high levels of stored iron with age (Connor et al., 1990). Unfortunately, there is a lack of information about the effect of NPs on organs such as the kidneys, liver and spleen (Buzea et al., 2007). However, it

might be assumed that because NPs can translocate to and accumulate in these organs, there is a possibility of adverse reaction and toxicity, which may lead to disease (Buzea et al., 2007). Some diseases with unknown source have been connected to the presence of NPs in the kidneys and liver. In healthy subjects, the liver and kidneys did not display any debris; but particles were discovered in the liver of patients with worn orthopaedic prostheses (Buzea et al., 2007). NPs have often been found in colon tissue of patients with Crohn's disease and ulcerative colitis, but not in healthy subjects (Buzea et al., 2007). The NPs found in these patients have various compositions and are not believed to be toxic in bulk form. After a microscopic and energy spectroscopy analysis of colon mucosa, NPs such as carbon, sulphur, silica and silver were found in abundance (Buzea et al., 2007). The size of these NPs varied between 50 and 100 nm; the smaller the NPs the further they can penetrate. These NPs were found in the layers between healthy and cancerous tissue.

Many potential benefits are predicted from NP commercial applications; however, these benefits should always be compared against the risks to humans and the environment (Buzea et al., 2007). Although the toxic effects of NPs have been highlighted, there is a lack of understanding about their interactions with biological systems (Buzea et al., 2007). These risks are often ignored even after knowing that NPs can cross the blood–brain barrier and can accumulate (Buzea et al., 2007). NP interactions with biological milieu are significantly associated with particles of a smaller size distribution, larger SA to mass ratio and surface characteristics (Buzea et al., 2007). Therefore, NPs can pass through tissues and cell membranes, deposit in the cellular compartments and cause cellular injury and toxicity (Buzea et al., 2007).

References

ABBOTT, M., WANG, W. C. & COHEN, B. 2011. The long-term reform of the water and wastewater industry: the case of Melbourne in Australia. *Utilities Policy,* 19, 115-122.

AGNIHOTRI, S., MUKHERJI, S. & MUKHERJI, S. 2014. Size-controlled silver nanoparticles synthesized over the range 5–100 nm using the same protocol and their antibacterial efficacy. *RSC Advances,* 4, 3974-3983.

ÅKERMAN, M. E., CHAN, W. C., LAAKKONEN, P., BHATIA, S. N. & RUOSLAHTI, E. 2002. Nanocrystal targeting in vivo. *Proceedings of the National Academy of Sciences,* 99, 12617-12621.

ALIABADI, H. M., SHAHIN, M., BROCKS, D. R. & LAVASANIFAR, A. 2008. Disposition of drugs in block copolymer micelle delivery systems. *Clinical Pharmacokinetics,* 47, 619-634.

ALLEN, T. M. & CULLIS, P. R. 2013. Liposomal drug delivery systems: from concept to clinical applications. *Advanced Drug Delivery Reviews,* 65, 36-48.

ALMUTARY, A. & SANDERSON, B. 2016. The MTT and crystal violet assays potential confounders in nanoparticle toxicity testing. *International Journal of Toxicology,* 35, 444-462.

ALTENBURGER, R. & KISSEL, T. 1999. The human keratinocyte cell line HaCaT: an i*n vitro* cell culture model for keratinocyte testosterone metabolism. *Pharmaceutical Research,* 16, 766-771.

ALTMAN, F. P. 1976. Tetrazolium salts and formazans. *Progress in Histochemistry & Cytochemistry,* 9, 1-56.

AMOABEDINY, G., NADERI, A., MALAKOOTIKHAH, J., KOOHI, M., MORTAZAVI, S., NADERI, M. & RASHEDI, H. 2009. Guidelines for safe handling, use and disposal of nanoparticles. *Journal of Physics: Conference Series*, 170, 012037.

AMOOZGAR, Z. & YEO, Y. 2012. Recent advances in stealth coating of nanoparticle drug delivery systems. *Wiley Interdisciplinary Reviews: Nanomedicine & Nanobiotechnology,* 4, 219-233.

ANSELMO, A. C. & MITRAGOTRI, S. 2016. Nanoparticles in the clinic. *Bioengineering & Translational Medicine,* 1, 10-29.

ANTONINI, J. M., SANTAMARIA, A. B., JENKINS, N. T., ALBINI, E. & LUCCHINI, R. 2006. Fate of manganese associated with the inhalation of welding fumes: potential neurological effects. *Neurotoxicology,* 27, 304-310.

ARGYLE, V. & ROBINSON, B. 2006. Are nanoparticles safe? *Chemistry in New Zealand,* 70, 12.

AUSTRALIA. 1999. *The South Australian Government Gazette*. Department for Administrative and Information Services, Adelaide.

AUSTRALIA. 2002. *Introduction to desalination technologies in Australia*. Report for Agriculture, Fisheries and Forestry, Canberra, Australia.

AUSTRALIA'S AGRICULTURE. 2012. Australia's agriculture, fisheries and forestry at a glance 2012, Department of Agriculture, Fisheries and Forestry, Canberra, Australia.

BALAGURU, R. J. B. & JEYAPRAKASH, B. 2012. *Introduction to materials and classification of low dimensional materials*.

BARBE, C., BARTLETT, J., KONG, L., FINNIE, K., LIN, H. Q., LARKIN, M., CALLEJA, S., BUSH, A. & CALLEJA, G. 2004. Silica particles: a novel drug-delivery system. *Advanced Materials,* 16, 1959-1966.

BAUN, A., HARTMANN, N. B., GRIEGER, K. & KUSK, K. O. 2008. Ecotoxicity of engineered nanoparticles to aquatic invertebrates: a brief review and recommendations for future toxicity testing. *Ecotoxicology,* 17, 387-395.

BELYANSKAYA, L., MANSER, P., SPOHN, P., BRUININK, A. & WICK, P. 2007. The reliability and limits of the MTT reduction assay for carbon nanotubes–cell interaction. *Carbon,* 45, 2643-2648.

BERNAS, T. & DOBRUCKI, J. 2002. Mitochondrial and nonmitochondrial reduction of MTT: interaction of MTT with TMRE, JC-1, and NAO mitochondrial fluorescent probes. *Cytometry,* 47, 236-242.

BERNEVIG, B. A., HUGHES, T. L. & ZHANG, S.-C. 2006. Quantum spin Hall effect and topological phase transition in HgTe quantum wells. *Science,* 314, 1757-1761.

BERRIDGE, M. V., HERST, P. M. & TAN, A. S. 2005. Tetrazolium dyes as tools in cell biology: new insights into their cellular reduction. *Biotechnology Annual Review,* 11, 127-152.

BERRIDGE, M. V. & TAN, A. S. 1993. Characterization of the cellular reduction of 3-(4, 5-dimethylthiazol-2-yl)-2, 5-diphenyltetrazolium bromide (MTT):

subcellular localization, substrate dependence, and involvement of mitochondrial electron transport in MTT reduction. *Archives of Biochemistry & Biophysics,* 303, 474-482.

BHABRA, G., SOOD, A., FISHER, B., CARTWRIGHT, L., SAUNDERS, M., EVANS, W. H., SURPRENANT, A., LOPEZ-CASTEJON, G., MANN, S. & DAVIS, S. A. 2009. Nanoparticles can cause DNA damage across a cellular barrier. *Nature Nanotechnology,* 4, 876-883.

BIJU, V., ITOH, T., ANAS, A., SUJITH, A. & ISHIKAWA, M. 2008. Semiconductor quantum dots and metal nanoparticles: syntheses, optical properties, and biological applications. *Analytical & Bioanalytical Chemistry,* 391, 2469-2495.

BOGOVSKI, P. & BOGOVSKI, S. 1981. Special report animal species in which n-nitroso compounds induce cancer. *International Journal of Cancer,* 27, 471-474.

BONDARENKO, O., JUGANSON, K., IVASK, A., KASEMETS, K., MORTIMER, M. & KAHRU, A. 2013. Toxicity of Ag, CuO and ZnO nanoparticles to selected environmentally relevant test organisms and mammalian cells *in vitro*: a critical review. *Archives of Toxicology,* 87, 1181-1200.

BORM, P. J., ROBBINS, D., HAUBOLD, S., KUHLBUSCH, T., FISSAN, H., DONALDSON, K., SCHINS, R., STONE, V., KREYLING, W. & LADEMANN, J. 2006. The potential risks of nanomaterials: a review carried out for ECETOC. *Particle & Fibre Toxicology,* 3, 1.

BORM, P. J., SCHINS, R. P. & ALBRECHT, C. 2004. Inhaled particles and lung cancer, part B: paradigms and risk assessment. *International Journal of Cancer,* 110, 3-14.

BOUKAMP, P., PETRUSSEVSKA, R. T., BREITKREUTZ, D., HORNUNG, J., MARKHAM, A. & FUSENIG, N. E. 1988. Normal keratinization in a spontaneously immortalized aneuploid human keratinocyte cell line. *Journal of Cell Biology,* 106, 761-771.

BOWMAN, C. R., BAILEY, F. C., ELROD- ERICKSON, M., NEIGH, A. M. & OTTER, R. R. 2012. Effects of silver nanoparticles on zebrafish (*Danio rerio*) and *Escherichia coli* (ATCC 25922): a comparison of toxicity based on total surface area versus mass concentration of particles in a model eukaryotic and prokaryotic system. *Environmental Toxicology & Chemistry,* 31, 1793-1800.

BRAACH-MAKSVYTIS, V. 2002. Nanotechnology in Australia—towards a national initiative. *Journal of Nanoparticle Research,* 4, 1-7.

BRAR, S. K., VERMA, M., TYAGI, R. & SURAMPALLI, R. 2010. Engineered nanoparticles in wastewater and wastewater sludge—evidence and impacts. *Waste Management,* 30, 504-520.

BROUWER, D., VAN DUUREN-STUURMAN, B., BERGES, M., JANKOWSKA, E., BARD, D. & MARK, D. 2009. From workplace air measurement results toward estimates of exposure? Development of a strategy to assess exposure to manufactured nano-objects. *Journal of Nanoparticle Research,* 11, 1867.

BROWN, D., DONALDSON, K., BORM, P., SCHINS, R., DEHNHARDT, M., GILMOUR, P., JIMENEZ, L. & STONE, V. 2004. Calcium and ROS-mediated activation of transcription factors and TNF-α cytokine gene expression in macrophages exposed to ultrafine particles. *American Journal of Physiology-Lung Cellular & Molecular Physiology,* 286, L344-L353.

BROWN, R. & FARRELLY, M. 2007. Barriers to advancing sustainable urban water management: a typology. *Rainwater & Urban Design 2007*, 229.

BROWN, S. C., KAMAL, M., NASREEN, N., BAUMURATOV, A., SHARMA, P., ANTONY, V. B. & MOUDGIL, B. M. 2007. Influence of shape, adhesion and simulated lung mechanics on amorphous silica nanoparticle toxicity. *Advanced Powder Technology*, 18, 69-79.

BROWN, T. 2009. Silica exposure, smoking, silicosis and lung cancer—complex interactions. *Occupational Medicine*, 59, 89-95.

BRUCHEZ, M., MORONNE, M., GIN, P., WEISS, S. & ALIVISATOS, A. P. 1998. Semiconductor nanocrystals as fluorescent biological labels. S*cience,* 281, 2013-2016.

BRUNNER, T. J., WICK, P., MANSER, P., SPOHN, P., GRASS, R. N., LIMBACH, L. K., BRUININK, A. & STARK, W. J. 2006. *In vitro* cytotoxicity of oxide nanoparticles: comparison to asbestos, silica, and the effect of particle solubility. *Environmental Science & Technology,* 40, 4374-4381.

BRUST, M., WALKER, M., BETHELL, D., SCHIFFRIN, D. J. & WHYMAN, R. 1994. Synthesis of thiol-derivatised gold nanoparticles in a two-phase liquid–liquid system. *Journal of the Chemical Society, Chemical Communications*, 7, 801-802.

BURIĆ, P., JAKŠIĆ, Ž., ŠTAJNER, L., SIKIRIĆ, M. D., JURAŠIN, D., CASCIO, C., CALZOLAI, L. & LYONS, D. M. 2015. Effect of silver nanoparticles on Mediterranean sea urchin embryonal development is species specific and

depends on moment of first exposure. *Marine Environmental Research,* 111, 50-59.

BUZEA, C., PACHECO, I. I. & ROBBIE, K. 2007. Nanomaterials and nanoparticles: sources and toxicity. *Biointerphases,* 2, MR17-MR71.

CANELAS, D. A., HERLIHY, K. P. & DESIMONE, J. M. 2009. Top- down particle fabrication: control of size and shape for diagnostic imaging and drug delivery. *Wiley Interdisciplinary Reviews: Nanomedicine & Nanobiotechnology,* 1, 391-404.

CASEY, A., DAVOREN, M., HERZOG, E., LYNG, F. M., BYRNE, H. J. & CHAMBERS, G. 2007a. Probing the interaction of single walled carbon nanotubes within cell culture medium as a precursor to toxicity testing. *Carbon,* 45, 34-40.

CASEY, A., HERZOG, E., DAVOREN, M., LYNG, F. M., BYRNE, H. J. & CHAMBERS, G. 2007b. Spectroscopic analysis confirms the interactions between single walled carbon nanotubes and various dyes commonly used to assess cytotoxicity. *Carbon,* 45, 1425-1432.

CASTRANOVA, V. & VALLYATHAN, V. 2000. Silicosis and coal workers' pneumoconiosis. *Environmental Health Perspectives,* 108, 675.

CEDERVALL, T., LYNCH, I., FOY, M., BERGGÅRD, T., DONNELLY, S. C., CAGNEY, G., LINSE, S. & DAWSON, K. A. 2007. Detailed identification of plasma proteins adsorbed on copolymer nanoparticles. *Angewandte Chemie,* 119, 5856-5858.

CHANG, E., THEKKEK, N., YU, W. W., COLVIN, V. L. & DREZEK, R. 2006. Evaluation of quantum dot cytotoxicity based on intracellular uptake. *Small,* 2, 1412-1417.

CHANG, J.-S., CHANG, K. L. B., HWANG, D.-F. & KONG, Z.-L. 2007. *In vitro* cytotoxicitiy of silica nanoparticles at high concentrations strongly depends on the metabolic activity type of the cell line. *Environmental Science & Technology,* 41, 2064-2068.

CHAUDHRY, Q., SCOTTER, M., BLACKBURN, J., ROSS, B., BOXALL, A., CASTLE, L., AITKEN, R. & WATKINS, R. 2008. Applications and implications of nanotechnologies for the food sector. *Food Additives & Contaminants,* 25, 241-258.

CHEN, J.-F., WANG, Y.-H., GUO, F., WANG, X.-M. & ZHENG, C. 2000. Synthesis of nanoparticles with novel technology: high-gravity reactive precipitation. *Industrial & Engineering Chemistry Research,* 39, 948-954.

CHEN, S., ZHAO, X., CHEN, J., CHEN, J., KUZNETSOVA, L., WONG, S. S. & OJIMA, I. 2010. Mechanism-based tumor-targeting drug delivery system. Validation of efficient vitamin receptor-mediated endocytosis and drug release. *Bioconjugate Chemistry,* 21, 979.

CHIBA, K., KAWAKAMI, K. & TOHYAMA, K. 1998. Simultaneous evaluation of cell viability by neutral red, MTT and crystal violet staining assays of the same cells. *Toxicology In Vitro,* 12, 251-258.

CHINEN, A. B., GUAN, C. M., FERRER, J. R., BARNABY, S. N., MERKEL, T. J. & MIRKIN, C. A. 2015. Nanoparticle probes for the detection of cancer biomarkers, cells, and tissues by fluorescence. *Chemical Reviews,* 115, 10530-10574.

CHO, K., WANG, X., NIE, S. & SHIN, D. M. 2008. Therapeutic nanoparticles for drug delivery in cancer. *Clinical Cancer Research,* 14, 1310-1316.

CHOU, C.-C., HSIAO, H.-Y., HONG, Q.-S., CHEN, C.-H., PENG, Y.-W., CHEN, H.-W. & YANG, P.-C. 2008. Single-walled carbon nanotubes can induce pulmonary injury in mouse model. *Nano Letters,* 8, 437-445.

CLOGSTON, J. D. & PATRI, A. K. 2011. Zeta potential measurement. In S. E. MCNEILL (ed.) *Characterization of nanoparticles intended for drug delivery*, Humana Press, New York, NY, pp. 63-70.

COLDITZ, G. A., SELLERS, T. A. & TRAPIDO, E. 2006. Epidemiology—identifying the causes and preventability of cancer? *Nature Reviews Cancer,* 6, 75-83.

COLVIN, V. L. 2003. The potential environmental impact of engineered nanomaterials. *Nature Biotechnology,* 21, 1166-1170.

CONNOR, J., MENZIES, S., ST MARTIN, S. & MUFSON, E. 1990. Cellular distribution of transferrin, ferritin, and iron in normal and aged human brains. *Journal of Neuroscience Research,* 27, 595-611.

COOLEN, L., SPINICELLI, P. & HERMIER, J.-P. 2009. Emission spectrum and spectral diffusion of a single CdSe/ZnS nanocrystal measured by photon-correlation Fourier spectroscopy. *Journal of the Optical Society of America B,* 26, 1463-1468.

CORNELIS, G., HUND-RINKE, K., KUHLBUSCH, T., VAN DEN BRINK, N. & NICKEL, C. 2014. Fate and bioavailability of engineered nanoparticles in soils: a review. *Critical Reviews in Environmental Science & Technology,* 44, 2720-2764.

CORRIN, B. & KING, E. 1969. Experimental endogenous lipid pneumonia and silicosis. *Journal of Pathology,* 97, 325-330.

CORTALEZZI, M. M., ROSE, J., BARRON, A. R. & WIESNER, M. R. 2002. Characteristics of ultrafiltration ceramic membranes derived from alumoxane nanoparticles. *Journal of Membrane Science,* 205, 33-43.

COTO-GARCÍA, A. M., SOTELO-GONZÁLEZ, E., FERNÁNDEZ-ARGÜELLES, M. T., PEREIRO, R., COSTA-FERNÁNDEZ, J. M. & SANZ-MEDEL, A. 2011. Nanoparticles as fluorescent labels for optical imaging and sensing in genomics and proteomics. *Analytical & Bioanalytical Chemistry,* 399, 29-42.

CROSERA, M., BOVENZI, M., MAINA, G., ADAMI, G., ZANETTE, C., FLORIO, C. & LARESE, F. F. 2009. Nanoparticle dermal absorption and toxicity: a review of the literature. *International Archives of Occupational & Environmental Health,* 82, 1043-1055.

CROWLEY, C., KLANRIT, P., BUTLER, C. R., VARANOU, A., PLATÉ, M., HYNDS, R. E., CHAMBERS, R. C., SEIFALIAN, A. M., BIRCHALL, M. A. & JANES, S. M. 2016. Surface modification of a POSS-nanocomposite material to enhance cellular integration of a synthetic bioscaffold. *Biomaterials,* 83, 283-293.

CSŐGÖR, Z., NACKEN, M., SAMETI, M., LEHR, C.-M. & SCHMIDT, H. 2003. Modified silica particles for gene delivery. *Materials Science & Engineering C,* 23, 93-97.

DABBOUSI, B., BAWENDI, M., ONITSUKA, O. & RUBNER, M. 1995. Electroluminescence from CdSe quantum- dot/polymer composites. *Applied Physics Letters,* 66, 1316-1318.

DAGLE, G., WEHNER, A., CLARK, M. & BUSCHBOM, R. 1986. Chronic inhalation exposure of rats to quartz. Silica, silicosis and cancer. Controversy in occupational medicine. *Cancer Research Monographs,* 2, 255-266.

DAHLE, J. T. & ARAI, Y. 2015. Environmental geochemistry of cerium: applications and toxicology of cerium oxide nanoparticles. *International Journal of Environmental Research & Public Health,* 12, 1253-1278.

DANIEL, M.-C. & ASTRUC, D. 2004. Gold nanoparticles: assembly, supramolecular chemistry, quantum-size-related properties, and applications toward biology, catalysis, and nanotechnology. *Chemical Reviews*, 104, 293-346.

DARRACQ, G., CHOKKI, J., RAGOT, A., BIGARNET, X., BARON, J. & JOYEUX, M. 2015. Clarification: impact on ultrafiltration membrane fouling in drinking water treatment. *Journal—American Water Works Association*, 107, 12.

DAS, M., MOHANTY, C. & SAHOO, S. K. 2009. Ligand-based targeted therapy for cancer tissue. *Expert Opinion on Drug Delivery,* 6, 285-304.

DAVIS, M. E. & SHIN, D. M. 2008. Nanoparticle therapeutics: an emerging treatment modality for cancer. *Nature Reviews Drug Discovery,* 7, 771-782.

DE JONG, W. H. & BORM, P. J. 2008. Drug delivery and nanoparticles: applications and hazards. *International Journal of Nanomedicine,* 3, 133.

DEIN, F. J., WILSON, A., FISCHER, D. & LANGENBERG, P. 1994. Avian leucocyte counting using the hemocytometer. *Journal of Zoo & Wildlife Medicine*, 432-437.

DERFUS, A. M., CHAN, W. C. & BHATIA, S. N. 2004. Probing the cytotoxicity of semiconductor quantum dots. *Nano Letters,* 4, 11-18.

DJURIŠIĆ, A. B., LEUNG, Y. H., NG, A., XU, X. Y., LEE, P. K. & DEGGER, N. 2015. Toxicity of metal oxide nanoparticles: mechanisms, characterization, and avoiding experimental artefacts. *Small,* 11, 26-44.

DOBROVOLSKAIA, M. A., CLOGSTON, J. D., NEUN, B. W., HALL, J. B., PATRI, A. K. & MCNEIL, S. E. 2008. Method for analysis of nanoparticle hemolytic properties in vitro. *Nano Letters*, 8, 2180-2187.

DONALDSON, K., AITKEN, R., TRAN, L., STONE, V., DUFFIN, R., FORREST, G. & ALEXANDER, A. 2006. Carbon nanotubes: a review of their properties in relation to pulmonary toxicology and workplace safety. *Toxicological Sciences,* 92, 5-22.

DONALDSON, K., TRAN, L., JIMENEZ, L. A., DUFFIN, R., NEWBY, D. E., MILLS, N., MACNEE, W. & STONE, V. 2005. Combustion-derived nanoparticles: a review of their toxicology following inhalation exposure. *Particle & Fibre Toxicology,* 2, 10.

DRESCHER, D., ORTS-GIL, G., LAUBE, G., NATTE, K., VEH, R. W., ÖSTERLE, W. & KNEIPP, J. 2011. Toxicity of amorphous silica nanoparticles on

eukaryotic cell model is determined by particle agglomeration and serum protein adsorption effects. *Analytical & Bioanalytical Chemistry,* 400, 1367-1373.

DU, H., CHANDAROY, P. & HUI, S. W. 1997. Grafted poly-(ethylene glycol) on lipid surfaces inhibits protein adsorption and cell adhesion. *Biochimica et Biophysica Acta (BBA)-Biomembranes,* 1326, 236-248.

DU, W., SHAN, J., WU, Y., XU, R. & YU, D. 2010. Preparation and characterization of polybenzoxazine/trisilanol polyhedral oligomeric silsesquioxanes composites. *Materials & Design,* 31, 1720-1725.

DUBERTRET, B., SKOURIDES, P., NORRIS, D. J., NOIREAUX, V., BRIVANLOU, A. H. & LIBCHABER, A. 2002. *In vivo* imaging of quantum dots encapsulated in phospholipid micelles. *Science,* 298, 1759-1762.

EDWARDS, G. 2006. Whose values count? Demand management for Melbourne's water. *Economic Record,* 82, S54-S63.

EFROS, A. L., LOCKWOOD, D. J. & TSYBESKOV, L. 2013. *Semiconductor nanocrystals: from basic principles to applications*. Springer Science & Business Media, New York, NY>

EL SALIBY, I., SHON, H., KANDASAMY, J. & VIGNESWARAN, S. 2008. Nanotechnology for wastewater treatment: in brief. In *Encyclopedia of Life Support System*.

ESPARZA, D., ZARAZÚA, I., LÓPEZ-LUKE, T., CERDÁN-PASARÁN, A., SÁNCHEZ-SOLÍS, A., TORRES-CASTRO, A., MORA-SERO, I. & DE LA ROSA, E. 2015. Effect of different sensitization technique on the photoconversion efficiency of CdS quantum dot and CdSe quantum rod sensitized TiO2 solar cells. *Journal of Physical Chemistry C,* 119, 13394-13403.

ESTEPHAN, Z. G., SCHLENOFF, P. S. & SCHLENOFF, J. B. 2011. Zwitteration as an alternative to PEGylation. *Langmuir,* 27, 6794-6800.

FABREGA, J., LUOMA, S. N., TYLER, C. R., GALLOWAY, T. S. & LEAD, J. R. 2011. Silver nanoparticles: behaviour and effects in the aquatic environment. *Environment International,* 37, 517-531.

FARADAY, M. 1857. The Bakerian lecture: experimental relations of gold (and other metals) to light. *Philosophical Transactions of the Royal Society of London,* 147, 145-181.

FAROKHZAD, O. C. & LANGER, R. 2009. Impact of nanotechnology on drug delivery. *ACS Nano,* 3, 16-20.

FARRÉ, M., GAJDA-SCHRANTZ, K., KANTIANI, L. & BARCELÓ, D. 2009. Ecotoxicity and analysis of nanomaterials in the aquatic environment. *Analytical & Bioanalytical Chemistry,* 393, 81-95.

FARRÉ, M., KELLER, J., HOLLING, N., POUSSADE, Y. & GERNJAK, W. 2011. Occurrence of N-nitrosodimethylamine precursors in wastewater treatment plant effluent and their fate during ultrafiltration-reverse osmosis membrane treatment. *Water Science & Technology,* 63, 605-612.

FEHER, F. J., WYNDHAM, K. D., SOULIVONG, D. & NGUYEN, F. 1999. Syntheses of highly functionalized cube-octameric polyhedral oligosilsesquioxanes (R 8 Si 8 O 12). *Journal of the Chemical Society, Dalton Transactions*, 9, 1491-1498.

FERNÁNDEZ-RODRÍGUEZ, M. A., SHEN, Q. & HARTWIG, J. F. 2006. A general and long-lived catalyst for the palladium-catalyzed coupling of aryl halides with thiols. *Journal of the American Chemical Society,* 128, 2180-2181.

FLANIGEN, E. M. & PATTON, R. L. 1978. Silica polymorph and process for preparing same. Google Patents.

FLIER, J. S., UNDERHILL, L. H. & FOLKMAN, J. 1995. Clinical applications of research on angiogenesis. *New England Journal of Medicine,* 333, 1757-1763.

FOLKMAN, J. 1971. Tumor angiogenesis: therapeutic implications. *New England Journal of Medicine*, 285, 1182-1186.

FØRELAND, S., BYE, E., BAKKE, B. & EDUARD, W. 2008. Exposure to fibres, crystalline silica, silicon carbide and sulphur dioxide in the Norwegian silicon carbide industry. *Annals of Occupational Hygiene,* 52, 317-336.

FOREVER, W. 2005. *Regional drought strategy*.

FOTAKIS, G. & TIMBRELL, J. A. 2006. In vitro cytotoxicity assays: comparison of LDH, neutral red, MTT and protein assay in hepatoma cell lines following exposure to cadmium chloride. *Toxicology Letters,* 160, 171-177.

FRENS, G. 1973. Controlled nucleation for the regulation of the particle size in monodisperse gold suspensions. *Nature,* 241, 20-22.

FUBINI, B., GHIAZZA, M. & FENOGLIO, I. 2010. Physico-chemical features of engineered nanoparticles relevant to their toxicity. *Nanotoxicology,* 4, 347-363.

FUKUMURA, D. & JAIN, R. K. 2007. Tumor microvasculature and microenvironment: targets for anti-angiogenesis and normalization. *Microvascular Research,* 74, 72-84.

GAO, D., NOLAN, D. J., MELLICK, A. S., BAMBINO, K., MCDONNELL, K. & MITTAL, V. 2008. Endothelial progenitor cells control the angiogenic switch in mouse lung metastasis. *Science,* 319, 195-198.

GARNER, K. L. & KELLER, A. A. 2014. Emerging patterns for engineered nanomaterials in the environment: a review of fate and toxicity studies. *Journal of Nanoparticle Research,* 16, 2503.

GARNETT, M. C. & KALLINTERI, P. 2006. Nanomedicines and nanotoxicology: some physiological principles. *Occupational Medicine,* 56, 307-311.

GENERALOV, R., LUKOSEVICIUTE, S., JUZENIENE, A. & JUZENAS, P. 2010. Cytotoxicity and phototoxicity of red fluorescent nontargeted quantum dots. *IEEE Journal of Selected Topics in Quantum Electronics,* 16, 997-1003.

GEORGIEVA, J. V., HOEKSTRA, D. & ZUHORN, I. S. 2014. Smuggling drugs into the brain: an overview of ligands targeting transcytosis for drug delivery across the blood–brain barrier. *Pharmaceutics,* 6, 557-583.

GERLIER, D. & THOMASSET, N. 1986. Use of MTT colorimetric assay to measure cell activation. *Journal of Immunological Methods,* 94, 57-63.

GEROFI, J. & FENTON, G. 1981. Comparison of solar RO and solar thermal desalination systems. *Desalination,* 39, 95-107.

GHANBARI, H., COUSINS, B. G. & SEIFALIAN, A. M. 2011. A nanocage for nanomedicine: polyhedral oligomeric silsesquioxane (POSS). *Macromolecular Rapid Communications,* 32, 1032-1046.

GNANASEKARAN, D., MADHAVAN, K. & REDDY, B. 2009. Developments of polyhedral oligomeric silsesquioxanes (POSS), POSSnanocomposites and their applications: a review. Journal of Scientific & Industrial Research, 68, 437-464.

GOODWIN, C. J., HOLT, S. J., DOWNES, S. & MARSHALL, N. J. 1995. Microculture tetrazolium assays: a comparison between two new tetrazolium salts, XTT and MTS. *Journal of Immunological Methods,* 179, 95-103.

GOTTSCHALK, F., ORT, C., SCHOLZ, R. & NOWACK, B. 2011. Engineered nanomaterials in rivers—exposure scenarios for Switzerland at high spatial and temporal resolution. *Environmental Pollution,* 159, 3439-3445.

GRASSHOFF, K., KREMLING, K. & EHRHARDT, M. 2009. *Methods of seawater analysis* 3rd edn, John Wiley & Sons.

GREENLEE, L. F., LAWLER, D. F., FREEMAN, B. D., MARROT, B. & MOULIN, P. 2009. Reverse osmosis desalination: water sources, technology, and today's challenges. *Water Research,* 43, 2317-2348.

GREF, R., LÜCK, M., QUELLEC, P., MARCHAND, M., DELLACHERIE, E., HARNISCH, S., BLUNK, T. & MÜLLER, R. 2000. 'Stealth'corona-core nanoparticles surface modified by polyethylene glycol (PEG): influences of the corona (PEG chain length and surface density) and of the core composition on phagocytic uptake and plasma protein adsorption. *Colloids & Surfaces B: Biointerfaces,* 18, 301-313.

GROSE, R. W. & FLANIGEN, E. M. 1977. Crystalline silica. Google Patents.

GUADAGNINI, R., HALAMODA KENZAOUI, B., WALKER, L., POJANA, G., MAGDOLENOVA, Z., BILANICOVA, D., SAUNDERS, M., JUILLERAT-JEANNERET, L., MARCOMINI, A. & HUK, A. 2015. Toxicity screenings of nanomaterials: challenges due to interference with assay processes and components of classic in vitro tests. *Nanotoxicology,* 9, 13-24.

GUPTA, A. K., BERRY, C., GUPTA, M. & CURTIS, A. 2003. Receptor-mediated targeting of magnetic nanoparticles using insulin as a surface ligand to prevent endocytosis. *IEEE Transactions on NanoBioscience,* 2, 255-261.

HAGENS, W. I., OOMEN, A. G., DE JONG, W. H., CASSEE, F. R. & SIPS, A. J. 2007. What do we (need to) know about the kinetic properties of nanoparticles in the body? *Regulatory Toxicology & Pharmacology,* 49, 217-229.

HAINFELD, J. F., O'CONNOR, M. J., LIN, P., QIAN, L., SLATKIN, D. N. & SMILOWITZ, H. M. 2014. Infrared-transparent gold nanoparticles converted by tumors to infrared absorbers cure tumors in mice by photothermal therapy. *PloS One,* 9, e88414.

HALDEN, R. U. 2015. Epistemology of contaminants of emerging concern and literature meta-analysis. *Journal of Hazardous Materials,* 282, 2-9.

HANAHAN, D. & FOLKMAN, J. 1996. Patterns and emerging mechanisms of the angiogenic switch during tumorigenesis. *Cell,* 86, 353-364.

HARDMAN, R. 2006. A toxicologic review of quantum dots: toxicity depends on physicochemical and environmental factors. *Environmental Health Perspectives,* 114, 165-172.

HARTUNG, T. 2014. Nanotoxicology: the case for *in vitro* tests. In B. FADEEL (ed.) *Handbook of safety assessment of nanomaterials: from toxicological testing to personalized medicine*, Pan Stanford, pp. 113-151.

HEALD, C., STOLNIK, S., KUJAWINSKI, K., DE MATTEIS, C., GARNETT, M., ILLUM, L., DAVIS, S., PURKISS, S., BARLOW, R. & GELLERT, P. 2002. Poly (lactic acid)-poly (ethylene oxide)(PLA-PEG) nanoparticles: NMR studies of the central solidlike PLA core and the liquid PEG corona. *Langmuir,* 18, 3669-3675.

HENSHER, D., SHORE, N. & TRAIN, K. 2005. Households' willingness to pay for water service attributes. *Environmental & Resource Economics,* 32, 509-531.

HIRAI, T., YOSHIKAWA, T., NABESHI, H., YOSHIDA, T., TOCHIGI, S., ICHIHASHI, K.-I., UJI, M., AKASE, T., NAGANO, K. & ABE, Y. 2012. Amorphous silica nanoparticles size-dependently aggravate atopic dermatitis-like skin lesions following an intradermal injection. *Particle & Fibre Toxicology,* 9, 3.

HOBBS, S. K., MONSKY, W. L., YUAN, F., ROBERTS, W. G., GRIFFITH, L., TORCHILIN, V. P. & JAIN, R. K. 1998. Regulation of transport pathways in tumor vessels: role of tumor type and microenvironment. *Proceedings of the National Academy of Sciences,* 95, 4607-4612.

HOET, P. H., BRÜSKE-HOHLFELD, I. & SALATA, O. V. 2004. Nanoparticles—known and unknown health risks. *Journal of Nanobiotechnology,* 2, 12.

HOLDER, A. L., GOTH-GOLDSTEIN, R., LUCAS, D. & KOSHLAND, C. P. 2012. Particle-induced artifacts in the MTT and LDH viability assays. *Chemical Research in Toxicology,* 25, 1885-1892.

HOLMAN, M., PEKARSKAYA, E., BRUNGER, M., SULLIVAN, T., KRULE, E., KAO, M., LIN, P. & YU, D. 2006. *Profiting from international nanotechnology*. Lux Research, Inc., New York, NY.

HOWARD, P. H. 1991. *Handbook of environmental fate and exposure data: for organic chemicals, volume III pesticides*. CRC Press.

HOYT, V. W. & MASON, E. 2008. Nanotechnology: emerging health issues. *Journal of Chemical Health & Safety,* 15, 10-15.

HSU, M. & JULIANO, R. 1982. Interactions of liposomes with the reticuloendothelial system: II. Nonspecific and receptor-mediated uptake of liposomes by mouse

peritoneal macrophages. *Biochimica et Biophysica Acta (BBA)—Molecular Cell Research*, 720, 411-419.

HUANG, N.-P., MICHEL, R., VOROS, J., TEXTOR, M., HOFER, R., ROSSI, A., ELBERT, D. L., HUBBELL, J. A. & SPENCER, N. D. 2001. Poly (L-lysine)-g-poly (ethylene glycol) layers on metal oxide surfaces: surface-analytical characterization and resistance to serum and fibrinogen adsorption. *Langmuir*, 17, 489-498.

HUANG, S. M., ZUO, X., LI, J. J. E., LI, S. F. Y., BAY, B. H. & ONG, C. N. 2012. Metabolomics studies show dose- dependent toxicity induced by SiO2 nanoparticles in MRC- 5 human fetal lung fibroblasts. *Advanced Healthcare Materials*, 1, 779-784.

HURT, R. H., MONTHIOUX, M. & KANE, A. 2006. Toxicology of carbon nanomaterials: status, trends, and perspectives on the special issue. *Carbon*, 44, 1028-1033.

IANNAZZO, D., PISTONE, A., SALAMÒ, M., GALVAGNO, S., ROMEO, R., GIOFRÉ, S. V., BRANCA, C., VISALLI, G. & DI PIETRO, A. 2017. Graphene quantum dots for cancer targeted drug delivery. *International Journal of Pharmaceutics*, 518, 185-192.

IBRAHIM, I. A., ZIKRY, A. & SHARAF, M. A. 2010. Preparation of spherical silica nanoparticles: Stober silica. *Journal of American Science*, 6, 985-989.

ISHIYAMA, M., TOMINAGA, H., SHIGA, M., SASAMOTO, K., OHKURA, Y. & UENO, K. 1996. A combined assay of cell viability and in vitro cytotoxicity with a highly water-soluble tetrazolium salt, neutral red and crystal violet. *Biological & Pharmaceutical Bulletin*, 19, 1518-1520.

ISOBE, H., TANAKA, T., MAEDA, R., NOIRI, E., SOLIN, N., YUDASAKA, M., IIJIMA, S. & NAKAMURA, E. 2006. Preparation, purification, characterization, and cytotoxicity assessment of water-soluble, transition-metal-free carbon nanotube aggregates. *Angewandte Chemie*, 118, 6828-6832.

IZQUIERDO-BARBA, I., COLILLA, M. & VALLET-REGÍ, M. 2016. Zwitterionic ceramics for biomedical applications. *Acta Biomaterialia*, 40, 201-211.

JAISWAL, J. K., MATTOUSSI, H., MAURO, J. M. & SIMON, S. M. 2003. Long-term multiple color imaging of live cells using quantum dot bioconjugates. *Nature Biotechnology*, 21, 47-51.

JANÁT-AMSBURY, M., RAY, A., PETERSON, C. & GHANDEHARI, H. 2011. Geometry and surface characteristics of gold nanoparticles influence their biodistribution and uptake by macrophages. *European Journal of Pharmaceutics & Biopharmaceutics,* 77, 417-423.

JANG, H. D., KIM, S.-K. & KIM, S.-J. 2001. Effect of particle size and phase composition of titanium dioxide nanoparticles on the photocatalytic properties. *Journal of Nanoparticle Research,* 3, 141-147.

JI, X., SONG, X., LI, J., BAI, Y., YANG, W. & PENG, X. 2007. Size control of gold nanocrystals in citrate reduction: the third role of citrate. *Journal of the American Chemical Society,* 129, 13939-13948.

JIA, G., WANG, H., YAN, L., WANG, X., PEI, R., YAN, T., ZHAO, Y. & GUO, X. 2005. Cytotoxicity of carbon nanomaterials: single-wall nanotube, multi-wall nanotube, and fullerene. *Environmental Science & Technology,* 39, 1378-1383.

JIANG, J., OBERDÖRSTER, G. & BISWAS, P. 2009. Characterization of size, surface charge, and agglomeration state of nanoparticle dispersions for toxicological studies. *Journal of Nanoparticle Research,* 11, 77-89.

JIN, S. & YE, K. 2007. Nanoparticle- mediated drug delivery and gene therapy. *Biotechnology Progress,* 23, 32-41.

JU-NAM, Y. & LEAD, J. R. 2008. Manufactured nanoparticles: an overview of their chemistry, interactions and potential environmental implications. *Science of the Total Environment,* 400, 396-414.

JUZENAS, P., CHEN, W., SUN, Y.-P., COELHO, M. A. N., GENERALOV, R., GENERALOVA, N. & CHRISTENSEN, I. L. 2008. Quantum dots and nanoparticles for photodynamic and radiation therapies of cancer. *Advanced Drug Delivery Reviews,* 60, 1600-1614.

KANG, B., MACKEY, M. A. & EL-SAYED, M. A. 2010. Nuclear targeting of gold nanoparticles in cancer cells induces DNA damage, causing cytokinesis arrest and apoptosis. *Journal of the American Chemical Society,* 132, 1517-1519.

KATEB, B. & HEISS, J. D. 2013. *The textbook of nanoneuroscience and nanoneurosurgery*. CRC Press.

KAUPPINEN, T., TOIKKANEN, J., PEDERSEN, D., YOUNG, R., AHRENS, W., BOFFETTA, P., HANSEN, J., KROMHOUT, H., BLASCO, J. M. & MIRABELLI, D. 2000. Occupational exposure to carcinogens in the European Union. *Occupational & Environmental Medicine,* 57, 10-18.

KELLER, A. A. & LAZAREVA, A. 2013. Predicted releases of engineered nanomaterials: from global to regional to local. *Environmental Science & Technology Letters,* 1, 65-70.

KENDALL, K., KENDALL, M. & REHFELDT, F. 2011. Adhesion of nanoparticles. *Adhesion of cells, viruses and nanoparticles.* Springer.

KHALIL, I. A., KOGURE, K., AKITA, H. & HARASHIMA, H. 2006. Uptake pathways and subsequent intracellular trafficking in nonviral gene delivery. *Pharmacological Reviews,* 58, 32-45.

KHUNG, Y. L. & NARDUCCI, D. 2015. Surface modification strategies on mesoporous silica nanoparticles for anti-biofouling zwitterionic film grafting. *Advances in Colloid & Interface Science,* 226, 166-186.

KIM, B., PARK, C.-S., MURAYAMA, M. & HOCHELLA JR, M. F. 2010. Discovery and characterization of silver sulfide nanoparticles in final sewage sludge products. *Environmental Science & Technology,* 44, 7509-7514.

KIM, J. & VAN DER BRUGGEN, B. 2010. The use of nanoparticles in polymeric and ceramic membrane structures: review of manufacturing procedures and performance improvement for water treatment. *Environmental Pollution,* 158, 2335-2349.

KIRCHNER, C., LIEDL, T., KUDERA, S., PELLEGRINO, T., MUÑOZ JAVIER, A., GAUB, H. E., STÖLZLE, S., FERTIG, N. & PARAK, W. J. 2005. Cytotoxicity of colloidal CdSe and CdSe/ZnS nanoparticles. *Nano Letters,* 5, 331-338.

KLAINE, S. J., ALVAREZ, P. J., BATLEY, G. E., FERNANDES, T. F., HANDY, R. D., LYON, D. Y., MAHENDRA, S., MCLAUGHLIN, M. J. & LEAD, J. R. 2008. Nanomaterials in the environment: behavior, fate, bioavailability, and effects. *Environmental Toxicology & Chemistry,* 27, 1825-1851.

KNIGHTS, D., MACGILL, I. & PASSEY, R. The sustainability of desalination plants in Australia: is renewable energy the answer? OzWater Conference, Sydney, 2007.

KOO, T., LEE, Y. & SHEIKHOLESLAMI, R. 2001. Silica fouling and cleaning of reverse osmosis membranes. *Desalination,* 139, 43-56.

KOVACIC, P. & SOMANATHAN, R. 2009. Pulmonary toxicity and environmental contamination: radicals, electron transfer, and protection by antioxidants. *Reviews of Environmental Contamination & Toxicology Vol 201.*

KROLL, A., PILLUKAT, M. H., HAHN, D. & SCHNEKENBURGER, J. 2009. Current in vitro methods in nanoparticle risk assessment: limitations and challenges. *European Journal of Pharmaceutics & Biopharmaceutics,* 72, 370-377.

KROLL, A., PILLUKAT, M. H., HAHN, D. & SCHNEKENBURGER, J. 2012. Interference of engineered nanoparticles with *in vitro* toxicity assays. *Archives of Toxicology,* 86, 1123-1136.

KRUSZEWSKI, M., BRZOSKA, K., BRUNBORG, G., ASARE, N., DOBRZYNSKA, M.-G., DUSINSKA, M., FJELLSBØ, L., GEORGANTZOPOULOU, A., GROMADZKA, J. & GUTLEB, A. C. 2011. Toxicity of silver nanomaterials in higher eukaryotes. *Advances in Molecular Toxicology,* 5, 179-218.

KUHLBUSCH, T. A., ASBACH, C., FISSAN, H., GÖHLER, D. & STINTZ, M. 2011. Nanoparticle exposure at nanotechnology workplaces: a review. *Particle & Fibre Toxicology,* 8, 22.

KUMAR, A., PANDEY, A. K., SHANKER, R. & DHAWAN, A. 2012. Microorganisms: a versatile model for toxicity assessment of engineered nanoparticles. *Nano-Antimicrobials.* Springer.

KUO, T.-C., LU, H.-P. & CHAO, C. C.-K. 2011. The tyrosine kinase inhibitor sorafenib sensitizes hepatocellular carcinoma cells to taxol by suppressing the HURP protein. *Biochemical Pharmacology,* 82, 184-194.

KUZMA, J. 2006. Moving forward responsibly: oversight for the nanotechnology–biology interface. *Nanotechnology & Occupational Health.* Springer.

LAKE, P. & BOND, N. R. 2007. Australian futures: freshwater ecosystems and human water usage. *Futures,* 39, 288-305.

LAM, C.-W., JAMES, J. T., MCCLUSKEY, R. & HUNTER, R. L. 2004. Pulmonary toxicity of single-wall carbon nanotubes in mice 7 and 90 days after intratracheal instillation. *Toxicological Sciences,* 77, 126-134.

LANGER, R. & TIRRELL, D. A. 2004. Designing materials for biology and medicine. *Nature,* 428, 487-492.

LARSON, D. R., ZIPFEL, W. R., WILLIAMS, R. M., CLARK, S. W., BRUCHEZ, M. P., WISE, F. W. & WEBB, W. W. 2003. Water-soluble quantum dots for multiphoton fluorescence imaging in vivo. *Science,* 300, 1434-1436.

LATTEMANN, S. & HÖPNER, T. 2008. Environmental impact and impact assessment of seawater desalination. *Desalination,* 220, 1-15.

LAWSON, R. J., SCHENKER, M. B., MCCURDY, S. A., JENKINS, B., LISCHAK, L. A., JOHN, W. & SCALES, D. 1995. Exposure to amorphous silica fibers and other particulate matter during rice farming operations. *Applied Occupational & Environmental Hygiene,* 10, 677-684.

LEE, D.-W., SHIRLEY, S. A., LOCKEY, R. F. & MOHAPATRA, S. S. 2006. Thiolated chitosan nanoparticles enhance anti-inflammatory effects of intranasally delivered theophylline. *Respiratory Research,* 7, 112.

LEE, Y., CHOI, J.-R., LEE, K. J., STOTT, N. E. & KIM, D. 2008. Large-scale synthesis of copper nanoparticles by chemically controlled reduction for applications of inkjet-printed electronics. *Nanotechnology,* 19, 415604.

LEWINSKI, N. A., BERTHET, A., MAURIZI, L., EISENBEIS, A. & HOPF, N. B. 2017. Effectiveness of hand washing on the removal of iron oxide nanoparticles from human skin *ex vivo*. *Journal of Occupational & Environmental Hygiene,* 00-00.

LI, G., WANG, L., NI, H. & PITTMAN, C. U. 2001. Polyhedral oligomeric silsesquioxane (POSS) polymers and copolymers: a review. *Journal of Inorganic & Organometallic Polymers,* 11, 123-154.

LI, J.-F., XU, Z.-L., YANG, H., YU, L.-Y. & LIU, M. 2009. Effect of TiO 2 nanoparticles on the surface morphology and performance of microporous PES membrane. *Applied Surface Science,* 255, 4725-4732.

LI, J. & ZHU, J.-J. 2013. Quantum dots for fluorescent biosensing and bio-imaging applications. *Analyst,* 138, 2506-2515.

LI, S.-D. & HUANG, L. 2010. Stealth nanoparticles: high density but sheddable PEG is a key for tumor targeting. *Journal of Controlled Release,* 145, 178.

LIMBACH, L. K., WICK, P., MANSER, P., GRASS, R. N., BRUININK, A. & STARK, W. J. 2007. Exposure of engineered nanoparticles to human lung epithelial cells: influence of chemical composition and catalytic activity on oxidative stress. *Environmental Science & Technology,* 41, 4158-4163.

LIN, W., HUANG, Y.-W., ZHOU, X.-D. & MA, Y. 2006. *In vitro* toxicity of silica nanoparticles in human lung cancer cells. *Toxicology & Applied Pharmacology,* 217, 252-259.

LINCH, K. D., MILLER, W. E., ALTHOUSE, R. B., GROCE, D. W. & HALE, J. M. 1998. Surveillance of respirable crystalline silica dust using OSHA compliance data (1979–1995). *American Journal of Industrial Medicine,* 34, 547-558.

LIPPMANN, M. 1990. Effects of fiber characteristics on lung deposition, retention, and disease. *Environmental Health Perspectives,* 88, 311.

LISON, D., THOMASSEN, L. C., RABOLLI, V., GONZALEZ, L., NAPIERSKA, D., SEO, J. W., KIRSCH-VOLDERS, M., HOET, P., KIRSCHHOCK, C. E. & MARTENS, J. A. 2008. Nominal and effective dosimetry of silica nanoparticles in cytotoxicity assays. *Toxicological Sciences,* 104, 155-162.

LIU, J., KERSHAW, W. & KLAASSEN, C. 1990. Rat primary hepatocyte cultures are a good model for examining metallothionein-induced tolerance to cadmium toxicity. *In Vitro Cellular & Developmental Biology,* 26, 75.

LIU, L., LI, W. & LIU, Q. 2014a. Recent development of antifouling polymers: structure, evaluation, and biomedical applications in nano/micro- structures. *Wiley Interdisciplinary Reviews: Nanomedicine & Nanobiotechnology,* 6, 599-614.

LIU, Y., TOURBIN, M., LACHAIZE, S. & GUIRAUD, P. 2014b. Nanoparticles in wastewaters: hazards, fate and remediation. *Powder Technology,* 255, 149-156.

LIZ-MARZÁN, L. M. 2013. Gold nanoparticle research before and after the Brust–Schiffrin method. *Chemical Communications,* 49, 16-18.

LONGMIRE, M. R., OGAWA, M., CHOYKE, P. L. & KOBAYASHI, H. 2011. Biologically optimized nanosized molecules and particles: more than just size. *Bioconjugate Chemistry,* 22, 993-1000.

LOVERN, S. B., STRICKLER, J. R. & KLAPER, R. 2007. Behavioral and physiological changes in *Daphnia magna* when exposed to nanoparticle suspensions (titanium dioxide, nano-C60, and C60HxC70Hx). *Environmental Science & Technology,* 41, 4465-4470.

LOW, K. G., GRANT, S. B., HAMILTON, A. J., GAN, K., SAPHORES, J. D., ARORA, M. & FELDMAN, D. L. 2015. Fighting drought with innovation: Melbourne's response to the Millennium Drought in Southeast Australia. *Wiley Interdisciplinary Reviews: Water,* 2, 315-328.

LOWRY, G. V., ESPINASSE, B. P., BADIREDDY, A. R., RICHARDSON, C. J., REINSCH, B. C., BRYANT, L. D., BONE, A. J., DEONARINE, A., CHAE, S. & THEREZIEN, M. 2012. Long-term transformation and fate of manufactured Ag nanoparticles in a simulated large scale freshwater emergent wetland. *Environmental Science & Technology,* 46, 7027-7036.

LUO, D., HAN, E., BELCHEVA, N. & SALTZMAN, W. M. 2004. A self-assembled, modular DNA delivery system mediated by silica nanoparticles. *Journal of Controlled Release,* 95, 333-341.

LUO, J. & WAN, Y. 2011. Effect of highly concentrated salt on retention of organic solutes by nanofiltration polymeric membranes. *Journal of Membrane Science,* 372, 145-153.

LYNCH, I. 2016. Water governance challenges presented by nanotechnologies: tracking, identifying and quantifying nanomaterials (the ultimate disparate source) in our waterways. *Hydrology Research,* 47, 552-568.

LYNCH, I. & DAWSON, K. A. 2008. Protein–nanoparticle interactions. *Nano Today,* 3, 40-47.

MA, H., WILLIAMS, P. L. & DIAMOND, S. A. 2013. Ecotoxicity of manufactured ZnO nanoparticles—a review. *Environmental Pollution,* 172, 76-85.

MACCORMACK, T. J., CLARK, R. J., DANG, M. K., MA, G., KELLY, J. A., VEINOT, J. G. & GOSS, G. G. 2012. Inhibition of enzyme activity by nanomaterials: potential mechanisms and implications for nanotoxicity testing. *Nanotoxicology,* 6, 514-525.

MACCORMACK, T. J., GOSS, G. G. & HANDY, R. D. 2013. Emerging threats to fishes: engineered organic nanomaterials. *Fish Physiology: Organic Chemical Toxicology of Fishes,* 1, 439-469.

MAEDA, H., WU, J., SAWA, T., MATSUMURA, Y. & HORI, K. 2000. Tumor vascular permeability and the EPR effect in macromolecular therapeutics: a review. *Journal of Controlled Release,* 65, 271-284.

MAHAPATRA, S. S. & KARAK, N. 2008. Silver nanoparticle in hyperbranched polyamine: synthesis, characterization and antibacterial activity. *Materials Chemistry & Physics,* 112, 1114-1119.

MAHMOUDI, M., HOFMANN, H., ROTHEN-RUTISHAUSER, B. & PETRI-FINK, A. 2011. Assessing the *in vitro* and *in vivo* toxicity of superparamagnetic iron oxide nanoparticles. *Chemical Reviews,* 112, 2323-38.

MALVINDI, M. A., DE MATTEIS, V., GALEONE, A., BRUNETTI, V., ANYFANTIS, G. C., ATHANASSIOU, A., CINGOLANI, R. & POMPA, P. P. 2014. Toxicity assessment of silica coated iron oxide nanoparticles and biocompatibility improvement by surface engineering. *PLoS One,* 9, e85835.

MARCHESI, S., CARNIATO, F. & BOCCALERI, E. 2014. Synthesis and characterisation of a novel europium (III)-containing heptaisobutyl-POSS. *New Journal of Chemistry*, 38, 2480-2485.

MARINELLI, M., GHOSH, A. & MERCURI, F. 2001. Small quartz silica spheres induced disorder in octylcyanobiphenyl (8CB) liquid crystals: a thermal study. *Physical Review E,* 63, 061713.

MARK, J. E. 2007. *Physical properties of polymers handbook.* Springer.

MARTIN, C. R. 1994. Nanomaterials—a membrane-based synthetic approach. *Science,* 266, 1961-1966.

MATSUMURA, Y. & MAEDA, H. 1986. A new concept for macromolecular therapeutics in cancer chemotherapy: mechanism of tumoritropic accumulation of proteins and the antitumor agent smancs. *Cancer Research,* 46, 6387-6392.

MATSUSAKI, M., LARSSON, K., AKAGI, T., LINDSTEDT, M., AKASHI, M. & BORREBAECK, C. A. 2005. Nanosphere induced gene expression in human dendritic cells. *Nano Letters,* 5, 2168-2173.

MATTSON, A. M., JENSEN, C. O. & DUTCHER, R. A. 1947. Triphenyltetrazolium chloride as a dye for vital tissues. *Science,* 106, 294-295.

MAYNARD, A. D., AITKEN, R. J., BUTZ, T., COLVIN, V., DONALDSON, K., OBERDÖRSTER, G., PHILBERT, M. A., RYAN, J., SEATON, A. & STONE, V. 2006. Safe handling of nanotechnology. *Nature,* 444, 267.

MAZUMDER, V. & SUN, S. 2009. Oleylamine-mediated synthesis of Pd nanoparticles for catalytic formic acid oxidation. *Journal of the American Chemical Society,* 131, 4588-4589.

MCCUSKER, C., CARROLL, J. B. & ROTELLO, V. M. 2005. Cationic polyhedral oligomeric silsesquioxane (POSS) units as carriers for drug delivery processes. *Chemical Communications,* 8, 996-998.

MCKINNON, W. B. 1982. Impact into the Earth's ocean floor: preliminary experiments, a planetary model, and possibilities for detection. *Geological Society of America Special Papers,* 190, 129-142.

MEESTERS, J. A., VELTMAN, K., HENDRIKS, A. J. & VAN DE MEENT, D. 2013. Environmental exposure assessment of engineered nanoparticles: why REACH needs adjustment. *Integrated Environmental Assessment & Management,* 9, e15-e26.

MERGET, R., BAUER, T., KÜPPER, H., PHILIPPOU, S., BAUER, H., BREITSTADT, R. & BRUENING, T. 2002. Health hazards due to the inhalation of amorphous silica. *Archives of Toxicology,* 75, 625-634.

MEZHER, T., FATH, H., ABBAS, Z. & KHALED, A. 2011. Techno-economic assessment and environmental impacts of desalination technologies. *Desalination,* 266, 263-273.

MICHALET, X., PINAUD, F., BENTOLILA, L., TSAY, J., DOOSE, S., LI, J., SUNDARESAN, G., WU, A., GAMBHIR, S. & WEISS, S. 2005. Quantum dots for live cells, *in vivo* imaging, and diagnostics. *Science,* 307, 538-544.

MICHELSON, E. S. & REJESKI, D. Falling through the cracks? Public perception, risk, and the oversight of emerging nanotechnologies. *IEEE International Symposium on Technology and Society, 2006*. IEEE, pp. 1-17.

MILLER, R. J., BENNETT, S., KELLER, A. A., PEASE, S. & LENIHAN, H. S. 2012. TiO_2 nanoparticles are phototoxic to marine phytoplankton. *PloS One,* 7, e30321.

MILLER, R. J., LENIHAN, H. S., MULLER, E. B., TSENG, N., HANNA, S. K. & KELLER, A. A. 2010. Impacts of metal oxide nanoparticles on marine phytoplankton. *Environmental Science & Technology,* 44, 7329-7334.

MILLS, N. L., AMIN, N., ROBINSON, S. D., ANAND, A., DAVIES, J., PATEL, D., DE LA FUENTE, J. M., CASSEE, F. R., BOON, N. A. & MACNEE, W. 2006. Do inhaled carbon nanoparticles translocate directly into the circulation in humans? *American Journal of Respiratory & Critical Care Medicine,* 173, 426-431.

MISRA, S. K., DYBOWSKA, A., BERHANU, D., LUOMA, S. N. & VALSAMI-JONES, E. 2012. The complexity of nanoparticle dissolution and its importance in nanotoxicological studies. *Science of the Total Environment,* 438, 225-232.

MITCH, W. A., SHARP, J. O., TRUSSELL, R. R., VALENTINE, R. L., ALVAREZ-COHEN, L. & SEDLAK, D. L. 2003. N-nitrosodimethylamine (NDMA) as a drinking water contaminant: a review. *Environmental Engineering Science,* 20, 389-404.

MIU, A. C. & BENGA, O. 2006. Aluminum and Alzheimer's disease: a new look. *Journal of Alzheimer's disease,* 10, 179-201.

MOFFATT, S. & CRISTIANO, R. J. 2006. Uptake characteristics of NGR-coupled stealth PEI/pDNA nanoparticles loaded with PLGA-PEG-PLGA tri-block

copolymer for targeted delivery to human monocyte-derived dendritic cells. *International Journal of Pharmaceutics*, 321, 143-154.

MOGHIMI, S. & PATEL, H. 1998. Serum-mediated recognition of liposomes by phagocytic cells of the reticuloendothelial system—the concept of tissue specificity. *Advanced Drug Delivery Reviews,* 32, 45-60.

MOGHIMI, S. M., HUNTER, A. C. & MURRAY, J. C. 2001. Long-circulating and target-specific nanoparticles: theory to practice. *Pharmacological Reviews,* 53, 283-318.

MOGHIMI, S. M. & SZEBENI, J. 2003. Stealth liposomes and long circulating nanoparticles: critical issues in pharmacokinetics, opsonization and protein-binding properties. *Progress in Lipid Research,* 42, 463-478.

MOHANRAJ, V. & CHEN, Y. 2006. Nanoparticles— review. *Tropical Journal of Pharmaceutical Research,* 5, 561-573.

MOMTAZ, S. & GLADSTONE, W. 2008. Ban on commercial fishing in the estuarine waters of New South Wales, Australia: community consultation and social impacts. *Environmental Impact Assessment Review,* 28, 214-225.

MONTEIRO-RIVIERE, N. A. & INMAN, A. O. 2006. Challenges for assessing carbon nanomaterial toxicity to the skin. *Carbon,* 44, 1070-1078.

MONTEIRO-RIVIERE, N. A., INMAN, A. O. & ZHANG, L. W. 2009. Limitations and relative utility of screening assays to assess engineered nanoparticle toxicity in a human cell line. *Toxicology & Applied Pharmacology*, 234, 222-235.

MOORE, M. 2006. Do nanoparticles present ecotoxicological risks for the health of the aquatic environment? *Environment International*, 32, 967-976.

MORROW, P. E., GIBB, F. R., GAZIOGLU, K. M., MAHONEY, E., DAVIES, H., FEINGOLD, B. & WOOD, D. 1967. A study of particulate clearance from the human lungs 1, 2, 3. *American Review of Respiratory Disease,* 96, 1209-1221.

MOSMANN, T. 1983. Rapid colorimetric assay for cellular growth and survival: application to proliferation and cytotoxicity assays. *Journal of Immunological Methods,* 65, 55-63.

MUELLER, N. C. & NOWACK, B. 2010. Nanoparticles for remediation: solving big problems with little particles. *Elements,* 6, 395-400.

MUGAVIN, D. 2004. Adelaide's greenway: river torrens linear park. *Landscape & Urban Planning,* 68, 223-240.

MULLER, J., HUAUX, F., MOREAU, N., MISSON, P., HEILIER, J.-F., DELOS, M., ARRAS, M., FONSECA, A., NAGY, J. B. & LISON, D. 2005. Respiratory toxicity of multi-wall carbon nanotubes. *Toxicology & Applied Pharmacology,* 207, 221-231.

MULVANEY, P., GIERSIG, M., UNG, T. & LIZ- MARZÁN, L. M. 1997. Direct observation of chemical reactions in silica- coated gold and silver nanoparticles. *Advanced Materials,* 9, 570-575.

MURPHY, T. F. & SETHI, S. 2002. Chronic obstructive pulmonary disease. *Drugs & Aging,* 19, 761-775.

NAGHAVI, N., DE MEL, A., ALAVIJEH, O. S., COUSINS, B. G. & SEIFALIAN, A. M. 2013. Nitric oxide donors for cardiovascular implant applications. *Small,* 9, 22-35.

NAPIERSKA, D., THOMASSEN, L. C., RABOLLI, V., LISON, D., GONZALEZ, L., KIRSCH- VOLDERS, M., MARTENS, J. A. & HOET, P. H. 2009. Size-dependent cytotoxicity of monodisperse silica nanoparticles in human endothelial cells. *Small,* 5, 846-853.

NARANG, A. S. & MAHATO, R. I. 2006. Biological and biomaterial approaches for improved islet transplantation. *Pharmacological Reviews,* 58, 194-243.

NAVARRO, E., BAUN, A., BEHRA, R., HARTMANN, N. B., FILSER, J., MIAO, A.-J., QUIGG, A., SANTSCHI, P. H. & SIGG, L. 2008. Environmental behavior and ecotoxicity of engineered nanoparticles to algae, plants, and fungi. *Ecotoxicology,* 17, 372-386.

NAWROCKI, J. & ANDRZEJEWSKI, P. 2011. Nitrosamines and water. *Journal of Hazardous Materials,* 189, 1-18.

NEL, A., XIA, T., MÄDLER, L. & LI, N. 2006. Toxic potential of materials at the nanolevel. *Science,* 311, 622-627.

NEL, A. E., MÄDLER, L., VELEGOL, D., XIA, T., HOEK, E. M., SOMASUNDARAN, P., KLAESSIG, F., CASTRANOVA, V. & THOMPSON, M. 2009. Understanding biophysicochemical interactions at the nano–bio interface. *Nature Materials,* 8, 543-557.

NEWCOMBE, G., MORRAN, J. & CULBERT, J. 2012. NDMA attracting international attention. *Water: Journal of the Australian Water Association,* 39, 76.

NINEHAM, A. 1955. The chemistry of formazans and tetrazolium salts. *Chemical Reviews,* 55, 355-483.

NOVELLI, A. A., ARGESE, E., TAGLIAPIETRA, D., BETTIOL, C. & GHIRARDINI, A. V. 2002. Toxicity of tributyltin and triphenyltin to early life-stages of *Paracentrotus lividus* (Echinodermata: Echinoidea). *Environmental Toxicology & Chemistry,* 21, 859-864.

NOVIKOFF, A. B., SHIN, W.-Y. & DRUCKER, J. 1961. Mitochondrial localization of oxidative enzymes: staining results with two tetrazolium salts. *Journal of Biophysical & Biochemical Cytology,* 9, 47-61.

NOWAK, A. K., ROBINSON, B. W. & LAKE, R. A. 2003. Synergy between chemotherapy and immunotherapy in the treatment of established murine solid tumors. *Cancer Research,* 63, 4490-4496.

NOWACK, B., BAALOUSHA, M., BORNHÖFT, N., CHAUDHRY, Q., CORNELIS, G., COTTERILL, J., GONDIKAS, A., HASSELLÖV, M., LEAD, J. & MITRANO, D. M. 2015. Progress towards the validation of modeled environmental concentrations of engineered nanomaterials by analytical measurements. *Environmental Science: Nano,* 2, 421-428.

OBERDÖRSTER, G. 2000. Pulmonary effects of inhaled ultrafine particles. *International Archives of Occupational & Environmental Health,* 74, 1-8.

OBERDÖRSTER, G., MAYNARD, A., DONALDSON, K., CASTRANOVA, V., FITZPATRICK, J., AUSMAN, K., CARTER, J., KARN, B., KREYLING, W. & LAI, D. 2005a. Principles for characterizing the potential human health effects from exposure to nanomaterials: elements of a screening strategy. *Particle & Fibre Toxicology,* 2, 8.

OBERDÖRSTER, G., OBERDÖRSTER, E. & OBERDÖRSTER, J. 2005b. Nanotoxicology: an emerging discipline evolving from studies of ultrafine particles. *Environmental Health Perspectives,* 113, 823.

OBERDÖRSTER, G., SHARP, Z., ATUDOREI, V., ELDER, A., GELEIN, R., KREYLING, W. & COX, C. 2004. Translocation of inhaled ultrafine particles to the brain. *Inhalation Toxicology,* 16, 437-445.

OMER, A. M. 2008. Energy, environment and sustainable development. *Renewable & Sustainable Energy Reviews,* 12, 2265-2300.

ONG, K. J., MACCORMACK, T. J., CLARK, R. J., EDE, J. D., ORTEGA, V. A., FELIX, L. C., DANG, M. K., MA, G., FENNIRI, H. & VEINOT, J. G. 2014.

Widespread nanoparticle-assay interference: implications for nanotoxicity testing. *PLoS One*, 9, e90650.

OWENS, D. E. & PEPPAS, N. A. 2006. Opsonization, biodistribution, and pharmacokinetics of polymeric nanoparticles. *International Journal of Pharmaceutics,* 307, 93-102.

PANÁČEK, A., KOLÁŘ, M., VEČEŘOVÁ, R., PRUCEK, R., SOUKUPOVÁ, J., KRYŠTOF, V., HAMAL, P., ZBOŘIL, R. & KVÍTEK, L. 2009. Antifungal activity of silver nanoparticles against *Candida* spp. *Biomaterials*, 30, 6333-6340.

PANDIT, S., DASGUPTA, D., DEWAN, N. & AHMED, P. 2016. Nanotechnology based biosensors and its application. *Pharma Innovation Journal*, 5, 18-25.

PANDURANGI, R. S., SEEHRA, M. S., RAZZABONI, B. L. & BOLSAITIS, P. 1990. Surface and bulk infrared modes of crystalline and amorphous silica particles: a study of the relation of surface structure to cytotoxicity of respirable silica. *Environmental Health Perspectives,* 86, 327.

PARENT, M.-É., SIEMIATYCKI, J. & FRITSCHI, L. 2000. Workplace exposures and oesophageal cancer. *Occupational & Environmental Medicine,* 57, 325-334.

PARK, E.-J., CHOI, J., PARK, Y.-K. & PARK, K. 2008. Oxidative stress induced by cerium oxide nanoparticles in cultured BEAS-2B cells. *Toxicology,* 245, 90-100.

PARK, M. V., NEIGH, A. M., VERMEULEN, J. P., DE LA FONTEYNE, L. J., VERHAREN, H. W., BRIEDÉ, J. J., VAN LOVEREN, H. & DE JONG, W. H. 2011. The effect of particle size on the cytotoxicity, inflammation, developmental toxicity and genotoxicity of silver nanoparticles. *Biomaterials,* 32, 9810-9817.

PATIL, S. S., SHEDBALKAR, U. U., TRUSKEWYCZ, A., CHOPADE, B. A. & BALL, A. S. 2016. Nanoparticles for environmental clean-up: a review of potential risks and emerging solutions. *Environmental Technology & Innovation,* 5, 10-21.

PATIL, Y., SADHUKHA, T., MA, L. & PANYAM, J. 2009. Nanoparticle-mediated simultaneous and targeted delivery of paclitaxel and tariquidar overcomes tumor drug resistance. *Journal of Controlled Release,* 136, 21-29.

PEER, D. & MARGALIT, R. 2006. Fluoxetine and reversal of multidrug resistance. *Cancer Letters,* 237, 180-187.

PEGEL, S., PÖTSCHKE, P., PETZOLD, G., ALIG, I., DUDKIN, S. M. & LELLINGER, D. 2008. Dispersion, agglomeration, and network formation of multiwalled carbon nanotubes in polycarbonate melts. *Polymer,* 49, 974-984.

PETERS, K., UNGER, R. E., KIRKPATRICK, C. J., GATTI, A. M. & MONARI, E. 2004. Effects of nano-scaled particles on endothelial cell function in vitro: studies on viability, proliferation and inflammation. *Journal of Materials Science: Materials in Medicine,* 15, 321-325.

PETERS, T. M., ELZEY, S., JOHNSON, R., PARK, H., GRASSIAN, V. H., MAHER, T. & O'SHAUGHNESSY, P. 2008. Airborne monitoring to distinguish engineered nanomaterials from incidental particles for environmental health and safety. *Journal of Occupational & Environmental Hygiene,* 6, 73-81.

PETROS, R. A. & DESIMONE, J. M. 2010. Strategies in the design of nanoparticles for therapeutic applications. *Nature Reviews Drug Discovery,* 9, 615-627.

PEYRON, M.-A., MISHELLANY, A. & WODA, A. 2004. Particle size distribution of food boluses after mastication of six natural foods. *Journal of Dental Research,* 83, 578-582.

PHILLIPS, S. H., HADDAD, T. S. & TOMCZAK, S. J. 2004. Developments in nanoscience: polyhedral oligomeric silsesquioxane (POSS)-polymers. *Current Opinion in Solid State & Materials Science,* 8, 21-29.

PIETERS, R., LOONEN, A., HUISMANS, D., BROEKEMA, G., DIRVEN, M., HEYENBROK, M., HAHLEN, K. & VEERMAN, A. 1990. *In vitro* drug sensitivity of cells from children with leukemia using the MTT assay with improved culture conditions. *Blood,* 76, 2327-2336.

PISTONE, A., IANNAZZO, D., ANSARI, S., MILONE, C., SALAMÒ, M., GALVAGNO, S., CIRMI, S. & NAVARRA, M. 2016. Tunable doxorubicin release from polymer-gated multiwalled carbon nanotubes. *International Journal of Pharmaceutics,* 515, 30-36.

POON, Z., CHANG, D., ZHAO, X. & HAMMOND, P. T. 2011. Layer-by-layer nanoparticles with a pH-sheddable layer for in vivo targeting of tumor hypoxia. *ACS Nano,* 5, 4284-4292.

PRADEEP, S., RAGHURAM, S., CHAUDHURY, M. G. & MAZUMDER, S. 2017. Synthesis and characterization of Fe3+ and Mn2+ doped ZnS quantum dots for photocatalytic applications: effect of 2-mercaptoethanol and chitosan as capping agents. *Journal of Nanoscience & Nanotechnology,* 17, 1125-1132.

PRATTEN, M. K. & LLOYD, J. B. 1986. Pinocytosis and phagocytosis: the effect of size of a particulate substrate on its mode of capture by rat peritoneal macrophages cultured in vitro. *Biochimica et Biophysica Acta (BBA)-General Subjects,* 881, 307-313.

PRAUSNITZ, M. R., MITRAGOTRI, S. & LANGER, R. 2004. Current status and future potential of transdermal drug delivery. *Nature Reviews Drug Discovery,* 3, 115-124.

PRICE, P. & MCMILLAN, T. J. 1990. Use of the tetrazolium assay in measuring the response of human tumor cells to ionizing radiation. *Cancer Research,* 50, 1392-1396.

PRIYA, K. K., RAMESH, M., SARAVANAN, M. & PONPANDIAN, N. 2015. Ecological risk assessment of silicon dioxide nanoparticles in a freshwater fish *Labeo rohita*: hematology, ionoregulation and gill Na+/K+ ATPase activity. *Ecotoxicology & Environmental Safety,* 120, 295-302.

PUMERA, M. 2011. Nanotoxicology: the molecular science point of view. *Chemistry—An Asian Journal,* 6, 340-348.

QIAN, Z. M., LI, H., SUN, H. & HO, K. 2002. Targeted drug delivery via the transferrin receptor-mediated endocytosis pathway. *Pharmacological Reviews,* 54, 561-587.

QUIGGIN, J. 2006. Urban water supply in Australia: the option of diverting water from irrigation. *Public Policy,* 1, 14.

QUIGGIN, J. 2007. Issues in Australian water policy. *Australian Chief Executive: Official Journal of the Committee for Economic Development of Australia,* February 2007, 38-47.

QUIK, J. T., VONK, J. A., HANSEN, S. F., BAUN, A. & VAN DE MEENT, D. 2011. How to assess exposure of aquatic organisms to manufactured nanoparticles? *Environment International,* 37, 1068-1077.

RAJAPAKSE, K., DROBNE, D., KASTELEC, D. & MARINSEK-LOGAR, R. 2013. Experimental evidence of false-positive Comet test results due to TiO2 particle-assay interactions. *Nanotoxicology,* 7, 1043-1051.

RAK, J. & JOANNE, L. Y. 2004. Oncogenes and tumor angiogenesis: the question of vascular ‘supply’and vascular ‘demand’. *Seminars in Cancer Biology,* 14, 93-104.

RALUY, G., SERRA, L. & UCHE, J. 2006. Life cycle assessment of MSF, MED and RO desalination technologies. *Energy,* 31, 2361-2372.

REZNICKOVA, A., NOVOTNA, Z., KVITEK, O., KOLSKA, Z. & SVORCIK, V. 2015. Gold, silver and carbon nanoparticles grafted on activated polymers for biomedical applications. *Journal of nanoscience & Nanotechnology,* 15, 10053-10073.

RISOM, L., MØLLER, P. & LOFT, S. 2005. Oxidative stress-induced DNA damage by particulate air pollution. *Mutation Research/Fundamental & Molecular Mechanisms of Mutagenesis,* 592, 119-137.

ROBERTS, D. A., JOHNSTON, E. L. & KNOTT, N. A. 2010. Impacts of desalination plant discharges on the marine environment: a critical review of published studies. *Water Research,* 44, 5117-5128.

ROGERS-HAYDEN, T. & PIDGEON, N. 2007. Moving engagement 'upstream'? Nanotechnologies and the Royal Society and Royal Academy of Engineering's inquiry. *Public Understanding of Science,* 16, 345-364.

ROSETH, N. 2006. Community views on water shortages and conservation. *Water: Journal of the Australian Water Association,* 33, 62.

ROTHEN-RUTISHAUSER, B. M., SCHÜRCH, S., HAENNI, B., KAPP, N. & GEHR, P. 2006. Interaction of fine particles and nanoparticles with red blood cells visualized with advanced microscopic techniques. *Environmental Science & Technology,* 40, 4353-4359.

ROY, I., OHULCHANSKYY, T. Y., BHARALI, D. J., PUDAVAR, H. E., MISTRETTA, R. A., KAUR, N. & PRASAD, P. N. 2005. Optical tracking of organically modified silica nanoparticles as DNA carriers: a nonviral, nanomedicine approach for gene delivery. *Proceedings of the National Academy of Sciences of the United States of America,* 102, 279-284.

RZIGALINSKI, B. A. & STROBL, J. S. 2009. Cadmium-containing nanoparticles: perspectives on pharmacology and toxicology of quantum dots. *Toxicology & Applied Pharmacology,* 238, 280-288.

SALATA, O. V. 2004. Applications of nanoparticles in biology and medicine. *Journal of Nanobiotechnology,* 2, 3.

SAMBUY, Y., DE ANGELIS, I., RANALDI, G., SCARINO, M., STAMMATI, A. & ZUCCO, F. 2005. The Caco-2 cell line as a model of the intestinal barrier:

influence of cell and culture-related factors on Caco-2 cell functional characteristics. *Cell Biology & Toxicology,* 21, 1-26.

SANAGI, M. M., CHONG, M. H., ENDUD, S., IBRAHIM, W. A. W. & ALI, I. 2015. Nano iron porphyrinated poly (amidoamine) dendrimer mobil composition matter-41 for extraction of N-nitrosodiphenylamine nitrosamine from water samples. *Microporous & Mesoporous Materials,* 213, 68-77.

SANTIAGO-MARTÍN, A. D., CONSTANTIN, B., GUESDON, G., KAGAMBEGA, N., RAYMOND, S. & CLOUTIER, R. G. 2015. Bioavailability of engineered nanoparticles in soil systems. *Journal of Hazardous, Toxic, & Radioactive Waste,* 20, B4015001.

SANZ, M. A. & STOVER, R. L. Low energy consumption in the Perth seawater desalination plant. IDA World Congress–Maspalomas, Gran Canaria, Spain, 2007.

SAVOLAINEN, K., ALENIUS, H., NORPPA, H., PYLKKÄNEN, L., TUOMI, T. & KASPER, G. 2010. Risk assessment of engineered nanomaterials and nanotechnologies—a review. *Toxicology,* 269, 92-104.

SCHIAVO, S., OLIVIERO, M., MIGLIETTA, M., RAMETTA, G. & MANZO, S. 2016. Genotoxic and cytotoxic effects of ZnO nanoparticles for *Dunaliella tertiolecta* and comparison with SiO 2 and TiO 2 effects at population growth inhibition levels. *Science of the Total Environment,* 550, 619-627.

SCHMID, K. & RIEDIKER, M. 2008. Use of nanoparticles in Swiss industry: a targeted survey. *Environmental Science & Technology,* 42, 2253-2260.

SCHOOP, V. M., MIRANCEA, N. & FUSENIG, N. E. 1999. Epidermal organization and differentiation of HaCaT keratinocytes in organotypic coculture with human dermal fibroblasts. *Journal of Investigative Dermatology,* 112, 343-353.

SCHOTTENFELD, D. & BEEBE- DIMMER, J. 2006. Chronic inflammation: a common and important factor in the pathogenesis of neoplasia. *CA: a Cancer Journal for Clinicians,* 56, 69-83.

SCHWAB, J. J. & LICHTENHAN, J. D. 1998. Polyhedral oligomeric silsesquioxane (POSS)-based polymers. *Applied Organometallic Chemistry,* 12, 707-713.

SEMPLE, S. C., CHONN, A. & CULLIS, P. R. 1998. Interactions of liposomes and lipid-based carrier systems with blood proteins: relation to clearance behaviour in vivo. *Advanced Drug Delivery Reviews,* 32, 3-17.

SENIOR, J. 1986. Fate and behavior of liposomes in vivo: a review of controlling factors. *Critical Reviews in Therapeutic Drug Carrier Systems,* 3, 123-193.

SHANNON, M. A., BOHN, P. W., ELIMELECH, M., GEORGIADIS, J. G., MARINAS, B. J. & MAYES, A. M. 2008. Science and technology for water purification in the coming decades. *Nature,* 452, 301-310.

SHEN, J.-N., RUAN, H.-M., WU, L.-G. & GAO, C.-J. 2011. Preparation and characterization of PES–SiO 2 organic–inorganic composite ultrafiltration membrane for raw water pretreatment. *Chemical Engineering Journal,* 168, 1272-1278.

SHENG, Y., YUAN, Y., LIU, C., TAO, X., SHAN, X. & XU, F. 2009. In vitro macrophage uptake and in vivo biodistribution of PLA–PEG nanoparticles loaded with hemoglobin as blood substitutes: effect of PEG content. *Journal of Materials Science: Materials in Medicine,* 20, 1881-1891.

SHI, J., VOTRUBA, A. R., FAROKHZAD, O. C. & LANGER, R. 2010. Nanotechnology in drug delivery and tissue engineering: from discovery to applications. *Nano Letters,* 10, 3223.

SHI, W., DOLAI, S., RIZK, S., HUSSAIN, A., TARIQ, H., AVERICK, S., L'AMOREAUX, W., EL IDRISSI, A., BANERJEE, P. & RAJA, K. 2007. Synthesis of monofunctional curcumin derivatives, clicked curcumin dimer, and a PAMAM dendrimer curcumin conjugate for therapeutic applications. *Organic Letters,* 9, 5461-5464.

SHINOHARA, Y. & KOHYAMA, N. 2004. Quantitative analysis of tridymite and cristobalite crystallized in rice husk ash by heating. *Industrial Health,* 42, 277-285.

SIMMONS, M. Y. & BARLOW, T. W. 2009. Nanotechnology in Australia. In L. LIU (ed.) *Emerging nanotechnology power: nanotechnology R&D and business trends in the Asia Pacific Rim,* World Scientific, Singapore, pp.

SKIRTACH, A. G., MUÑOZ JAVIER, A., KREFT, O., KÖHLER, K., PIERA ALBEROLA, A., MÖHWALD, H., PARAK, W. J. & SUKHORUKOV, G. B. 2006. Laser- induced release of encapsulated materials inside living cells. *Angewandte Chemie International Edition,* 45, 4612-4617.

SMART, R. H. & ANDERSON, W. M. 1952. Pneumoconiosis due to diatomaceous earth. Clinical and x-ray aspects. *Industrial Medicine & Surgery.,* 21, 509-18.

SMITH, A. M., DUAN, H., MOHS, A. M. & NIE, S. 2008. Bioconjugated quantum dots for in vivo molecular and cellular imaging. *Advanced Drug Delivery Reviews,* 60, 1226-1240.

SMITH, S. M., WUNDER, M. B., NORRIS, D. A. & SHELLMAN, Y. G. 2011. A simple protocol for using a LDH-based cytotoxicity assay to assess the effects of death and growth inhibition at the same time. *PloS One,* 6, e26908.

SOHAEBUDDIN, S. K., THEVENOT, P. T., BAKER, D., EATON, J. W. & TANG, L. 2010. Nanomaterial cytotoxicity is composition, size, and cell type dependent. *Particle & Fibre Toxicology,* 7, 22.

SONUNE, A. & GHATE, R. 2004. Developments in wastewater treatment methods. *Desalination,* 167, 55-63.

SPAIN, B. A., CUMMINGS, O. & GARCIA, J. G. 1995. Bronchiolitis obliterans in an animal feed worker. *American Journal of Industrial Medicine,* 28, 437-443.

STEBOUNOVA, L. V., GUIO, E. & GRASSIAN, V. H. 2011. Silver nanoparticles in simulated biological media: a study of aggregation, sedimentation, and dissolution. *Journal of Nanoparticle Research,* 13, 233-244.

STEENLAND, K., BURNETT, C., LALICH, N., WARD, E. & HURRELL, J. 2003. Dying for work: the magnitude of US mortality from selected causes of death associated with occupation. *American Journal of Industrial Medicine,* 43, 461-482.

STEFANIUK, M., OLESZCZUK, P. & OK, Y. S. 2016. Review on nano zerovalent iron (nZVI): from synthesis to environmental applications. *Chemical Engineering Journal,* 287, 618-632.

STONE, V., JOHNSTON, H. & SCHINS, R. P. 2009. Development of in vitro systems for nanotoxicology: methodological considerations. *Critical Reviews in Toxicology,* 39, 613-626.

STREET, R. A. 2005. *Hydrogenated amorphous silicon,* Cambridge University Press, Cambridge, England.

STUEKER, O., ORTEGA, V. A., GOSS, G. G. & STEPANOVA, M. 2014. Understanding interactions of functionalized nanoparticles with proteins: a case study on lactate dehydrogenase. *Small,* 10, 2006-2021.

SUN, T., ZHANG, Y. S., PANG, B., HYUN, D. C., YANG, M. & XIA, Y. 2014. Engineered nanoparticles for drug delivery in cancer therapy. *Angewandte Chemie International Edition,* 53, 12320-12364.

SURESH, A. K., PELLETIER, D. A., WANG, W., MORRELL-FALVEY, J. L., GU, B. & DOKTYCZ, M. J. 2012. Cytotoxicity induced by engineered silver nanocrystallites is dependent on surface coatings and cell types. *Langmuir,* 28, 2727-2735.

SUTRADHAR, K. B. & AMIN, M. L. 2014. Nanotechnology in cancer drug delivery and selective targeting. *ISRN Nanotechnology,* 2014, 939378.

TEMPLETON, M. R. & CHEN, Z. 2010. NDMA and seven other nitrosamines in selected UK drinking water supply systems. *Journal of Water Supply: Research & Technology—AQUA,* 59, 277-283.

TEOW, Y., ASHARANI, P., HANDE, M. P. & VALIYAVEETTIL, S. 2011. Health impact and safety of engineered nanomaterials. *Chemical Communications,* 47, 7025-7038.

THOMAS, K., AGUAR, P., KAWASAKI, H., MORRIS, J., NAKANISHI, J. & SAVAGE, N. 2006. Research strategies for safety evaluation of nanomaterials, part VIII: international efforts to develop risk-based safety evaluations for nanomaterials. *Toxicological Sciences,* 92, 23-32.

TIMBAL, B. 2004. Southwest Australia past and future rainfall trends. *Climate Research,* 26, 233-249.

TIWARI, A. J. & MARR, L. C. 2010. The role of atmospheric transformations in determining environmental impacts of carbonaceous nanoparticles. *Journal of Environmental Quality,* 39, 1883-1895.

TOI, M., BICKNELL, R. & HARRIS, A. L. 1992. Inhibition of colon and breast carcinoma cell growth by interleukin-4. *Cancer Research,* 52, 275-279.

TROUILLER, B., RELIENE, R., WESTBROOK, A., SOLAIMANI, P. & SCHIESTL, R. H. 2009. Titanium dioxide nanoparticles induce DNA damage and genetic instability *in vivo* in mice. *Cancer Research,* 69, 8784-8789.

TROY, P. 1995. *Australian cities: issues, strategies and policies for urban Australia in the 1990s*, Cambridge University Press, Melbourne, Australia.

TURKEVICH, J., STEVENSON, P. C. & HILLIER, J. 1951. A study of the nucleation and growth processes in the synthesis of colloidal gold. *Discussions of the Faraday Society,* 11, 55-75.

UBOLDI, C., GIUDETTI, G., BROGGI, F., GILLILAND, D., PONTI, J. & ROSSI, F. 2012. Amorphous silica nanoparticles do not induce cytotoxicity, cell

transformation or genotoxicity in Balb/3T3 mouse fibroblasts. *Mutation Research/Genetic Toxicology & Environmental Mutagenesis,* 745, 11-20.

VERDON- KIDD, D. C. & KIEM, A. S. 2009. Nature and causes of protracted droughts in southeast Australia: comparison between the Federation, WWII, and Big Dry droughts. *Geophysical Research Letters,* 36.

VERRECCHIA, T., SPENLEHAUER, G., BAZILE, D., MURRY-BRELIER, A., ARCHIMBAUD, Y. & VEILLARD, M. 1995. Non-stealth (poly (lactic acid/albumin)) and stealth (poly (lactic acid-polyethylene glycol)) nanoparticles as injectable drug carriers. *Journal of Controlled Release,* 36, 49-61.

VERTESSY, R. 2010. *Australian water resources assessment 2010*. Bureau of Meteorology, Canberra, Australia.

VIGGERS, J., WEAVER, H. & LINDENMAYER, D. 2013. *Melbourne's water catchments: perspectives on a world-class water supply,* CSIRO Publishing, Melbourne, Australia.

VO, N. T. K., BUFALINO, M. R., HARTLEN, K. D., KITAEV, V. & LEE, L. E. J. 2014. Cytotoxicity evaluation of silica nanoparticles using fish cell lines. *In Vitro Cellular & Developmental Biology—Animal,* 50, 427-438.

VON MEDEAZZA, G. M. 2005. 'Direct' and socially-induced environmental impacts of desalination. *Desalination,* 185, 57-70.

VON MOOS, N. The toxicity of nanoplastics to marine organisms. CIESM Workshop Monographs, Genève, 2014.

VRČEK, I. V., PAVIČIĆ, I., CRNKOVIĆ, T., JURAŠIN, D., BABIČ, M., HORÁK, D., LOVRIĆ, M., FERHATOVIĆ, L., ĆURLIN, M. & GAJOVIĆ, S. 2015. Does surface coating of metallic nanoparticles modulate their interference with in vitro assays? *RSC Advances,* 5, 70787-70807.

WADDON, A. J. & COUGHLIN, E. B. 2003. Crystal structure of polyhedral oligomeric silsequioxane (POSS) nano-materials: a study by X-ray diffraction and electron microscopy. *Chemistry of Materials,* 15, 4555-4561.

WALLACE, W., GUTTMAN, C. & ANTONUCCI, J. 1999. Molecular structure of silsesquioxanes determined by matrix-assisted laser desorption/ionization time-of-flight mass spectrometry. *Journal of the American Society for Mass Spectrometry,* 10, 224-230.

WANG, L., WANG, K., SANTRA, S., ZHAO, X., HILLIARD, L. R., SMITH, J. E., WU, Y. & TAN, W. 2006. Watching silica nanoparticles glow in the biological world. *Analytical Chemistry,* 78, 646-654.

WANG, L., WANG, Y., XU, T., LIAO, H., YAO, C., LIU, Y., LI, Z., CHEN, Z., PAN, D. & SUN, L. 2014. Gram-scale synthesis of single-crystalline graphene quantum dots with superior optical properties. *Nature Communications,* 5, 5357.

WANG, L., YANG, C. & TAN, W. 2005. Dual-luminophore-doped silica nanoparticles for multiplexed signaling. *Nano Letters,* 5, 37-43.

WANG, W., REN, S., ZHANG, H., YU, J., AN, W., HU, J. & YANG, M. 2011. Occurrence of nine nitrosamines and secondary amines in source water and drinking water: Potential of secondary amines as nitrosamine precursors. *Water Research,* 45, 4930-4938.

WARHEIT, D. B., LAURENCE, B., REED, K. L., ROACH, D., REYNOLDS, G. & WEBB, T. 2004. Comparative pulmonary toxicity assessment of single-wall carbon nanotubes in rats. *Toxicological Sciences,* 77, 117-125.

WARHEIT, D. B., WEBB, T. R., COLVIN, V. L., REED, K. L. & SAYES, C. M. 2007. Pulmonary bioassay studies with nanoscale and fine-quartz particles in rats: toxicity is not dependent upon particle size but on surface characteristics. *Toxicological Sciences,* 95, 270-280.

WARREN, J. K. 1982. The hydrological setting, occurrence and significance of gypsum in late Quaternary salt lakes in South Australia. *Sedimentology,* 29, 609-637.

WASHINGTON, C. 2005. *Particle size analysis in pharmaceutics and other industries: theory and practice.* CRC Press,

WATER, M. 2004. *Melbourne's rivers and creeks 2004,* Melbourne Water, Melbourne, Australia.

WEISSLEDER, R., KELLY, K., SUN, E. Y., SHTATLAND, T. & JOSEPHSON, L. 2005. Cell-specific targeting of nanoparticles by multivalent attachment of small molecules. *Nature Biotechnology,* 23, 1418-1423.

WESTERHOFF, P. K., KISER, M. A. & HRISTOVSKI, K. 2013. Nanomaterial removal and transformation during biological wastewater treatment. *Environmental Engineering Science,* 30, 109-117.

WIESNER, M., HOTZE, E., BRANT, J. & ESPINASSE, B. 2008. Nanomaterials as possible contaminants: the fullerene example. *Water Science & Technology,* 57, 305-310.

WILSON, M., KANNANGARA, K., SMITH, G., SIMMONS, M. & RAGUSE, B. 2002. *Nanotechnology: basic science and emerging technologies*, CRC Press.

WIN, K. Y. & FENG, S.-S. 2005. Effects of particle size and surface coating on cellular uptake of polymeric nanoparticles for oral delivery of anticancer drugs. *Biomaterials*, 26, 2713-2722.

WÖRLE-KNIRSCH, J. M., PULSKAMP, K. & KRUG, H. F. 2006. Oops they did it again! Carbon nanotubes hoax scientists in viability assays. *Nano Letters*, 6, 1261-1268.

WRIGHT, M. T. & COX, G. 2006. Independent panel major project: Kurnell Desalination Plant and associated infrastructure.

WU, J. & MATHER, P. T. 2009. POSS polymers: physical properties and biomaterials applications. *Polyer Reviews*, 49, 25-63.

XIA, T., KOVOCHICH, M., BRANT, J., HOTZE, M., SEMPF, J., OBERLEY, T., SIOUTAS, C., YEH, J. I., WIESNER, M. R. & NEL, A. E. 2006. Comparison of the abilities of ambient and manufactured nanoparticles to induce cellular toxicity according to an oxidative stress paradigm. *Nano Letters*, 6, 1794-1807.

XIONG, D., FANG, T., YU, L., SIMA, X. & ZHU, W. 2011. Effects of nano-scale TiO_2, ZnO and their bulk counterparts on zebrafish: acute toxicity, oxidative stress and oxidative damage. *Science of the Total Environment*, 409, 1444-1452.

YAMAMOTO, Y., NAGASAKI, Y., KATO, Y., SUGIYAMA, Y. & KATAOKA, K. 2001. Long-circulating poly (ethylene glycol)–poly (d, l-lactide) block copolymer micelles with modulated surface charge. *Journal of Controlled Release*, 77, 27-38.

YANG, H., LIU, C., YANG, D., ZHANG, H. & XI, Z. 2009. Comparative study of cytotoxicity, oxidative stress and genotoxicity induced by four typical nanomaterials: the role of particle size, shape and composition. *Journal of Applied Toxicology*, 29, 69-78.

YANG, X., LIU, J., HE, H., ZHOU, L., GONG, C., WANG, X., YANG, L., YUAN, J., HUANG, H. & HE, L. 2010. SiO_2 nanoparticles induce cytotoxicity and protein expression alteration in HaCaT cells. *Part Fibre Toxicol*, 7, 1.

YANG, Y. & RIOUX, R. M. 2014. Highly stereoselective anti-Markovnikov hydrothiolation of alkynes and electron-deficient alkenes by a supported Cu-NHC complex. *Green Chemistry*, 16, 3916-3925.

YASSIN, A., YEBESI, F. & TINGLE, R. 2005. Occupational exposure to crystalline silica dust in the United States, 1988-2003. *Environmental Health Perspectives*, 113, 255-260.

YEH, H.-C. & SCHUM, G. 1980. Models of human lung airways and their application to inhaled particle deposition. *Bulletin of Mathematical Biology*, 42, 461-480.

YIN, J.-J., LIU, J., EHRENSHAFT, M., ROBERTS, J. E., FU, P. P., MASON, R. P. & ZHAO, B. 2012. Phototoxicity of nano titanium dioxides in HaCaT keratinocytes—generation of reactive oxygen species and cell damage. *Toxicology & Applied Pharmacology*, 263, 81-88.

YONEZAWA, T. & KUNITAKE, T. 1999. Practical preparation of anionic mercapto ligand-stabilized gold nanoparticles and their immobilization. *Colloids & Surfaces A: Physicochemical & Engineering Aspects*, 149, 193-199.

YOUNG, F. M., PHUNGTAMDET, W. & SANDERSON, B. J. 2005. Modification of MTT assay conditions to examine the cytotoxic effects of amitraz on the human lymphoblastoid cell line, WIL2NS. *Toxicology In Vitro*, 19, 1051-1059.

YOUNG, R. 2005. National trends in urban water resource management. *Address to Gold Coast Water Future Advisory Communities, Water Service Association of Australia*.

ZHANG, L., GU, F., CHAN, J., WANG, A., LANGER, R. & FAROKHZAD, O. 2008a. Nanoparticles in medicine: therapeutic applications and developments. *Clinical Pharmacology & Therapeutics*, 83, 761-769.

ZHANG, L. W., YU, W. W., COLVIN, V. L. & MONTEIRO-RIVIERE, N. A. 2008b. Biological interactions of quantum dot nanoparticles in skin and in human epidermal keratinocytes. *Toxicology & Applied Pharmacology*, 228, 200-211.

ZHANG, T., GE, J., HU, Y., ZHANG, Q., ALONI, S. & YIN, Y. 2008c. Formation of hollow silica colloids through a spontaneous dissolution–regrowth process. *Angewandte Chemie*, 120, 5890-5895.

ZHANG, Y.-H. P., HIMMEL, M. E. & MIELENZ, J. R. 2006. Outlook for cellulase improvement: screening and selection strategies. *Biotechnology Advances*, 24, 452-481.

ZHANG, Y., CHEN, Y., WESTERHOFF, P., HRISTOVSKI, K. & CRITTENDEN, J. C. 2008d. Stability of commercial metal oxide nanoparticles in water. *Water Research*, 42, 2204-2212.

ZHANG, Y., HU, L., YU, D. & GAO, C. 2010. Influence of silica particle internalization on adhesion and migration of human dermal fibroblasts. *Biomaterials,* 31, 8465-8474.

ZHAO, X., HILLIARD, L. R., MECHERY, S. J., WANG, Y., BAGWE, R. P., JIN, S. & TAN, W. 2004. A rapid bioassay for single bacterial cell quantitation using bioconjugated nanoparticles. *Proceedings of the National Academy of Sciences of the United States of America,* 101, 15027-15032.

ZHAO, Y. & SCHIRALDI, D. A. 2005. Thermal and mechanical properties of polyhedral oligomeric silsesquioxane (POSS)/polycarbonate composites. *Polymer,* 46, 11640-11647.

ZHU, M., NIE, G., MENG, H., XIA, T., NEL, A. & ZHAO, Y. 2012. Physicochemical properties determine nanomaterial cellular uptake, transport, and fate. *Accounts of Chemical Research,* 46, 622-631.

ZHU, X., WANG, J., ZHANG, X., CHANG, Y. & CHEN, Y. 2009. The impact of ZnO nanoparticle aggregates on the embryonic development of zebrafish (*Danio rerio*). *Nanotechnology,* 20, 195103.

ZHU, X., ZHU, L., DUAN, Z., QI, R., LI, Y. & LANG, Y. 2008. Comparative toxicity of several metal oxide nanoparticle aqueous suspensions to Zebrafish (*Danio rerio*) early developmental stage. *Journal of Environmental Science & Health Part A,* 43, 278-284.

Appendices

Appendix 1: Dose Responses of Methanol Used in the Preparation of the Crystal Violet Assay

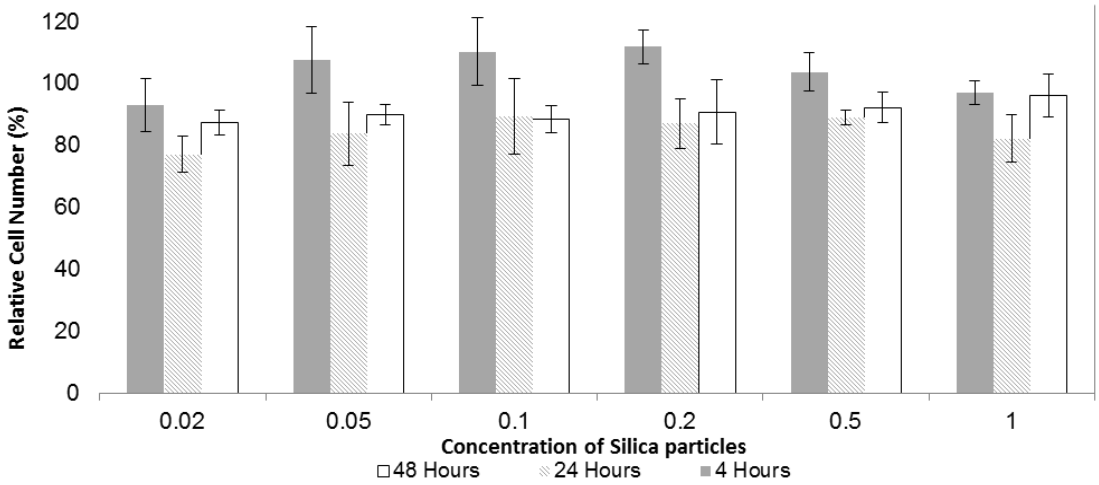

Figure A.1: Effect of treatment with methanol for 4, 24 and 48 h on the viability of HaCaT cells using the crystal violet assay. The effect of methanol was minimal and only seen after 24-h exposure. The concentration of methanol in the crystal violet assay was adjusted according to this result.

Appendix 2: Preparation of Solutions Used in this Study

A2.1 Phosphate Buffered Saline Stock Solution

The stock solution was prepared and stored in the tissue culture lab at a concentration of 10 × PBS. It was prepared by dissolving 2 g of KCI, 80 g of NaCl, 14.4 g of Na_2HPO and 2.4 g of KH_2PO_4 into 900 mL Baxter water and then completed to 1 L. The pH was then adjusted to 7.4. 1 × PBS was used in this study and it was prepared by adding 100 mL of stock PBS to 900 mL Baxter water; the pH was then adjusted to 7.4 and it was autoclaved and stored at room temperature.

A2.2 MTT Stock Solution

Thiazolyl blue tetrazolium bromide (MTT) (Sigma Aldrich, MO, USA) was prepared in a stock solution at a concentration of 5 mg/mL by dissolving 250 mg of MTT powder in 50 mL of 1 × PBS. The solution was prepared in a beaker covered with foil and then filtered through a 0.22-µm sterile syringe filter to produce sterile 10-mL aliquots. The tubes were then stored at –20°C.

A2.3 Roswell Park Memorial Institute Medium

Two L of RPMI medium was prepared as needed for the study. In detail, 20.88 g of RPMI powder (Sigma cat no. R6504 + phenol red) was added to 0.592 g L-glutamine (Sigma Aldrich, MO, USA). Twenty mL penicillin (HyQ®, HyClone, UT, USA) was added and 1.7 mL of Baxter water was used to dissolve the mixture. The pH was adjusted to 7 and 35.6 mL of sodium bicarbonate (Pfizer, WA, Australia) and 200 mL of FBS (HyQ®) was added. The total volume was then completed to 2 L using Baxter water. The medium was filtered using a 0.22-µm filter and stored at 4°C; unfiltered medium was stored at –20°C.

A2.4 DMEM Medium

Dulbecco's minimal essential medium (DMEM) powder (13.5 g/L); 17.8 mL/L sodium bicarbonate (Pfizer); L-glutamine (0.592 g/L); 10 mL penicillin/streptomycin (Gibco®, HyClone) and 10% heat-inactivated FBS (HyClone, Victoria, Australia) were added to 0.5 L of sterile MQ water (Baxter). The medium was adjusted to pH 7.4 and sterilised

using a 0.22-µm filter before storage at 4°C. The temperature and pH of the media were equilibrated for 30 min in a 37°C incubator immediately before use.

A2.5 0.5 M Sodium Phosphate Buffer

Stock solutions of 0.5 M monobasic sodium (Sigma Aldrich, MO, USA) and 0.5 M dibasic sodium phosphate (Sigma Aldrich) were prepared for dissolving the QDs. For monobasic sodium, 6 g of powder was dissolved in a final volume of 100 mL Baxter water. For dibasic sodium phosphate, 7.098 g of powder was dissolved in a final volume of 100 mL Baxter water. Ten mL of monobasic solution was added to 52.5 mL of dibasic solution. The mixture was stirred on a magnetic stirrer and the pH adjusted to 7.5. The mixture was then sterilised using a re-usable 250-mL filter and stored at room temperature.

A2.6 20% Sodium Dodecyl Sulphate in 0.02 M HCI

Initially, 400 mL of RO water was added to a 500-mL volumetric flask. In the fume hood, 0.8333 mL of 12 M HCI was added to a flask and the volume brought up to 500 mL with RO water. The 500 mL was stored in a glass Schott bottle with a clear label in the fume hood. Forty g of SDS powder was added to 200 mL of 0.02 M HCI and stored in the fume hood.

A2.7 Crystal Violet Stain

Fifty % methanol was prepared by adding 50 mL of RO water to 50 mL 100% methanol and was kept in a volumetric flask in the fume hood. To prepare crystal violet stain, 0.5 g per 100 mL was weighed and added to the prepared 50% methanol and mixed well before storing in the fume hood. Crystal violet stain is toxic; therefore, a mask was worn during the weighing.

A2.8 Trypan Blue

To prepare 100 mL of TB, 0.9 g NaCl was added to a volumetric flask along with 0.2 g of TB powder, and mixed with 100 mL MQ water for 3 min. The mixture was sterilised using a 0.22-µm filter or 250-mL re-usable filter and stored at 4°C.

A2.9 33% Acetic Acid

Seven7-seven mL of MQ water was transferred to a Schott bottle. Thirty-three mL of acetic acid was added to the measured MQ water in the Schott bottle. The solution was stored at room temperature in a fume hood.

Appendix 3: Details about the Human Cell Lines Used in this Study

Table A3.1: Human skin keratinocyte cell line

Designation	HaCaT
Organism	*Homo sapiens* (human)
Ethnicity	Caucasian
Age/stage	62 years
Gender	Male
Tissue	Skin
Cell type	Keratinocyte
Growth properties	Monolayer
Description	*In vitro* spontaneously transformed keratinocytes from histologically normal skin
Culture medium	DMEM or RPMI medium (high glucose) supplemented with 2 mM L-glutamine and 10% FCS
Split ratio	A ratio of 1:5 to 1:10 is recommended
Fluid renewal	2 times weekly
Freeze medium	CM-1 (CLS—Cell Lines Service)
Sterility	Tests for mycoplasma, bacteria and fungi were negative
Biosafety level	1
Tumorigenic	No
Karyotype	Aneuploid (hypotetraploid)

Table A3.2: Human colon carcinoma cell line

Designation:	Caco-2
Organism	*Homo sapiens*, human
Ethnicity	Caucasian
Age/stage	72 years
Gender	Male
Tissue	Colon
Cell type	Epithelial cells
Morphology	Epithelial like
Cultural properties	Adherent
Culture medium	DMEM or RPMI medium (high glucose) supplemented with 2 mM L-glutamine and 10% FCS
Split ratio	A ratio of 1:5 to 1:10 is recommended
Fluid renewal	2–3 times weekly
Freeze medium	CM-1 (CLS—Cell Lines Service)
Sterility	Tests for mycoplasma, bacteria and fungi were negative
Biosafety level	1
Diseases	Colorectal adenocarcinoma